



JOANA FÉLIX PEREIRA  
BSc in Biochemistry

# THERAPEUTIC DEEP EUTECTIC SYSTEMS AS PROMISING NEW TOOLS IN THE ANTICANCER BATTLE

MASTER IN MOLECULAR GENETICS AND BIOMEDICINE

NOVA University Lisbon

November, 2021





JOANA FÉLIX PEREIRA  
BSc in Biochemistry

THERAPEUTIC DEEP EUTECTIC  
SYSTEMS AS PROMISING NEW TOOLS IN  
THE ANTICANCER BATTLE

MASTER IN MOLECULAR GENETICS AND BIOMEDICINE  
NOVA University Lisbon  
November, 2021





# THERAPEUTIC DEEP EUTECTIC SYSTEMS AS PROMISING NEW TOOLS IN THE ANTICANCER BATTLE

**JOANA FÉLIX PEREIRA**

BSc in Biochemistry

**Adviser:** Ana Rita Cruz Duarte  
*Associate Professor, NOVA University Lisbon*

**Examination Committee:**

**Chair:** Maria Alexandra Nuncio de Carvalho Ramos  
Fernandes,  
Assistant Professor, FCT-NOVA

**Rapporteurs:** Carina Alexandra Marques Esteves,  
Post-Doctoral Researcher, FCT-NOVA

**Adviser:** Ana Rita Cruz Duarte,  
Associate Professor, FCT-NOVA



## **THERAPEUTIC DEEP EUTECTIC SYSTEMS AS PROMISING NEW TOOLS IN THE ANTICANCER BATTLE**

Copyright © Joana Félix Pereira, NOVA School of Science and Technology, NOVA University Lisbon.

The NOVA School of Science and Technology and the NOVA University Lisbon have the right, perpetual and without geographical boundaries, to file and publish this dissertation through printed copies reproduced on paper or on digital form, or by any other means known or that may be invented, and to disseminate through scientific repositories and admit its copying and distribution for non-commercial, educational or research purposes, as long as credit is given to the author and editor.





## ACKNOWLEDGEMENTS

I would like to express my gratitude to my supervisor Ana Rita Duarte for giving me this project that I loved and for her time, help and support. Thank you so much for this opportunity and the doors that it opened for my future. It was amazing to participate in your projects and to have the opportunity of working in one of the most prestigious investigation centers on deep eutectic systems.

I also want to thank my co-supervisor Filipe Oliveira for all his time, patience, guidance and kindness. Thank you so much for the opportunities that you opened for me and for all the support that you gave me, without you I would not be able to finish my thesis. Thank you for all the hours spent in the lab and reading and discussing my thesis to improve the final result.

I want to thank all the members of DES.Solve group. You are a great team. I never imagine to be welcomed in the way that I was.

Thank you also to our sponsors, this work has received funding from the ERC-2016-CoG 725034 and was supported by the Associate Laboratory for Green Chemistry- LAQV financed by national funds from FCT/MCTES (UIDB/50006/2020).

Thank you so much to my friends Inês Almeida and Cátia Oliveira Soares. You are the best friends that I could ever get and without you and your support I wouldn't had the courage to finish my thesis and do what was necessary.

Finally, I would like to thank my parents. Without you nothing would be possible. Thank you for giving me the opportunity to continue my studies and for all the conditions I need to succeed.



## ABSTRACT

Cancer remains a major health problem worldwide, with colorectal cancer (CRC) being the third most incident and the second most lethal. Inflammation has been highly associated with cancer development and maintenance, therefore, the reduction of the inflammatory microenvironment represents a promising therapeutic strategy.

Deep eutectic systems (DES) are based on the combination of different components which together, at a certain molar ratio, present a deep decrease in their melting point compared with the individual compounds. When an active pharmaceutical ingredient is part of a DES it is designated by therapeutic deep eutectic system (THEDES).

New THEDES combining terpenes with anticancer properties, such as safranal, menthol and linalool, with NSAIDs, like ibuprofen, ketoprofen and flurbiprofen were produced. To evaluate THEDES therapeutic potential activity, their physico-chemical properties, bioavailability and bioactivity, were explored using an integrative approach to determine their anti-CRC activity. Our results show that Safranal:Ibuprofen (3:1), Safranal:Ibuprofen (4:1) and Menthol:Ibuprofen (3:1) present promising therapeutic activity towards CRC cells due to a selective cytotoxic action towards cancer cells. Menthol:Ibuprofen (3:1) anti-proliferative action seems to be related with cell membrane disruption, reduction of the inflammation through the reduction of ROS production, and induction of apoptosis via caspase-3. On the other hand, Safranal:Ibuprofen (3:1) and Safranal:Ibuprofen (4:1) seem to prevent tumour cells expansion only through the induction of apoptosis via caspase-3. These systems also present an increasement in Ibuprofen permeability, with Menthol:Ibuprofen (3:1) increasing also Ibuprofen solubility and the overall bioavailability.

**Keywords:** Colorectal cancer, Deep eutectic systems, THEDES, NSAID, Natural compounds, Terpenes



## RESUMO

O cancro continua a ser um dos maiores problemas de saúde em todo o mundo, sendo que o cancro colorretal é o terceiro mais incidente e o segundo mais letal. A inflamação está altamente associada ao desenvolvimento e persistência do cancro, por esse motivo, a redução do microambiente inflamatório representa uma estratégia terapêutica promissora.

Sistemas eutéticos, em inglês, *Deep eutectic systems* (DES) são sistemas baseados na combinação de diferentes componentes que em conjunto e a um determinado rácio molar apresentam uma grande diminuição do ponto de fusão em comparação com os compostos individuais. Quando um dos componentes do DES é um ingrediente farmacêutico ativo ele é designado de sistemas eutéticos terapêuticos, *therapeutic deep eutectic system* (THEDES).

Novos THEDES a conjugar terpenos com propriedades anticancerígenas, como mentol, safranal e linalool, com anti-inflamatórios não esteroides, como ibuprofeno, cetoprofen e flurbiprofeno. Para avaliar o potencial terapêutico dos THEDES, as suas propriedades físico-químicas, biodisponibilidade e bioatividade foram exploradas ao longo da tese como uma análise integrativa para determinar as suas atividades contra o cancro colorretal. Os nossos resultados demonstram que o Safranal:Ibuprofeno (3:1), Safranal:Ibuprofeno (4:1) e Mentol:Ibuprofeno (3:1) apresentam uma atividade terapêutica promissora contra as células do cancro colorretal devido a uma ação citotóxica seletiva contra as células cancerígenas. A ação do Mentol:Ibuprofeno (3:1) como anti-proliferativo contra as células cancerígenas aparenta estar relacionada com a disrupção da membrana celular, redução da inflamação através da redução da produção de ROS, e através da indução da apoptose via caspase-3. Por outro lado, Safranal:Ibuprofeno (3:1) e Safranal:Ibuprofeno (4:1) aparentam prevenir a expansão das células tumorais apenas através da indução da apoptose via caspase-3. Adicionalmente, estes sistemas também apresentam um aumento da permeabilidade do Ibuprofeno, com o sistema Mentol:Ibuprofeno (3:1) aumentando também a solubilidade do Ibuprofeno e a sua biodisponibilidade no geral.

**Palavras-chave:** Cancro colorretal, sistemas eutéticos, THEDES, anti-inflamatórios não esteroides, Compostos naturais, Terpenos



# TABLE OF CONTENTS

ACKNOWLEDGEMENTS .....	IX
ABSTRACT .....	XI
RESUMO.....	XIII
TABLE OF CONTENTS .....	XV
LIST OF FIGURES .....	XVII
LIST OF TABLES .....	XXI
GLOSSARY .....	XXIII
<b>1 INTRODUCTION .....</b>	<b>1</b>
1.1. MODERN WORLD AND THE CANCER CHALLENGE.....	1
1.1.1. <i>Cancer</i> .....	3
1.1.2. <i>Colorectal Cancer</i> .....	6
1.2. SUSTAINABLE CHEMISTRY AND DEEP EUTECTIC SYSTEMS .....	12
1.2.1. <i>DES</i> .....	12
1.2.2. <i>Terpenes</i> .....	15
1.2.3. <i>Nonsteroidal Anti-inflammatory Drugs (NSAIDs)</i> .....	19
<b>2 AIM.....</b>	<b>25</b>
<b>3 MATERIALS AND METHODS.....</b>	<b>27</b>
3.1. THEDES PREPARATION.....	27
3.2. POM .....	27
3.3. NMR.....	27
3.4. SOLUBILITY ASSESSMENT .....	28
3.5. PERMEABILITY STUDIES .....	28
3.6. CELL CULTURE AND SUB-CULTURING .....	29
3.7. CELL THAWING .....	30
3.8. CELL FREEZING.....	30
3.9. CELL VIABILITY ASSESSMENT.....	31
3.9.1. <i>Cytotoxicity Assay</i> .....	32
3.9.2. <i>Antiproliferative Assay</i> .....	32
3.10. LACTATE DEHYDROGENASE (LDH) RELEASE.....	33
3.11. ANTI-INFLAMMATORY POTENTIAL ASSESSMENT.....	34
3.11.1. <i>Intracellular ROS Production</i> .....	34

3.11.2.	<i>NO Production</i> .....	35
3.11.3.	<i>IL-8 ELISA</i> .....	36
3.12.	CASPASE-3 ACTIVITY.....	38
3.13.	STATISTICAL ANALYSIS.....	38
<b>4</b>	<b>RESULTS AND DISCUSSION</b> .....	<b>39</b>
4.1.	THEDES PREPARATION .....	39
4.2.	NMR STUDIES .....	40
4.3.	POM .....	48
4.4.	NSAIDS SOLUBILITY AND PERMEABILITY ASSESSMENT.....	50
4.5.	THEDES CYTOTOXICITY AND ANTIPROLIFERATIVE EFFECTS.....	54
4.6.	LDH RELEASE .....	57
4.7.	THEDES ANTI-INFLAMMATORY EFFECTS .....	58
4.7.1.	<i>Intracellular ROS e NO</i> .....	58
4.7.2.	<i>IL-8 Measurement</i> .....	60
4.8.	EFFECTS OF THEDES ON APOPTOSIS VIA CASPASE-3 .....	61
<b>5</b>	<b>CONCLUSIONS</b> .....	<b>65</b>
	<b>BIBLIOGRAPHY</b> .....	<b>67</b>
<b>A</b>	<b>SUPPLEMENTARY INFORMATION</b> .....	<b>77</b>
A.1.	NMR STUDIES .....	77
A.2.	THEDES CYTOTOXICITY AND ANTIPROLIFERATIVE POTENTIALS .....	83
A.3.	LDH RELEASE .....	85
A.4.	IL-8 MEASUREMENT.....	85
A.4.1.	<i>Bradford</i> .....	86



# LIST OF FIGURES

**FIGURE 1.1.** TUMOUR PROGRESSION DURING COLON CARCINOMA DEVELOPMENT. A SINGLE COLON EPITHELIAL MUTATED CELL STARTS TO PROLIFERATE AND TRANSMITS ITS MUTATION TO DAUGHTER CELLS. DURING CELL PROLIFERATION A SMALL BENIGN ADENOMA IS FORMED. CONSEQUENT ROUNDS OF CLONAL SELECTION LEADS TO ADENOMA GROWTH AND INCREASED PROLIFERATIVE POTENTIAL. THE BENIGN ADENOMA THEN EVOLVES TO A MALIGNANT CARCINOMA DUE TO INVASION OF THE TUMOUR CELLS THROUGH THE BASEMENT MEMBRANE INTO THE CONNECTIVE TISSUE. AFTER THAT, CANCER CELLS CONTINUE TO MULTIPLY AND PROPAGATE IN THE CONNECTIVE TISSUE OF THE COLON WALL. ULTIMATELY, CANCER CELLS PENETRATE THE COLON WALL AND INVADE THE SURROUNDING ORGANS, BLOOD AND LYMPHATIC VESSELS, ALLOWING CANCER CELLS TO METASTASIZE TO ALL THE BODY (ADAPTED FROM [19]).....4

**FIGURE 1.2.** EMT ENHANCES METASTASIS. DURING TUMOUR FORMATION THE GENETIC AND EPIGENETIC MODIFICATIONS THAT TUMOUR CELLS SURFER PROMOTES EMT AND COLLECTIVE MIGRATION. THESE TWO INVASIVE MECHANISMS ENABLE TUMOUR CELLS TO DETACH FROM THEIR SURROUNDING CELLS, INVADE THROUGH THE BASEMENT MEMBRANE AND MIGRATE TO OTHER TISSUES AS A SINGLE CELL (DARK BLUE) OR AS A CLUSTER OF CELLS (LIGHT BLUE). THIS INVASION IS THE START OF THE METASTATIC DISSEMINATION AND SPREAD TO THE LYMPHATIC NODES AND BLOOD VESSELS. THE MIGRATION TO BLOOD VESSELS ENABLES THE DEVELOPMENT OF DISTANT METASTASIS, WHERE CELLS ONCE AGAIN EXPRESS AN EPITHELIAL PHENOTYPE DUE TO UNDERGO MESENCHYMAL-EPITHELIAL TRANSITION (MET) (ADAPTED FROM [21]).....5

**FIGURE 1.3.** INFLAMMATORY PROCESS ASSOCIATED WITH CRC AND CAC DEVELOPMENT. **(A)** IN SPORADIC CRC, ONE OF THE FIRST EVENTS THAT OCCUR IS THE MUTATION IN THE GENE ENCODING APC, ASSOCIATED WITH THE WNT PATHWAY, THAT LEADS TO THE ACTIVATION OF B-CATENIN AND CONSEQUENTLY TO ADENOMA DEVELOPMENT. THE APC MUTATION IS ALSO ASSOCIATED WITH LOSS OF TIGHT JUNCTIONS WHICH ALLOWS MICROBIAL INVASION FROM THE INTESTINAL MICROBIOME, INDUCING IL-17 AND IL-23 PRODUCTION. FOR AN EARLY-STAGE ADENOMA EVOLVE TO A CARCINOMA, ACTIVATION OF ONCOGENE KRAS AND INACTIVATION OF TUMOUR SUPPRESSORS TGF- $\beta$  RECEPTOR AND P53 MUST OCCUR. THIS TRANSITION ALSO INVOLVES INCREASED EXPRESSION OF COX2. **(B)** IN CAC, CHRONIC INFLAMMATION IS CONSTANT AND MUCOSAL PRODUCTION OF PROINFLAMMATORY CYTOKINES INCREASES IN A PROCESS MEDIATED BY NF- $\kappa$ B THAT IS RESPONSIBLE FOR B-CATENIN ACTIVATION. MUTATION ON THE GENE THAT ENCODE P53 IS ONE OF THE FIRST STEPS IN CAC AND IS ASSOCIATED WITH INCREASING PRODUCTION OF IL-6. IL-6 CONSEQUENTLY ACTIVATES TRANSDUCER AND ACTIVATOR OF TRANSCRIPTION 3 (STAT3) THAT EXTENDS NF- $\kappa$ B ACTIVATION. TUMOUR NECROSIS FACTOR (TNF) IS ANOTHER TUMOUR-PROMOTING CYTOKINE PRODUCED IN THE INITIAL INFLAMMATORY RESPONSE AND INCREASES VASCULAR PERMEABILITY THAT PROMOTES THE MICROBIAL INVASION, AND CONSEQUENTLY FURTHER ENHANCES THE INFLAMMATORY RESPONSE WITH INCREASING ACTIVATION OF NF- $\kappa$ B AND STAT3. MOREOVER, CHRONIC INFLAMMATION AND THE CONSTANT ACTIVATION OF NF- $\kappa$ B IS ALSO RESPONSIBLE FOR OXIDATIVE STRESS THAT LEADS TO DNA DAMAGE, RESULTING IN MUTATIONS OF THE GENE THAT ENCODES APC AND THE DEVELOPMENT OF CARCINOMA (ADAPTED FROM [24]). ..... 9

**FIGURE 1.4.** THEORETICAL TEMPERATURE-CONCENTRATION PHASE DIAGRAM FOR A BINARY EUTECTIC SYSTEM (ADAPTED FROM [57])..... 13

**FIGURE 1.5.** MENTHOL STRUCTURE..... 16

**FIGURE 1.6.** LINALOOL STRUCTURE. .... 17

**FIGURE 1.7.** SAFRANAL STRUCTURE..... 18

<b>FIGURE 1.8.</b> IBUPROFEN STRUCTURE. ....	20
<b>FIGURE 1.9.</b> FLURBIPROFEN STRUCTURE. ....	21
<b>FIGURE 1.10.</b> KETOPROFEN STRUCTURE. ....	22
<b>FIGURE 1.11.</b> KETOPROFEN ACTS AS ANTI-INFLAMMATORY THROUGH THE INHIBITION OF COX1 AND COX2 AND CONSEQUENT DECREASE OF PROSTAGLANDIN SYNTHESIS, AND ALSO THROUGH THE INHIBITION OF THE LIPOXYGENASE PATHWAY OF THE ARACHIDONIC ACID CASCADE THAT IS RESPONSIBLE FOR THE PRODUCTION OF NONCYCLIZED MONOHYDROXY ACIDS (HETE) AND LEUKOTRIENES. ....	23
<b>FIGURE 3.1.</b> HEMOCYTOMETER CHAMBER SCHEME FOR CELL COUNTING. ....	30
<b>FIGURE 3.2.</b> HT29 CELL LINE IN CULTURE. ....	31
<b>FIGURE 3.3.</b> CACO-2 CELL LINE IN CULTURE. ....	32
<b>FIGURE 3.4.</b> COLORIMETRIC REACTION TO MEASURE LDH RELEASE. LDH IS RESPONSIBLE FOR THE CONVERSION OF LACTATE IN PYRUVATE COUPLED WITH THE REDUCTION OF NAD <sup>+</sup> TO NADH. THE NADH WILL REDUCE THE WATER-SOLUBLE TETRAZOLIUM SALT (WST) IN THE PRESENCE OF AN ELECTRON MEDIATOR, ORIGINATING AN ORANGE FORMAZAN DYE. ....	33
<b>FIGURE 3.5.</b> DCFH-DA REACTION FOR DETECTION OF ROS. DCFH-DA CROSSES THE CELL MEMBRANE WHERE IT IS HYDROLYZED BY ESTERASES ORIGINATING DCFH. THEN, DCFH REACTS WITH ROS AND IS OXIDATED TO THE FLUORESCENT DCF (ADAPTED FROM [136]). ....	35
<b>FIGURE 3.6.</b> SANDWICH ELISA METHOD. FIRST THE PLATE WELLS ARE COATED WITH CAPTURE ANTIBODY AND BLOCKING BUFFER TO AVOID UNSPECIFIC PROTEIN BINDINGS. AFTER THE COATING THE SAMPLES ARE ADDED TO THE WELLS. SECONDLY, THE IL-8 BINDS SPECIFICALLY TO THE CAPTURE ANTIBODY. THIRDLY, THE BIOTINYLATED DETECTION ANTIBODY IS ADDED AND BINDS TO THE IMMOBILIZED IL-8. FINALLY, STREPTAVIDIN-HRP BINDS TO THE BIOTIN AND CATALYSES AN ENZYMATIC COLOUR REACTION, ORIGINATING A BLUE SOLUTION. IMAGE CREATED WITH BIORENDER.COM. ....	36
<b>FIGURE 4.1.</b> <sup>1</sup> H NMR SPECTRA AND PICK ASSIGNMENT OF (A) IBU, (B) SAF, (C) LIN, (D) ME, (E) FLU AND (F) KET. SAMPLES PREPARED IN DMSO-D <sub>6</sub> . ....	43
<b>FIGURE 4.2.</b> <sup>1</sup> H NMR SPECTRA AND SIGNAL ASSIGNMENT OF THEDES (A) SAF:IBU (3:1), (B) SAF:IBU (4:1) (C) LIN:FLU (4:1), (D) LIN:KET (4:1), (E) ME:FLU (4:1) AND (F) ME:KET (4:1). SAMPLES PREPARED IN DMSO-D <sub>6</sub> . ....	46
<b>FIGURE 4.3.</b> NOESY NMR SPECTRA, SIGNAL ASSIGNMENT AND INTERACTIONS ASSIGNMENT OF THEDES ME:KET (4:1). SAMPLES PREPARED IN DMSO-D <sub>6</sub> . ....	48
<b>FIGURE 4.4.</b> POM RESULTS OBTAINED FOR A) LIN:FLU (4:1), B) LIN:KET (4:1), C) ME:FLU (4:1), D) ME:KET (4:1), E) SAF:IBU (3:1), F) SAF:IBU (4:1) AND G) ME:IBU (3:1). ....	49
<b>FIGURE 4.5.</b> SOLUBILITY RESULTS OBTAINED FOR THE NSAIDs IN PURE FORM, IN THEDES FORM AND AS A PHYSICAL MIXTURE. A) SOLUBILITY RESULTS FOR IBU AND IBU CONTAINING SYSTEMS. B) SOLUBILITY RESULTS FOR KET AND KET CONTAINING SYSTEMS. C) SOLUBILITY RESULTS FOR FLU AND FLU CONTAINING SYSTEMS. RESULTS WERE PERFORMED IN TRIPLICATE. <sup>b</sup> VALOUR RETRIEVED FROM [58]. DATA INDICATED AS MEAN + SD (STANDARD DEVIATION). *P<0.05 AND **P<0.01. "##" - STATISTICAL SIGNIFICANCE COMPARED WITH THE CONTROL. "#" - STATISTICAL SIGNIFICANCE BETWEEN DIFFERENT CONDITIONS. ....	50
<b>FIGURE 4.6.</b> PERMEABILITY RESULTS OBTAINED FOR THE NSAIDs IN PURE FORM AND IN THEDES FORM. A) PERMEABILITY RESULTS FOR IBU AND IBU CONTAINING SYSTEMS. B) PERMEABILITY RESULTS FOR KET AND KET CONTAINING SYSTEMS. C) PERMEABILITY RESULTS FOR FLU AND FLU CONTAINING SYSTEMS. RESULTS WERE PERFORMED IN TRIPLICATE. DATA INDICATED AS MEAN + SD. ....	52
<b>FIGURE 4.7.</b> CYTOTOXICITY AND ANTIPROLIFERATIVE VIABILITY CURVES OBTAINED AFTER CACO-2 AND HT29 CELLS, RESPECTIVELY, HAD BEEN EXPOSED TO DIFFERENT CONCENTRATIONS OF A) SAF:IBU (3:1) AND B)	

SAF:IBU (4:1). EC <sub>50</sub> RESULTS INDICATED IN THE GRAPHICS. RESULTS WERE EXPRESSED RELATIVELY TO THE CONTROL AS THE MEAN ± SD OF THREE INDEPENDENT EXPERIMENTS PERFORMED IN TRIPLICATE. ....	56
<b>FIGURE 4.8.</b> LDH RELEASED BY HT29 CELL LINE AFTER BEING EXPOSED TO DIFFERENT CONCENTRATIONS OF A) ME:IBU (3:1), B) SAF:IBU (3:1) AND C) SAF:IBU (4:1). RESULTS WERE OBTAINED FROM THREE INDEPENDENT EXPERIMENTS PERFORMED IN DUPLICATE. DATA INDICATED AS MEAN ± SD. ....	58
<b>FIGURE 4.9.</b> INTRA ROS RESULTS OBTAINED FOR THE SAF:IBU (3:1) AND SAF:IBU (4:1) IN THEDES FORM AND THE RESPECTIVE INDIVIDUAL COMPOUNDS AT THE SAME CONCENTRATION PRESENT IN THEDES. RESULTS WERE OBTAINED FROM THREE INDEPENDENT EXPERIMENTS PERFORMED IN TRIPLICATE. DATA INDICATED AS MEAN ± SD. ....	59
<b>FIGURE 4.10.</b> INTRA ROS RESULTS OBTAINED FOR THE A) ME:IBU (3:1) IN THEDES FORM AND THE RESPECTIVE INDIVIDUAL COMPOUNDS [B) ME AND C) IBU] AT THE SAME CONCENTRATION PRESENT IN THEDES. RESULTS WERE OBTAINED FROM THREE INDEPENDENT EXPERIMENTS PERFORMED IN TRIPLICATE. DATA INDICATED AS MEAN + SD. ****p<0.0001, AS THE STATISTICAL SIGNIFICANCE COMPARED WITH THE CONTROL. ....	59
<b>FIGURE 4.11.</b> CONCENTRATION OF IL-8 (PG/MG PROTEIN) AFTER 24H OF EXPOSER TO A) THEDES SAF:IBU (3:1), SAF:IBU (4:1) AND ME:IBU (3:1) AND TO THE RESPECTIVE INDIVIDUAL COMPOUNDS (B). RESULTS WERE PERFORMED IN TRIPLICATE. DATA INDICATED AS MEAN + SD. ....	61
<b>FIGURE 4.12.</b> RESULTS OBTAINED FOR SAF:IBU (3:1), SAF:IBU (4:1), ME:IBU (3:1) AND THE RESPECTIVE INDIVIDUAL COMPOUNDS REGARDING APOPTOSIS VIA CASPASE-3. RESULTS WERE PERFORMED IN TRIPLICATE. ....	62
<b>FIGURE A.1.</b> HSQC NMR SPECTRA AND SIGNAL ASSIGNMENT OF THEDES (A) SAF:IBU (3:1), (B) SAF:IBU (4:1) (C) LIN:FLU (4:1), (D) LIN:KET (4:1), (E) ME:FLU (4:1) AND (F) ME:KET (4:1). SAMPLES PREPARED IN CHLOROFORM-D. ....	80
<b>FIGURE A.2.</b> COSY NMR SPECTRA AND SIGNAL ASSIGNMENT OF THEDES ME:FLU (4:1). SAMPLE PREPARED IN CHLOROFORM-D. ....	80
<b>FIGURE A.3.</b> NOESY NMR SPECTRA, SIGNAL ASSIGNMENT AND INTERACTIONS ASSIGNMENT OF THEDES (A) SAF:IBU (3:1), (B) SAF:IBU (4:1) (C) LIN:FLU (4:1), (D) LIN:KET (4:1) AND (E) ME:FLU (4:1). SAMPLES PREPARED IN DMSO-D <sub>6</sub> . ....	83
<b>FIGURE A.4.</b> ANTIPROLIFERATIVE AND CYTOTOXIC GRAPHIC RESULTS OBTAIN AFTER HT29 AND CACO-2 CELLS, RESPECTIVELY, HAD BEEN EXPOSED TO DIFFERENT CONCENTRATIONS OF A) IBU, B) KET, C) FLU, D) LIN, E) SAF, F) LIN:KET (4:1), G) LIN:FLU (4:1), H) ME:KET (4:1) AND I) ME:FLU (4:1). EC <sub>50</sub> (EFFECTIVE CONCENTRATION - CONCENTRATION NECESSARY TO DECREASE 50 % OF CELL VIABILITY) RESULTS INDICATED IN THE GRAPHICS. RESULTS WERE EXPRESSED RELATIVELY TO THE CONTROL AS THE MEAN ± SD OF THREE INDEPENDENT EXPERIMENTS PERFORMED IN TRIPLICATE. ....	84
<b>FIGURE A.5.</b> DETERMINATION OF OPTIMAL CELL CONCENTRATION TO THE LDH RELEASE ASSAY. THE OPTIMAL CONCENTRATION IS OBTAINED WHEN THE LOW CONTROL HAS AN ABSORBANCE VALUE MINOR THAN 0,8 AND WHEN THE GREATEST DIFFERENCE BETWEEN THE ABSORBANCE OF THE HIGH CONTROL AND LOW CONTROL IS OBSERVABLE. IN THIS CASE, THE OPTIMAL CELL CONCENTRATION IS AT 2.5 x 10 <sup>5</sup> CELL/ML. RESULTS WERE PERFORMED IN TRIPLICATE. ....	85
<b>FIGURE A.6.</b> IL-8 CALIBRATION CURVES OBTAINED WITH THE ELISA ASSAY FOR BOTH PLATES PREPARED. ABS MEASURED OBTAINED BY THE SUBTRACTION OF ABS (450 NM) MINUS ABS (620 NM). RESULTS WERE OBTAINED FROM AN EXPERIMENT PERFORMED IN TRIPLICATE. ....	85
<b>FIGURE A.7.</b> BSA CALIBRATION CURVE OBTAINED USING THE BRADFORD ASSAY. RESULTS WERE OBTAINED FROM AN EXPERIMENT PERFORMED IN TRIPLICATE. ....	86



## LIST OF TABLES

<b>TABLE 3.1.</b> FREEZING CULTURE MEDIUM AND CRYOPROTECTANT AGENT VOLUME TO FREEZE HT29 AND CACO-2 CELL LINES. ....	31
<b>TABLE 4.1.</b> DIFFERENT THEDES PREPARED. <sup>A</sup> VALOUR RETRIEVED FROM [138] .....	39
<b>TABLE 4.2.</b> SOLUBILITY RESULTS OBTAINED FOR NSAIDS IN PURE FORM, IN THEDES FORM AND AS A PHYSICAL MIXTURE. RESULTS WERE PERFORMED IN TRIPLICATE. DATA INDICATED AS MEAN + SD. <sup>B</sup> VALOUR RETRIEVED FROM [58]. ....	51
<b>TABLE 4.3.</b> PERMEABILITY RESULTS AND DIFFUSION COEFFICIENTS OBTAINED FOR THE NSAIDS IN PURE FORM AND IN THEDES FORM. RESULTS WERE PERFORMED IN TRIPLICATE. DATA INDICATED AS MEAN + SD. <sup>B</sup> VALOUR RETRIEVED FROM [58]. ....	53
<b>TABLE 4.4.</b> CYTOTOXICITY AND ANTIPROLIFERATIVE RESULTS OBTAINED FOR THEDES AND CORRESPONDING INDIVIDUAL COMPOUNDS. THE RESULTS ARE EXPRESSED IN TERMS OF EC <sub>50</sub> AND CORRESPONDING SELECTIVITY INDEXES. RESULTS WERE OBTAINED FROM THREE INDEPENDENT EXPERIMENTS PERFORMED IN TRIPLICATE. <sup>C</sup> VALUES RETRIEVED FROM [60]. <sup>D</sup> VALUE RETRIEVED FROM [56]. NC - NOT CALCULATED. DATA INDICATED AS MEAN ± SD. ....	55



## GLOSSARY

<b>5-FU</b>	5-fluorouracil
<b>AAPH</b>	2,2'-azobis(2-amidinopropane) dihydrochloride
<b>APC</b>	Adenomatous polyposis coli
<b>APIs</b>	Active pharmaceutical ingredients
<b>BCS</b>	Biopharmaceutical classification system
<b>BSA</b>	Bovine serum albumin
<b>CAC</b>	Colitis-associated cancer
<b>COSY</b>	Correlated spectroscopy
<b>COX</b>	Cyclooxygenase
<b>CPA</b>	Cryoprotectant agent
<b>CRC</b>	Colorectal cancer
<b>COVID-19</b>	Coronavirus disease 2019
<b>DAN</b>	2,3-Diaminonaphthalene
<b>DCF</b>	Dichlorofluorescein
<b>DCFH</b>	Dichlorofluorescin
<b>DCFH-DA</b>	dichlorofluorescin-diacetate
<b>DES</b>	Deep eutectic systems
<b>DMEM</b>	Dulbecco's Modification Eagle's Medium
<b>DMSO</b>	Dimethyl sulfoxide
<b>DNA</b>	Deoxyribonucleic acid
<b>DPBS</b>	Dulbecco's phosphate-buffered saline
<b>EC<sub>50</sub></b>	Effective concentration
<b>ECM</b>	Extracellular matrix

<b>ELISA</b>	Enzyme-linked immunosorbent assay
<b>EMT</b>	Epithelial-mesenchymal transition
<b>FBS</b>	Fetal bovine serum
<b>FDA</b>	Food and Drug Administration
<b>Flu</b>	Flurbiprofen
<b>FTIR</b>	Fourier transform infrared spectroscopy
<b>GC-MS</b>	Gas chromatography coupled with mass spectroscopy
<b>HBA</b>	Hydrogen bond acceptor
<b>HBD</b>	Hydrogen bond donor
<b>HETE</b>	5-Hydroxyeicosatetraenoic acid
<b>HMBC</b>	Heteronuclear multiple bond correlation
<b>HPLC</b>	High-performance liquid chromatography
<b>HRP</b>	Horse radish peroxidase
<b>IBD</b>	Inflammatory bowel diseases
<b>IBU</b>	Ibuprofen
<b>IL</b>	Interleukin
<b>ILs</b>	Ionic liquids
<b>Ket</b>	Ketoprofen
<b>LDH</b>	Lactate dehydrogenase
<b>Lin</b>	Linalool
<b>LV</b>	Leucovorin
<b>Me</b>	Menthol
<b>MET</b>	Mesenchymal-epithelial transition
<b>MMP</b>	Matrix metalloproteinase
<b>MMR</b>	Mismatch repair
<b>MTS</b>	3-(4,5-dimethylthiazol-2-yl)-5-(3-carboxymethoxyphenyl)-2-(4-sulfophenyl)-2H-tetrazolium
<b>NADH</b>	Nicotinamide-adenine dinucleotide
<b>NF-κB</b>	Nuclear factor-κB
<b>NMR</b>	Nuclear magnetic resonance spectroscopy



<b>NOESY</b>	Nuclear Overhauser effect spectroscopy
<b>NSAIDs</b>	Nonsteroidal anti-inflammatory drugs
<b>PBS</b>	Phosphate-buffered saline
<b>PES-U</b>	Polyethersulphone
<b>PG</b>	Prostaglandin
<b>PGE2</b>	Prostaglandin E2
<b>PLK1</b>	Polo-like kinase 1
<b>POM</b>	Polarized optical microscope
<b>PS</b>	Penincilin-strepmycin
<b>RNA</b>	Ribonucleic acid
<b>RNS</b>	Reactive nitrogen species
<b>ROS</b>	Reactive oxygen species
<b>RPMI</b>	Roswell Park Memorial Institute
<b>RT</b>	Room temperature
<b>Saf</b>	Safranal
<b>SD</b>	Standard deviation
<b>SI</b>	Selectivity index
<b>STAT3</b>	Signal transducer and activator of transcription 3
<b>TF</b>	Tissue factor
<b>TGF</b>	Transforming growth factor
<b>THEDES</b>	Therapeutic deep eutectic systems
<b>TMB</b>	3,3',5,5'-Tetramethylbenzidine
<b>TMS</b>	Tetramethylsilane
<b>TNF-<math>\alpha</math></b>	Tumour necrosis factor- $\alpha$
<b>TRPM8</b>	Transient receptor potential melastatin 8
<b>VEGF</b>	Vascular endothelial growth factor
<b>WHO</b>	World Health Organization



## INTRODUCTION

### 1.1. Modern World and the Cancer Challenge

Cancer is the second leading cause of morbidity and mortality after cardiovascular diseases, and it is estimated to become the leading cause of premature death in this century [1]. In 2018, 18.1 million new cancer cases and 9.6 million cancer deaths were estimate to occur, and this numbers are expected to increase up to 24.1 million by 2030 and to 29.5 million by 2040 [1,2]. A. S. Ahmad *et al.* concluded that 50 % of adults currently with less than 65 years will be diagnosed with cancer during their live [3].

These increasing cancer numbers and the growing of regional inequalities in tumour types are primarily due to countries' socioeconomical development, including poor lifestyle choices, hygiene levels, environmental pollution, spread of transmitted diseases and the economic resources available for medicine [2]. Additionally, under the current COVID-19 (Coronavirus disease 2019) pandemic cancer healthcare has been postponed to avoid patient's exposure to COVID-19 in hospitals, making virtual consulting and reschedule surgeries. Moreover, patients with COVID-19 symptoms are advised to stay at home instead of going to the treatments and most of the treatments were altered to non-intravenous therapies (oral, subcutaneous regiments or stop completely the treatment) to avoid dislocations to the hospitals and possible cytotoxic complications that may require hospital admission [4].

The main avoidable cancer risk factors that contribute to 70-95 % of cancers development are infections enhanced by biological agents, exposure to synthetic chemicals during work or through ingesting of products, exposure to sunlight, poor diet, overweight, tobacco and alcohol consumption. On the other hand, family inheritance and ageing are unavoidable cancer risk factors [2].

In terms of mortality, the countries more affected will be the low- and middle-income countries, since they will not be able to deal with costs associated with the disease [2].

In Europe cancer follows the global tendency, being the second most common cause of death and the most frequent illness of noncommunicable diseases [2]. The main causes that contribute for these outcome include: 1) industrialized environment, 2) high urbanization and a high age distribution, with continuous exposure to carcinogens and medicines, 3) chronic exposure to particulate matter and other pollutants, and 4) the implementation of early

detection and screening programs that increase the number of diagnosed cancers due to early detection [2].

Europe also present high differences in tumour types across European countries, mainly because of different environments and occupational exposure and due to differences on the budgets that the countries dispense on healthcare [2].

In 2018, Europe spent in total €199 billion in cancer. From these, cancer health expenditure accounted for €103 billion, being €32 billion of which used to buy cancer drugs [5,6]. The total productivity loss was €70 billion, €50 billion due to premature death and €20 billion for morbidity [5]. In United States, the health care expenditures are four times higher for cancer patients than for individuals without cancer, and it is expected to increase dramatically by 2030, increasing from \$183 billion in 2015 to \$246 billion in 2030 (an increase of 34 %), based only on the aging and growth of the United States population [7,8].

Between 1995 and 2018, cancer incidence increased by 50 %, from 2.1 million to 3.1 million cases only in Europe. Fortunately, cancer mortality only increased 20 %. However, the amount of money spent on cancer care doubled, mainly due to the triplicate of costs on cancer drugs between 2005 and 2018 [5,6]. However, due to progresses in modern medicine, productivity loss from premature deaths decreased [5].

Because of the increasing cancer care costs, cancer patients tend to delay the necessary medical care and do not purchase the medication required, increasing adverse health consequences [7]. These expenses related with cancer can include treatment costs, the travel needed to make the treatments and personal care costs [9]. Additionally, cancer patients that live in rural areas have increased costs related with accessing healthcare facilities, associated with an increased difficult to maintain work and life balance due to travels and long periods away from home [10].

There are still large country differences in terms of access to new cancer medicines mainly due to countries' economy [5]. That is why there is the need to find alternatives equal or more effective than the cancer drugs now available, but with lower costs associated [5,7].

Although economic costs are a critical factor in cancer patients' life, the emotional impact that cancer provokes in patients and their families is equally important. This emotional impact can have two sources, the cancer diagnostic itself and the economic distress that it brings associated. These two effects of cancer can be influenced by the employment circumstances and salary of the patients, and the family and friends support [9].

The quality of life of cancer patients affects the cancer prognosis and involves not only their physical health/disease but also their psychological, social/family and environmental wellbeing, since there is a direct relation between stress and immune system [11,12].

Since cancer is detected until the treatment is concluded, a lot of changes occurs on the patient's life that has a great impact on his/her quality of life and adjustment. One of those adjustments is in terms of family and marital life, since couples need to adapt themselves in order to overcome the new changes that they face. This is a huge problem specially for patients with breast and prostate cancer that suffer feminine and masculine modifications due to their disease [12].

In order to decrease cancer deaths and improve patients quality of life, the search for specific biomarkers associated with signalling pathways involved in carcinogenesis and the analysis of cancer epidemiology, can allow an earlier diagnostic and more specific therapeutic targets [2,13]. After the early diagnostic, the "watch and wait" strategy can be applied to minimize the risks and increase patients' quality of life, since it gives time to study the tumour behaviour, which is important to decide a better clinical strategy.

### **1.1.1. Cancer**

Cancer remains has one of the major health problems worldwide [14]. It is characterized by a multistep process, called carcinogenesis, that leads to genetic alterations, allowing the acquisition of important functional capacities for survival, unregulated proliferation and dissemination of cells [15–17]. These functions are a result of several factors, such as genomic instability and consequent aleatory mutations, an inflammatory state promoted by immune cells, and some will lead to tumour development [15,16].

Cancer is a complex disease with highly proliferative characteristics that comprehends three phases, the initiation phase that is followed by the promotion and the progression phase.

Carcinogenesis initiates with a mutation on a gene that regulates cell proliferation, differentiation, and/or survival within a cell, acquiring the capacity to divide and propagate this mutation [18,19]. The mutations that enhance cancer, can be spontaneous (replication defects) or chemically and physically induced, which promote the production of reactive oxygen species (ROS) [17]. Within the key target genes that can be mutated to initiate carcinogenesis, there are proto-oncogenes, that control cell division, and tumour suppressor genes, which are involved in monitorization and repair of deoxyribonucleic acid (DNA) mutations, and initiation of programmed cell death [18]. This first mutation is the initiation step and gives rise to an abnormal single cell [18,19].

Then, the mutated cell is stimulated to divide by growth factors and factors that promote mitosis, and originates a mass of mutated cells [18,19]. This moment of cell division is the promotion phase and does not involve the acquisition of new mutations, only epigenetic modifications may occur, such as DNA methylation and histone acetylation [18,20].

During clone multiplication, the new formed cells acquire more mutations giving rise to different sets of mutations within the clones. This phenomenon characterizes the progression phase and continues to occur during the tumour life, being responsible for the great heterogeneity that is present on malignant neoplasms [18].

Some of the new mutations originated during tumour progression will confer a selective advantage to some of its cell and, consequently its descendants will be dominant in the tumour population. Consequently, a clonal selection will occur since a new set of tumour cells will arise with improved characteristics, such as increased growth rate, survival, invasion, or metastasis. This clonal selection will continue during tumour development, increasing even more tumour growth rate and tumour malignancy, and often associated to tumour drug resistance [19].

These cancer cells acquired capabilities are designated by hallmarks, which include the maintenance of proliferative signals, the insensitivity to growth suppressors, tissue invasion

and metastasis, immortality, induction of angiogenesis, resist cell death, avoid immune destruction and cellular energy metabolism reprogramming [15,16,18].

During tumour progression, cells suffer morphology changes and start to behave differently from the normal ones [18,19]. The alterations that occur during the initial phase of cancer development give rise to a dysplasia, that include alterations in size and shape, loss of ordered tissue architecture and characteristics of systematic differentiation. Normally, dysplasia is not visible, however, in the case of intestinal adenomas, a dysplastic cell mass is observable (**Figure 1.1**) [18].

Dysplasia can be classified into low-grade or high-grade dysplasia, depending on the risk of further progression to invasive tumour, that will occur due to continue accumulation of mutations during cancer progression. Tumours can be originated from different cell types, such as those from nervous tissue, muscle, connective tissue, and epithelium. In the case of epithelial-originated tumours the increased divergency from normal cells appearance and tissue architecture, gives rise to a carcinoma [18].

When an epithelial tumour evolves to a carcinoma, infiltration through the basement membrane into the stroma occurs. This will give cells access to blood and lymphatic vessels, and capacity to invade adjacent and distant tissues (**Figure 1.1**) [18]. This infiltration moment differentiates a benign tumour from a malignant one, since benign tumour are confined to its original location and the malignant tumour are able to invade and disseminate to other locations. Only malignant tumours are referrer as cancer and it is their capacity to metastasize that makes cancer so difficult to be treated [19,21].

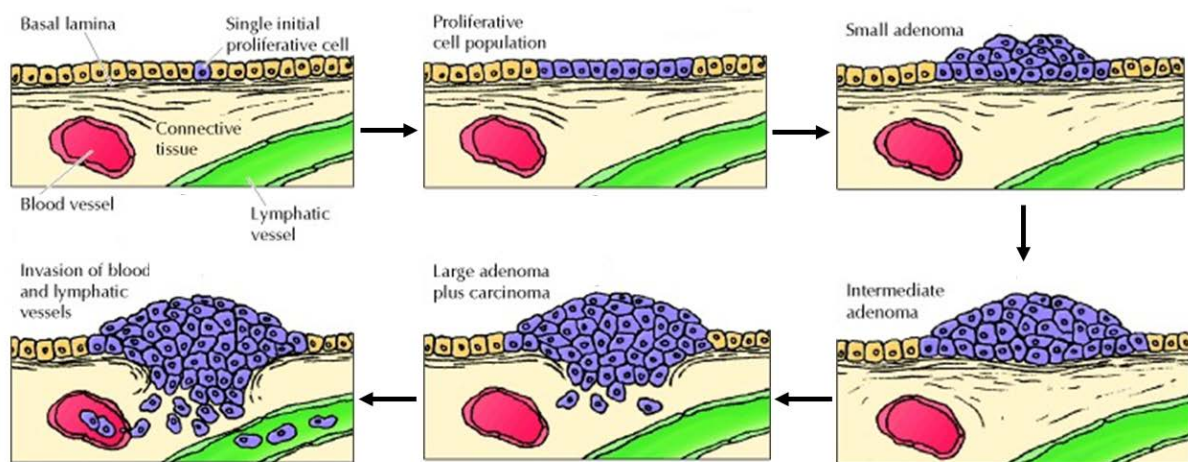


**Figure 1.1.** Tumour progression during colon carcinoma development. A single colon epithelial mutated cell starts to proliferate and transmits its mutation to daughter cells. During cell proliferation a small benign adenoma is formed. Consequent rounds of clonal selection leads to adenoma growth and increased proliferative potential. The benign adenoma then evolves to a malignant carcinoma due to invasion of the tumour cells through the basement membrane into the connective tissue. After that, cancer cells continue to multiply and propagate in the connective tissue of the colon wall. Ultimately, cancer cells penetrate the colon wall and invade the surrounding organs, blood and lymphatic vessels, allowing cancer cells to metastasize to all the body (Adapted from [19]).

In order for cells to be able to invade, new capabilities need to be acquired: cells need to be able to i) digest, disrupt and penetrate the basement membrane, through the secretion of protease that digest extracellular components, ii) break free of epithelial attachments to the basement membrane and between cells (loss of E-cadherin and some integrins), and iii)

increase their motility [18,19]. These properties are acquired due to epithelial-mesenchymal transition (EMT), meaning that epithelial cells behave as connective tissue cells [18].

Epithelial cells are responsible for cell-to-cell cohesion which is essential to maintain integrity of multicellular organisms' tissues. This acts as a selective barrier for the regulation of internal environment which has a very confined and immobile behaviour. However, for more flexible structures and functions, mesenchymal cells are needed. Mesenchymal cells present a highly motile and invasive phenotype, and are responsible for the production of an extracellular matrix (ECM), providing structure and support to epithelial cells. EMT increases flexibility during embryogenesis, wound healing and regeneration. Unfortunately, EMT is also observed during tumour invasion, spread and metastization processes. Additionally to EMT, epithelial cells can also migrate and spread during tumour development via collective migration, where epithelial cells move as a group that is physically and functionally connected. Although during collective migration cell-to-cell interactions are maintained, some EMT characteristics are observed, like modification of the ECM and acquisition of an invasive and motile phenotype. In epithelial cancers, EMT allows tumour cells to leave the primary tumour site, to migrate and invade neighbouring tissues and blood vessels, initiating the metastatic spread (**Figure 1.2**) [21].

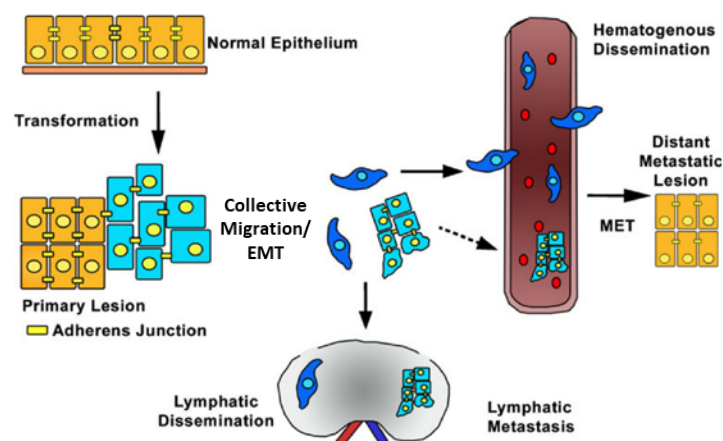


**Figure 1.2.** EMT enhances metastasis. During tumour formation the genetic and epigenetic modifications that tumour cells suffer promotes EMT and collective migration. These two invasive mechanisms enable tumour cells to detach from their surrounding cells, invade through the basement membrane and migrate to other tissues as a single cell (dark blue) or as a cluster of cells (light blue). This invasion is the start of the metastatic dissemination and spread to the lymphatic nodes and blood vessels. The migration to blood vessels enables the development of distant metastasis, where cells once again express an epithelial phenotype due to undergo mesenchymal-epithelial transition (MET) (Adapted from [21]).

Cancer cells are also able to enhance the development of new blood vessels through angiogenesis. Angiogenesis is a fundamental step to maintain the growth of a tumour when it is composed by more than a million cells, because, when a tumour becomes this large, malignant cells have low supply of nutrients and oxygen due to their distance to blood vessels. The new blood vessels are formed in response to growth factors secreted by cancer cells, that promote proliferation of endothelial cells present in the walls of capillaries in neighbouring tissue, causing the extension of capillaries into the tumour. These capillaries are also

important for metastasis, due to the fact that they can be easily penetrated by tumour cells, enabling malignant cells to enter the circulatory system and start the metastatic process [19].

#### **1.1.1.1. The role of inflammation on cancer development**

Focusing on the involvement of inflammation in tumour progression, the tumour acts like a wound that does not heal. During normal tissue damage, cell proliferation occurs to allow tissue regeneration, and immune inflammatory cells are recruited for a short period of time, to clean dead cells and cellular debris. However, in tumours and in chronic inflammation, immune inflammatory cells persist, due to a failure on the mechanisms that solve the inflammatory response or a persistence of the initiating factors, thus DNA damaged proliferating cells continue to multiply, giving rise to tissue pathologies, like abnormal angiogenesis and tumorigenesis [16,22,23]. This inflammatory response is an enhancer of tumorigenesis and tumour progression and facilitates the acquisition of cancer hallmarks through the provision of proliferative signals, survival factors, proangiogenic factors and enzymes that alter de ECM to facilitate angiogenesis, invasion and metastasis [16,23]. In addition, the inflammatory cells release certain molecules, such as ROS and reactive nitrogen species (RNS), that are normally necessary to fight infections, but in tumours they react to form peroxynitrite that cause mutations in proliferating cells, resulting in genomic modifications such as point mutations, deletions or rearrangements, increasing the genomic instability and resulting in higher malignancies [16,22]. Macrophages and T lymphocytes may also secrete tumour necrosis factor- $\alpha$  (TNF- $\alpha$ ) and macrophage migration inhibitory factor that are also responsible for DNA damage [23]. Thus, for a cancer to form, it has to sustain cell proliferation in the presence of inflammatory cells, growth factors and DNA damage agents [22].

These inflammatory cells are a part of the cancer, being recruited by cytokines and chemokines produced by the tumour, and can act as tumour-antagonists or tumour-promoters. Chemokines are expressed by tumours, tumour-associated leukocytes and platelets, not only to attract inflammatory cells but also to increase tumour growth and progression due to their involvement in the regulation of angiogenesis and metastasis [22,23]. The growth, migration and differentiation of the tumour microenvironment cells, such as neoplastic cells, fibroblasts and endothelial cells, are, hence, influenced by inflammatory cells, chemokines and cytokines [22].

One of the best examples of cancers associated with chronic inflammation is colorectal cancer (CRC), when it develops in the presence of inflammatory bowel diseases (IBD), such as chronic ulcerative and Crohn's disease, which is characterized by a persistent inflammatory response to luminal bacteria or to continual mucosal danger signals [22,24].

#### **1.1.2. Colorectal Cancer**

Cancer of the colon and rectum, or simply called colorectal cancer, is the third cancer with more incidence and the second most mortal, being expected 1.8 million new CRC cases and 881.000 deaths in 2018, representing about 1 in 10 cancer cases and deaths [1]. CRC appears sporadically, being only a few cases inherited, and is present mainly in people with more than 65 years old [25]. External causes, such as dietary patterns, obesity, lifestyle factors,



environmental and food mutagens, intestinal commensals and pathogens, and chronic intestinal inflammation, that precedes tumour development, are the main risks factors for the development of CRC [1,25-27]. The intestine is populated by countless bacterial strains and inflammatory reactions are linked to microbial responses, so any alterations in the number of bacteria (dysbiosis) can cause an inflammatory response and facilitate cancer development [24].

There are different types of CRC, being Colitis-associated cancer (CAC) the one developed during IBD [27-29]. This type of cancer is difficult to treat and more than 50 % of patients die from it [27].

The development of CAC and sporadic CRC involve the formation of polyps, adenomas and carcinomas, in a multistep process involving successive losses of genes and signalling pathways mutations, like those involving  $\beta$ -catenin, K-ras, p53, transforming growth factor (TGF)- $\beta$  and DNA mismatch repair (MMR) proteins, although the time of p53 mutation, adenomatous polyposis coli (APC) inactivation and K-ras activation can be different in CAC and CRC [25,27,28]. Additionally, the development of CAC also requires chronic inflammation, in which mucosal production of proinflammatory cytokines increases in a process mediated by nuclear factor- $\kappa$ B (NF- $\kappa$ B) [27,28]. Moreover, chronic inflammation is also responsible for oxidative stress that leads to cellular damages, contributing to colorectal carcinogenesis [29]. Nevertheless, IBD non-associated CRC also induces an inflammatory response, exhibiting inflammatory infiltration, due to constitutive activation of transcription factors of multiple inflammatory pathways, and increased expression of proinflammatory cytokines [27,30].

All the mutations that occur during cancer development promote chromosomal and microsatellite instability. Chromosomal instability is the most common in CRC, resulting in DNA abnormal content and loss of function of important tumour suppressors as APC and p53. Microsatellite instability (where the number of repeated DNA bases in a microsatellite - a short, repeated sequence of DNA - is different from the originally inherited microsatellite) is present in some CRC, normally associated with MMR genes loss of function due to hypermethylation [28,29].

The p53 tumour suppressor is inactivated in a later stage of non-IBD associate CRC, being these inactivation responsible for the conversion of a benign adenoma to an invasive carcinoma, however in CAC development its inactivation is one of the first steps, preventing its actions as inhibitor of abnormal cell proliferation, maintainer of genomic stability, suppressor of transformation and tumorigenesis, and regulator of inflammatory pathways [24,28-30]. Inactivation of p53 also enhances interleukin (IL)-6 signalling (**Figure 1.3**) [30].

Another frequent mutated gene in CRC is KRAS. This gene is activated and promotes the synthesis of pro-inflammatory cytokines and chemokines, like IL-6, prevents apoptosis and promotes invasion (**Figure 1.3**) [30].

Mutations in APC are associated with early development of sporadic CRC, but normally occurs later in CAC [29]. APC is a tumour suppressor that inhibits  $\beta$ -catenin. When APC is mutated  $\beta$ -catenin is activated and can migrate to the nucleus where it acts as a transcription

factor and promotes cellular proliferation [31]. This occurrence is essential for adenoma development (**Figure 1.3**) [27].

$\beta$ -catenin activation is an essential step in all CRC tumorigenesis. However, APC mutation is not the only way to activate  $\beta$ -catenin, other events such as i) activation of the receptor EP2 by prostaglandin (PG), which is produced in acute and chronic inflammation, leads to an increase of  $\beta$ -catenin in the nucleus; ii) mutations in  $\beta$ -catenin itself; iii) some inflammatory pathways influence the casein kinases that control the activation of  $\beta$ -catenin; iv) and there are proinflammatory signals that activate NF- $\kappa$ B pathway, promoting  $\beta$ -catenin activation [27].

$\beta$ -catenin activation is also regulated by the Wnt signalling. The Wnt signalling pathway regulates the nuclear localization of  $\beta$ -catenin and maintain the normal homeostasis in intestinal stem cells. When Wnt is inactivated,  $\beta$ -catenin binds to a protein complex for proteosomal degradation. When the pathway is active (through the presence of Wnt ligand or mutation in the pathway genes), the protein complex does not bind to  $\beta$ -catenin and  $\beta$ -catenin accumulates in the cytoplasm and migrates into the nucleus, where it binds to transcription factors, activating transcription of target genes and increasing proliferation, differentiation, migration and adhesion of colonic cells [32,33].

The Wnt signalling is not only involved in the early stages but it also participates in the invasive capacity of metastasis, being the activation of  $\beta$ -catenin essential for the transcription of aggressiveness, invasiveness and migration tumour genes [34].

As mentioned earlier, the intestinal microbiome is associated with CRC development and one of its roles is related with tumour-infiltrating microbes that induce IL-23 production, by myeloid progenitors, which increase the expression of pro-tumorigenic cytokine IL-17, that promotes epithelial cells growth and survival, initiating tumour development in sporadic CRC [24].

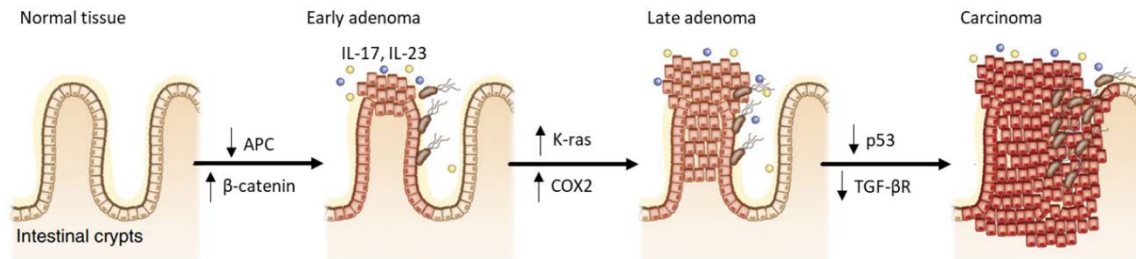
The inflammatory cells responsible for colitis and the constitutive activation of NF- $\kappa$ B also generate ROS and RNS. In addition, neutrophils and macrophages, involved in acute inflammation, generate free radicals and more prooxidant molecules. These free radicals are capable of targeting DNA, ribonucleic acid (RNA), proteins and lipids, affecting several metabolic processes, such those involved in tumour suppressing, and induce inflammatory and carcinogenic genes, leading to cancer [24,29].

For an early-stage adenoma evolve to a carcinoma and a metastatic carcinoma, activation of oncogenes KRAS and B-Raf and inactivation of tumour suppressors TGF- $\beta$  receptor, p53 and proapoptotic protein Bax must occur. This transition also involves increased expression of cyclooxygenase 2 (COX2) and mutations in DNA integrity checkpoints genes, leading to chromosome instability, which results in a great number of different mutations observed in CRC and, consequently, to resistance to therapy [27].

COX2 is upregulated in colorectal tumours, specially sporadic CRC, and acts as a pro-tumorigenic, inhibiting apoptosis, through i) the increasing expression of the anti-apoptotic protein Bcl-2, ii) activating indirectly  $\beta$ -catenin pathway, iii) promoting survival and proliferation, iv) inducing angiogenesis, by the production of vascular endothelial growth factor (VEGF), v) increasing tumour dissemination, by the alteration of cells adhesive

properties, and vi) indirectly producing free radicals [27–29]. COX2 is responsible for the synthesis of PG, and high levels of PG, specially prostaglandin E2 (PGE2), are observed in colon adenocarcinomas (**Figure 1.3**) [27].

#### A. Sporadic CRC



#### B. CAC

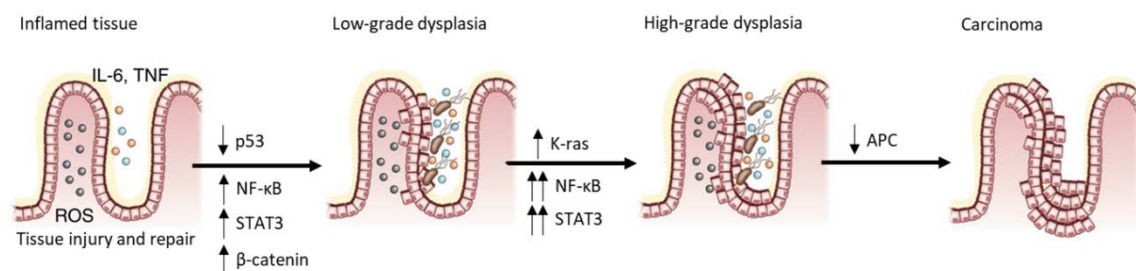


**Figure 1.3.** Inflammatory process associated with CRC and CAC development. **(A)** In sporadic CRC, one of the first events that occur is the mutation in the gene encoding APC, associated with the Wnt pathway, that leads to the activation of  $\beta$ -catenin and consequently to adenoma development. The APC mutation is also associated with loss of tight junctions which allows microbial invasion from the intestinal microbiome, inducing IL-17 and IL-23 production. For an early-stage adenoma evolve to a carcinoma, activation of oncogene KRAS and inactivation of tumour suppressors TGF- $\beta$  receptor and p53 must occur. This transition also involves increased expression of COX2. **(B)** In CAC, chronic inflammation is constant and mucosal production of proinflammatory cytokines increases in a process mediated by NF- $\kappa$ B that is responsible for  $\beta$ -catenin activation. Mutation on the gene that encode p53 is one of the first steps in CAC and is associated with increasing production of IL-6. IL-6 consequently activates transducer and activator of transcription 3 (STAT3) that extends NF- $\kappa$ B activation. Tumour necrosis factor (TNF) is another tumour-promoting cytokine produced in the initial inflammatory response and increases vascular permeability that promotes the microbial invasion, and consequently further enhances the inflammatory response with increasing activation of NF- $\kappa$ B and STAT3. Moreover, chronic inflammation and the constant activation of NF- $\kappa$ B is also responsible for oxidative stress that leads to DNA damage, resulting in mutations of the gene that encodes APC and the development of carcinoma (Adapted from [24]).

CRC and CAC are infiltrated by multiple types of immune cells, such as neutrophils, mast cells, natural killers, dendritic cells, tumour-associated macrophages and myeloid progenitors. Cells of the adaptative immunity are also present and have pro- and anti-tumorigenic effects, being T cells required for inflammation, cancer development and tumour progression, but also for anticancer immunity. Some T cells and natural killers are responsible for immunosurveillance, but innate immune cells, B cells and other subtypes of T cells are involved in tumour-promoting inflammation and pro-tumorigenic inflammatory cytokines and chemokines production [27].

Macrophages and dendritic cells produce tumour-promoting cytokines in early stages of tumour development and in later stages cytokines are produced by T cells [27]. Most of these cytokines activate receptors on intestine epithelial cells that activate oncogenic signalling pathways and oncogenic transcription factors, being NF- $\kappa$ B and signal transducer and activator of transcription 3 (STAT3) the most important in colorectal tumorigenesis,

because of their involvement in the activation of multiple genes needed for all the steps that occur during cancer development [27,28]. NF- $\kappa$ B also regulates the promoters of many genes critical for inflammatory processes, such as the proinflammatory cytokines TNF- $\alpha$  and IL-6 and COX2, and plays an anti-apoptotic role through the suppression of caspase-8 activation [24,28].

The IL-6 is produced by macrophages and cancer-associated mesenchymal stem cells and has a fundamental role in the start and progression of CAC, being able to stimulate proliferation of premalignant epithelial cells, protects them from apoptosis, promotes tumour growth and is required after injury for tissue protection and regeneration. IL-6 also activates STAT3, which protects and stimulates the regeneration of the gastrointestinal epithelium, increases expression of antiapoptotic genes (like Bcl-2), proliferative genes, VEGF, which encodes a proangiogenic factor, and extends activation of NF- $\kappa$ B (**Figure 1.3**) [24,27,30].

Another interleukin associated with tumour development, progression, angiogenesis, metastases and therapeutic resistance is IL-8. IL-8, in conjugation with other anti-inflammatory cytokines, are potent chemoattractants for neutrophils and natural killer cells thus promoting healing processes but also stimulating inflammatory diseases such as IBD. It has been reported that IL-8 is significantly upregulated by NF- $\kappa$ B pathway in the CRC tumour and in its microenvironment and its upregulation increases the activation of NF- $\kappa$ B [35,36].

TNF is another tumour-promoting cytokine produced in the initial inflammatory response. It acts as a promoter of inflammation, angiogenesis and tumour dissemination, due to being responsible for the production of other cytokines, chemokines and endothelial adhesion molecules, and increase vascular permeability that allows the recruitment of leukocytes (**Figure 1.3**) [24,27].

The inflammation process and immune cells are also involved in metastasis. TGF- $\beta$  is the major regulator of EMT. In EMT, tumour cells lose their cell-cell adhesion and increase their motility, allowing tumour cells to dissociate from the primary tumour and invade epithelial basal membranes, resulting in blood or lymphatic vessels intravasation. Then, extravasation occurs through invasion of the vascular basement membrane and ECM. These cells metastasize and attach to other organs and re-initiate proliferation [27,30,37,38]. This process is characterized by loss of E-cadherin, the most important molecule for cell-cell adhesion, that is regulated by  $\beta$ -catenin [27,34]. In addition, EMT can be promoted by activation of NF- $\kappa$ B and STAT3 and is also regulated by various proinflammatory cytokines, like TNF- $\alpha$  and IL-6 [27].

EMT is a natural occurring biological process during embryogenesis and organogenesis, but can also be activated under inflammation, during wound healing and tissue repair, and in the occurrence of carcinomas. This process is characterized by the development of apoptosis resistance, capacity to migrate and invade, and production of ECM components by cells [38].

Chemokines can directly promote the migration of tumour cells to blood vessels. Additionally, cytokines, like TNF, increase vascular permeability and facilitate the intra- and extravasation of metastatic cells [27]. TNF- $\alpha$  and TGF- $\beta$  increases the expression of matrix

metalloproteinase (MMP), a proteinase overexpressed in CRC, that allows the degradation of ECM and also facilitates invasion and extravasation of tumour cells [27].

#### **1.1.2.1. Treatment**

The majority of CRC diagnosis are achieved in an advanced stage of the disease, when metastasis already occurred, because when colon cancer starts to develop there are no symptoms and when they appear are not specific, manifesting as general abdominal pain, weight loss and tiredness. The specific symptoms, like intermittent abdominal pain, nausea and vomiting, only appear after bleeding, obstruction or perforation [25].

This late diagnosis decreases the treatment effectiveness and consequently decreases the survival rate [39]. As a consequence of being late diagnosed the first approach to treat CRC in most cases is surgery, but recurrence is frequent which represents a major problem since often ultimately lead to death. For that reason, it is often required the administration of adjuvant therapy.

There are two types of surgery available to treat CRC, laparoscopy (minimally invasive) and open surgery. The laparoscopic method has higher operational costs and longer surgery time, however, it requires half of the hospitalization time compared to open surgery and, because it is less invasive, it has less associated complications, since it reduces blood loss, has better and faster postoperative recovery, has better immune and inflammatory responses and causes less pain [40,41]. Although, laparoscopy seems to be safer, some local conditions like inflammation or adhesion can disable the use of this approach [42].

After surgery, patients can suffer some surgical complications, the most common are prolonged absence of muscle contractions of the intestines, wound infection and abdominopelvic collection. In terms of medical complications, cardiac arrhythmias, respiratory infections and impaired renal function are the most common [43].

There are other treatments available, working as an alternative or complementary to surgery, like radiation and chemotherapy based on biological agents, that target signalling pathways, or chemicals, that damage DNA or inhibit its synthesis [25,27]. The standard treatment for CRC is surgery followed by chemotherapy with 5-fluorouracil (5-FU), leucovorin (LV) and oxaliplatin during 6 months [25]. However, usually, metastatic CRC reveals to be resistant to these conventional therapies [39].

Although, the use of these standard treatment prevents recurrence and reduce tumour size [25,27], they have cytotoxic effects not only on the cancer cells but also on normal cells, leading to a variety of side effects [44].

A better prevention, earlier detection and alternative treatments with less side effects are necessary to have a more efficient treatment and better CRC patient's survival rates [40,45].

Modern medicine has been focusing on the enhancement of the properties of old therapeutics and finding alternative treatments based on products from natural origin, which present a great chemical diversity and unique mechanisms of action, making them valuable for the development of new drugs. Natural products efficacy is linked to their three-dimensional chemical and steric properties that increase efficiency and selectivity towards

specific molecular targets [45]. In addition, the use of these natural occurring compounds should be associated with green processes during their pharmaceutical preparation.

## 1.2. Sustainable Chemistry and Deep Eutectic Systems

Our planet and its natural resources are being damaged and overexploited as a consequence of human progress and development. The solution to overcome some of these problems is the search for alternative energy sources and new solutions for industrial processes. Green Chemistry is a concept created to increase production while at the same time be good for human health and reduce environmental stress [46,47]. It is defined as “the invention, design, and application of chemical products and processes to reduce or eliminate the use and generation of hazardous substances” [47,48].

Green Chemistry is based on twelve principles: i) Prevention (waste prevention), ii) Atom economy, iii) Less hazardous chemical synthesis, iv) Designing safer chemicals, v) Safer solvents and auxiliaries, vi) Design for energy efficiency, vii) Use of renewable feedstocks, viii) Reduce derivatives, ix) Catalyses, x) Design for degradation, xi) Real-time analysis for pollution prevention, xii) Inherently safer chemistry for accident prevention [47].

It is in this pursue for green solvents and systems that Deep Eutectic Systems (DES) arise. DES combine the universality and physicochemical properties of Ionic Liquids (ILs) (high thermal stabilities, low volatility and low vapor pressures) with the principles of Green Chemistry at lower production cost. DES preparation consists in directly combine two or more compounds until a homogeneous liquid is formed, with no need for further purification steps. Therefore, during DES production no waste, no undesired byproducts and no chemical reaction occur, so the yield of the processes and the atom economy can be considered 100 % [49-51]. Another factor used to determine the sustainability of the process is the E-factor (environmental factor), that is calculated by dividing the total waste produced by the total amount of product. For DES an E-factor of 0 is achievable.

Additionally, DES are tailor-made solvents, allowing the preparation of a system with specific characteristics for a certain application [51,52]. The ease of production, lower cost, the tailor-made capability, and biodegradability of the components, makes DES a suitable solvent alternative in a wide range of applications [53].

### 1.2.1. DES

DES are defined as combinations of two or more compounds, that, in a specific molar ratio, present a lower melting point than its individual elements. This phenomena may be attributed to the charge delocalization resultant of the hydrogen bonding between a hydrogen bond donor (HBD) and a hydrogen bond acceptor (HBA), together with steric effects and ionic contributions from the anion and cation [49,50,54].

The interactions that occur during DES formation between the HBA and the HBD originates a new identity with different physical and chemical properties from the individual elements. This is highly dependent on the initial components, entropy changes arising from the intermolecular arrangements, and the chosen molar ratio. The composition also have a

great effect on the physical properties of the DES such as viscosity, thermal behaviour, density, polarity, and conductivity [54–56].

**Figure 1.4** represents a theoretical temperature-concentration phase diagram for a simple binary eutectic system composed by X and Y. The lines AB and BC represent temperatures at which the compounds X and Y respectively begin to crystallize while temperature decreases. Above these lines the compounds are completely liquid. The line DBE is the temperature at which the mixture of X and Y begin to melt and below which the system is solid. The area under ABD represents the liquid mixture of X and Y in equilibrium with solid Y; and the area under BCE represents the liquid mixture of X and Y in equilibrium with solid X. The point B is where the liquid meets the solid, which is nominated by eutectic point, and it corresponds to molar ratio between the two components where a eutectic system can be formed. Therefore, the eutectic system is the situation that when cool downed will not deposit any pure solid X or Y, but will go from a liquid system of X and Y to a solid mixture of X and Y [50,57].

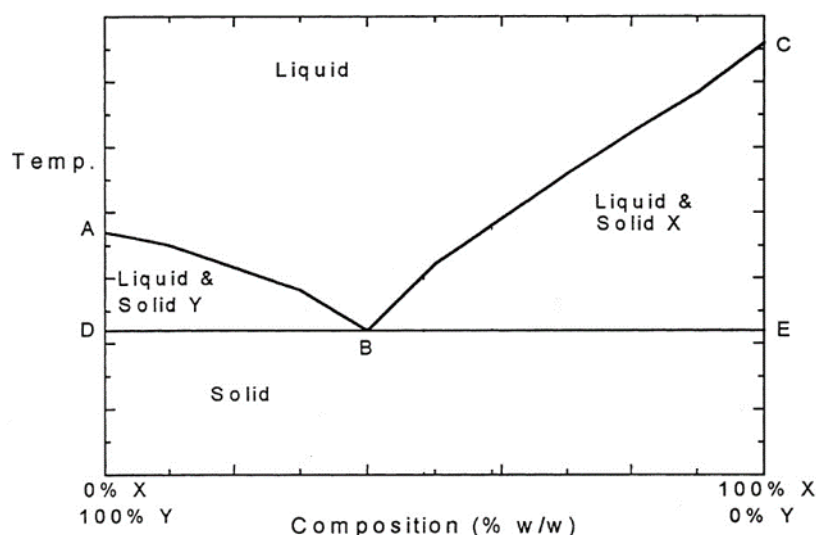


**Figure 1.4.** Theoretical temperature-concentration phase diagram for a binary eutectic system (Adapted from [57]).

From glass and ceramic industries to energy storage devices and pharmaceutical formulations DES have been employed in a so number of applications. On the pharmaceutical field, DES is used as a drug delivery system, as medium for enzymatic reactions, where enzymes are able to maintain their activity, and for drug solubilization [49,54]. Recently, active pharmaceutical ingredients (APIs) were included in DES formulations, giving rise to therapeutic deep eutectic systems (THEDES), which can have a range of bioactivities such as anti-fungal, anti-bacterial, anti-viral and anticancer activities [54].

THEDES have been showing features than can overcome conventional pharmaceutical drugs drawbacks. APIs efficacy is dependent on its transport, solubility, permeability and consequent bioavailability, being these properties a limiting factor for the drug efficiency [52,54]. However, THEDES have been reported as enhancers of solubility of poorly water soluble APIs, increasing its bioavailability and their skin permeation [54].

The permeability of a drug allows its transdermal delivery, an important process for example, to enhance healing efficiency, reduce side effects and avoid the initial liver metabolism. One of the tactics to increase drug permeability is to turn it into a liquid using DES, which reduces crystallization, enhances drug bioavailability and transdermal delivery [54,58]. Additionally, other problem associated with APIs is the existence of polymorphisms in crystalline formulations, that can alter the properties of the drug. To overcome this problem and enhance API solubility and permeability, the development of amorphous formulations, like THEDES, has been studied [52].

Carolina V. Pereira *et al.* and Paul W. Stott *et al.*, observed that it was possible to combine terpenes with ibuprofen as an eutectic system, and that this system promoted the transdermal delivery, since the terpene is a skin permeator enhancer [56,57].

It has been reported that THEDES containing APIs have a greater dissolution rate than the API alone, because they are in a different form, some of them going from a solid to a liquid. Dissolution capacity is dependent on the API physicochemical properties, and results from the disruption of the interaction between the API and the other component of the THEDES when it is dissolved in our physiological medium or in a similar solution, like phosphate-buffered saline (PBS) [54].

Among THEDES therapeutical applications, there have been evidences that the complexation of two or more components as an eutectic entity may represent an important role in the anticancer battle, since it is observed a more acute destruction on cancer cells in comparison with individual components alone. The DES anticancer activity is dependent on their initial compounds, the combination of HBA and HBD, their physical properties, chemical structure, presence of water in the system and the cell type where they are tested [51,54]. One of the mechanisms suggested for this increased destruction is through the disruption of cell membrane, that also increases ROS production which stimulates apoptosis [59].

Furthermore, Carolina V. Pereira *et al* observed that it was possible to combine the terpene limonene with ibuprofen (IBU) as a THEDES formulation, and that these systems presented enhanced and selective anticancer activities, associated with increased IBU solubility [56,57]. In another work, Menthol:Ibuprofen (3:1) as already been described as a DES [60] capable of increasing both IBU solubility and permeability associated with antiproliferative activity [58,60]. Moreover, different THEDES of ibuprofen with the terpenes thymol and menthol were already reported, showing different mechanisms of action, although terpenes structure similarity. Menthol:Ibuprofen (3:1) is capable of increase IBU solubility while THEDES with thymol did not show the same result, additionally thymol based THEDES do not show a specific action towards cancer cells contrary to Menthol:Ibuprofen (3:1), highlighting the tailor-made characteristic of THEDES [60].

For all of the above stated we believe that coupling a natural anticancer agent, like a terpene, with an anti-inflammatory drug as a THEDES formulation can be an important combination to fight cancer, through a specific action against cancer cells associated with an inflammatory state decrease.



### 1.2.2. Terpenes

Terpenes are volatile hydrocarbons that extensively occur in nature, produced by numerous plants and some animals. In plants, terpenes are produced as secondary metabolites in response to stress, acting as infochemicals, attractants or repellents, and at higher concentrations they act as weapons against pathogens due to terpenes high toxicity [61,62].

Terpenes are formed by multiple units of isoprene ( $C_5H_8$ ), that can be linked head to tail to form linear chains, or can be arranged to form rings [61,63]. In addition to isoprene units, some terpenes, the terpenoids, are also formed with oxygen-containing compounds [61,63,64].

Terpenes are used as therapeutics since ancient times because of their high presence in essential oils and easily extraction from plants [63]. They have been described as useful as antimicrobial, antifungal, antiviral, antiallergenic, anti-inflammatory, antihyperglycemic, as immunomodulation agent, but also in the prevention and therapy of cancer [61].

It was reported that consumption of monoterpenes - terpenes that consist only in two units of isoprene ( $C_{10}H_{16}$ ) - can be important in the prevention and therapy of cancers [61,64]. The monoterpene limonene, for example, has already shown chemopreventive and therapeutic effects towards several human cancers, such those from the liver, skin, lung, prostate, pancreatic and colon carcinomas [61].

Terpenes chemopreventive action can occur during the initiation phase of carcinogenesis, avoiding the interaction of cancer-causing agents with DNA, or during the promotion phase, where they inhibit cancer cells development and migration through the induction of apoptosis, re-differentiation and by influencing the molecular mechanisms responsible for cellular functions [61]. One of the mechanisms influenced by terpenes is post-translational isoprenylation of proteins, that consists on the covalent binding of a lipid containing three or four isoprene units to a thiol group of a cysteine side chain of a protein [61,65]. These prenylated proteins are responsible for the regulation of cell growth and transformation, and consequently their disruption inhibit cell growth and cancer development [61].

Terpenes can also act as skin penetration-enhancing agents thus, nowadays, they are used in topical dermal preparations and cosmetics. Furthermore, there are studies proving that the transdermal pathway can be an alternative for antitumour drug administration, a feature safe and clinically acceptable for the usage of lipophilic/hydrophobic and hydrophilic drugs, both transdermal enhanced by terpenes [61,63].

In general, small terpenes such as menthol, limonene and linalool, are better enhancers than larger ones, as phytol, nerolidol and humulene. Additionally, non-polar terpenes are better enhancers for lipophilic agents than polar ones. However, terpenes containing polar groups facilitate hydrophobic permeants to cross the skin and cellular membrane, much more easily than non-polar terpenes [61,63].

Therefore, penetration-enhancers should be incorporated into formulations to increase drug flux through diverse membranes including skin, epithelial or nasal membranes [66].

To date, terpenes have been mainly investigated in the pharmaceutical field as transdermal delivery, analgesics and antimicrobial agents. However, with the advent of DES,

several combinations of terpenes have been further studied, specifically as transdermal and dissolution enhancers of APIs, having demonstrated great potential in, for example menthol-based eutectic systems [67].

### 1.2.2.1. Menthol

Menthol (C<sub>10</sub>H<sub>20</sub>O) (**Figure 1.5**) is a cyclic monoterpene alcohol obtained from essential oils of *Mentha canadensis* L. (cornmint) and *Mentha x piperita* L. (peppermint) [63,68]. It is known for its upper respiratory tract decongestant properties and its multiple biological properties, such as analgesic, antimicrobial, antifungal, antipruritic, penetration-enhancing, chemopreventive, anticancer and anti-inflammatory activities [63,68]. Moreover, menthol is an agonist of the transient receptor potential melastatin 8 (TRPM8) thus, it can chemically activate this cold-sensitive receptor and elicit a cooling effect or sensation and an analgesic effect [68,69].

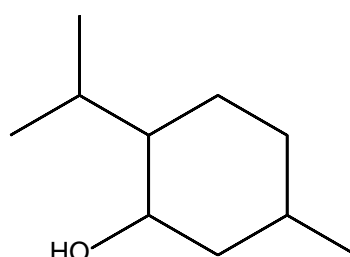


Figure 1.5. Menthol structure.

TRPM8 is tissue-selective when normally expressed, but it is overexpressed in a variety of malignant tumours [70]. TRPM8 is a Ca<sup>2+</sup> channel involved in tumour proliferation, survival, migration, invasion, growth and metastasis that is dependent on the cellular and molecular context [69,70]. When TRPM8 is activated naturally by temperature or by cooling agents, like menthol, a transient increase in Ca<sup>2+</sup> occur [70].

Caco-2 and HCT 116 colorectal adenocarcinoma cell lines over-express TRPM8, a receptor required for proliferation and survival of these cells, so the activation of TRPM8 by menthol sustain cancer development [70].

However, in melanoma and urinary bladder carcinoma cell lines, when menthol activates TRPM8 channel it decreases cell viability. This may be due to a sustained increase in Ca<sup>2+</sup> concentration, since TRP channels activation leads to the accumulation of Ca<sup>2+</sup> in mitochondria that increases the production of ROS [70-72]. Both ROS and mitochondria are involved in apoptosis induction, since cytochrome c release from mitochondria activates caspases and consequently apoptosis [73].

So, the role of TRPM8 in survival and apoptosis depends on the cancer cell line and the way that TRPM8 expression/activity is modulated [70].

Menthol anticancer properties have been studied on different types of cancers and can occur via the TRPM8-dependent or TRPM8-independent pathway. In the case of prostate cancer was reported that menthol caused cell cycle arrest at the G<sub>0</sub>/G<sub>1</sub> phase and inhibit the movement of DU145 cells that expressed TRPM8 [68]. Other authors reported that menthol induced apoptosis and mitochondrial ROS production through increased intracellular Ca<sup>2+</sup> release independently of TRPM8 channels in DU145 cell line, affecting instead purinergic

signalling pathways (a common pathway for neural and mesenchymal stem cell maintenance and differentiation) [74,75]. In another prostate cancer cell line (PC3 cell line), menthol induced G2/M cell cycle arrest through the inhibition of downstream signalling of polo-like kinase 1 (PLK1). In a different cancer model, using a rat mammary carcinogenesis model, the chemopreventive effects of menthol were studied and the induction of phase II carcinogen-metabolism enzymes, induction of apoptosis and tumour redifferentiation was reported [68].

Menthol is the most effective penetration enhancer and has been used as enhancer for transdermal delivery for a variety of drugs, due to permeate the epidermis, and probably other tissues, and in turn facilitate the accessibility of other drugs [63,68].

### 1.2.2.2. Linalool

Linalool ( $C_{10}H_{18}O$ ) (**Figure 1.6**) is a naturally occurring acyclic monoterpene alcohol obtain from *Coriandrum sativum* fruits that has a variety of commercial applications in cosmetics, soaps, perfumes and detergents due to their fragrance and odour, but it is also used in traditional medicine to alleviate pain, relax, sedate or eliminate certain Bacteria [63,76–78]. It is a cheap and well-known chemical with no irritation and sensitization reactions on the human body [77,79], that present antimicrobial, anti-inflammatory, analgesic, anticancer and antihypertensive activities [76,78–81]. Its anticancer properties have been already studied and three mechanisms of action have been described: induction of apoptosis [82,83], induction of oxidative stress [84,85] and immunomodulation [80].

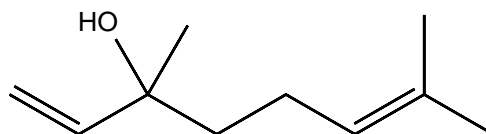


**Figure 1.6.** Linalool structure.

Kenichi I. *et al.* observed that linalool induces rapid ROS production which triggers an apoptotic cascade via lipid peroxidation. This mechanism is cancer specific since it did not affect normal organs in a human cancer xenografted mice model [86]. Another study has revealed that linalool has dose-dependent and time-dependent anticancer effects on prostate cancer cells through the induction of apoptosis, DNA fragmentation and sub-G1 cell cycle arrest [87].

Mei-Yin Chang and Yi-Ling Shen saw that linalool could effectively suppress the growth of four different cancer cells: SW620, T-47D, HepG2 and A549 cells. In the case of the T-47D cell line it was observed that linalool affected its migration and cell cycle through cancer immunity system modulation. Cells were arrested at the sub-G1 phase of the cell cycle, in a concentration dependent way, which normally means that cells are suffering apoptosis [80]. Linalool effect on HepG2 cell line were reported by other authors, which concluded that linalool had the capacity to permeate the membrane, due to its lipophilic feature, and interact with intracellular components, including mitochondria. This capacity allows mitochondrial derangements through inhibition of complexes I (NADH (nicotinamide-adenine dinucleotide) oxidase and NADH UQ-reductase) and II (succinate dehydrogenase) involved in electron transport chain coupled with proton release to the cytosol. This inhibition causes a disequilibrium on the proton gradient, a decrease on ATP level and an increase on ROS

generation. All these will cause an accumulation of dysfunctional proteins that will inhibit mitochondria function and lead to aging and cell death [84].

Like other terpenes, linalool has also the capacity to enhance conventional drugs permeability through skin and mucous membranes [76,88].

### 1.2.2.3. Safranal

Safranal ( $C_{10}H_{14}O$ ) (**Figure 1.7**) is a cyclical terpenic aldehyde that is the active carotenoid secondary metabolite of saffron (*Crocus sativus L.*) and the major volatile component responsible for the saffron aroma [89,90]. It is widely used as a food additive because of its taste, flavour, and colour along with its therapeutic properties. It has been described as therapeutic for many illnesses, such as hepatic diseases, neurodegenerative disorders, spasm, depression, acute and chronic inflammation, asthma, cardiovascular diseases and cancer [89].

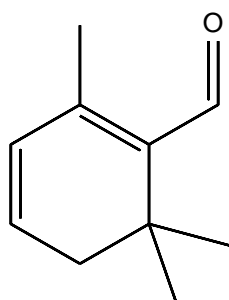


**Figure 1.7.** Safranal structure.

Carotenoids are known for present antioxidant activity, alter cell growth regulation, modulate gene expression and regulate immune response [89,90]. They are also well tolerated and their use in cancer chemoprevention and chemotherapy has been reported [91,92]. Thus, nowadays, safranal is being studied for its activities as anticarcinogenic and antitumour in different cancer models [92].

In one study, three different colon cancer cell lines were treated with saffron extracts and growth inhibition was observed. In addition, when a normal cell line was in contact with saffron no inhibition were observed and the cells were able to proliferate [89]. Another study with prostate cancer cells also reported that safranal was toxic for the cancer cell line used, but was less sensitive to normal cells [93]. Samarghandian S. *et al.* studied the use of saffron against human lung cancer cells, and reported that saffron inhibit these cells growth, but had no effect on normal human cells [94]. With these results it is possible to observe a tendency of safranal to be cancer specific, probably due to the existence of different cell surface receptors, intracellular retention transport, drug uptake mechanisms [92], or maybe safranal are able to affect specifically rapidly dividing cells [95]. However its toxicity is dependent on dose, time and cancer cell type [91,93,96].

Since safranal is lipophilic, has a low molecular size and present antioxidant properties, it can diffuse through the cell membranes [89,91] and prevent DNA, RNA and protein damages provoked by free radicals [89,93], suggesting that the anticancer activity of safranal can be related with its antioxidant property [89]. In addition, safranal is also cytotoxic, inducing DNA fragmentation and apoptosis [89,93,96,97]. Thus, it is proposed that the

antioxidant properties prevent cancer progression, while the cytotoxic effect direct cancer cells towards apoptosis and cell death [93].

The mechanisms behind safranal's anticarcinogenic and antitumour actions are not well known and different hypotheses have been proposed. One of the hypotheses is that safranal inhibits DNA and RNA synthesis but does not affect protein synthesis. Another possible mechanism for the antitumour action is the inhibition of free radical chain reactions, due to safranal antioxidant properties and its capacity to associate with membranes. The third mechanism is based on the interaction of carotenoids with topoisomerase II, that is involved in cellular DNA-protein interaction and is important for DNA repair [92]. It was also described that safranal binds DNA through intercalation and external binding and can incite a partial transition from B- to A-DNA conformation, provoking high levels of DNA vibrations due to helix destabilization. These associations are important to protect DNA from harmful oxidant damages [90,98]. The last mechanism proposed is based on the hypothesis that safranal targets specifically rapidly dividing cells through the inhibition of tubulin assembly and consequent diminishing of microtubules polymerization, a process needed for DNA migration on cell division and proliferation [95,97].

Zhang Y. *et al.* studied the effect of safranal in a colon carcinoma cell line (colo-205). They observed that safranal exhibit antiproliferative activity in a dose-dependence way. This antiproliferative effect is a consequence of DNA damage, cell cycle arrestment at G2/M phase and mitochondrial apoptosis, supported by increased expression of Bax, decrease Bcl-2 expression and accumulation of ROS [99]. Cell cycle arrest in G2/M phase and inhibition of DNA repair, leading to increase DNA damage, was also reported in HepG2 cells treated with safranal, moreover intrinsic and extrinsic apoptosis and endoplasmic reticulum stress was observed [100].

In addition to the anticancer potential of saffron, it was also described that saffron and its constituents can inhibit anticancer drugs toxicity [97].

Although safranal has all these anticancer properties and presents a good potential therapeutic, as a carotenoid it is poor soluble in water which makes its administration difficult [91], however, if combined as a DES, safranal solubility may increase and facilitate its use, since DES are described as solubility enhancers [54].

### **1.2.3. Nonsteroidal Anti-inflammatory Drugs (NSAIDs)**

As mentioned herein, inflammation is highly involved in neoplastic progression, especially in CRC [22,24], and because of that, CRC might be a potential candidate for treatment or prevention by NSAIDs.

There are several reports indicating that the use of NSAIDs reduces CRC and tumour recurrence risk by 40-50 %, through the reduction of growth and subsequent reduction of colorectal neoplasia development [22,23,27,29].

NSAIDs are nonselective or selective inhibitors of COX1/2 enzymes, and are normally prescribed for pain, fever and inflammation control, but they are also able to influence tumour development, metastasis and angiogenesis [23,101]. The analgesic, anti-pyretic and anti-inflammatory properties of NSAIDs are due to their COX inhibition capacity [102]. The firsts

NSAIDs developed had the capacity to inhibit both COX1 and COX2, but that brought same concerns, because COX1 is constitutively expressed in most tissues and is involved in physiological processes and its inhibition could bring dangerous side effects. As a result, a new generation of NSAIDs appear, the COX2-specific inhibitors, that target COX2 which is only induced in endothelial cells, macrophages and intestinal epithelial cells and its overexpression is a feature of malignant cells [101,102]. Furthermore, this new NSAIDs have shown effective treatment for CRC, which overexpresses PG and COX2 (in more than 95 % of human colon tumours), but not COX1 [22,24,101,102].

COX2 catalyses the synthesis of PG by converting arachidonic acid in PG, which is part of the lipid mediators family, and its involved in multiple tumour-promoting pathways, inducing inflammation in damaged tissues [22,24,101].

NSAIDs are also involved in inhibition of metastasis either by inhibiting COX2/PG pathways or by disruption of cancer-associated thrombosis. Thrombosis formation can be promoted by tissue factor (TF), a key regulator of hemostasis that is expressed by metastatic cancer cells and cancer-associated monocytes and macrophages, which activates the extrinsic coagulation cascade pathway leading to thrombosis. The inflammation produced by thrombosis leads to endothelial damage that result in vascular leak, enabling the escape of cancer cells [23]. Thus, the use of NSAIDs inhibit cancer-associated thrombosis via the suppression of platelet aggregation, that is fundamental for cancer cells dissemination [22,23].

The use of anti-inflammatory therapies may also avoid the fast development of drug resistance [27].

The down side effects of the use of NSAIDs are gastrointestinal related, especially the development of gastritis (inflammation of the lining of the stomach), since stomach's physiology is modified by PG. Unlike COX2, COX1 is constitutively expressed in the body and its responsible for kidney and stomach protection against damage and is also involved in PG synthesis needed for housekeeping functions [103,104]. PG is responsible for protective mucous production, decreases acid secretion and increases mucosal blood flow. When COX1 is inhibited, PG production is reduced, and the reverse effects occur, making the perfect environment for peptic-ulcer formation. Although the potent PG inhibitory effect, the propionic-acid derivates NSAIDs, like ibuprofen, flurbiprofen and ketoprofen, are much less harmful to the stomach than other [105–107].

### 1.2.3.1. Ibuprofen

Ibuprofen ( $C_{13}H_{18}O_2$ ) (**Figure 1.8**) is a racemic 2-phenylpropionic acid and the most used analgesic, antipyretic and anti-inflammatory drug [105,108].

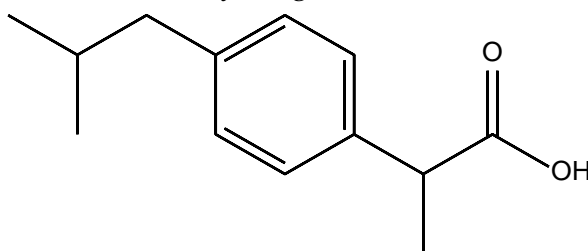


**Figure 1.8.** Ibuprofen structure.

Ibuprofen is one of the NSAIDs with lowest risks for severe gastrointestinal toxicity [109]. It inhibits COX by substrate competition with arachidonic acid, showing greater inhibitory effects on COX2 than COX1, due to differences on enzyme accessibility and arachidonic acid concentration present in the different systems [103]. This phenomena, together with the fact that it is used in clinical practice in lower doses than other NSAIDs, can be one of the mechanisms by which ibuprofen present less side effects [103,109].

The S-enantiomer of ibuprofen is pharmacologic active as a PG synthesis inhibitor unlike the R-enantiomer. However R-enantiomer present pharmacological properties important for the anti-inflammatory activities of ibuprofen [108,110].

HT29 cells overexpress Rac1b, triggered by colon inflammation [111,112]. Rac1b is a member of the Rho family of small GTPases associated with chronic inflammation and cancer, that promotes NF- $\kappa$ B activation and signalling [113]. P. Matos *et al.* reported that ibuprofen exercise its antitumour, and probably anti-inflammatory, activity by inhibiting COX2 as well as inhibiting specifically Rac1b overexpressed [112].

Ibuprofen has already been studied in THEDES form. The combination of ibuprofen and terpenes in THEDES has revealed an increase in solubility, transdermal delivery and flux of ibuprofen through the skin, being the increased on ibuprofen flux associated with the melting point depression of the THEDES [54,58]. These systems have already been tested against cancer cells, revealing that, in comparison to the individual elements, ibuprofen in THEDES present different mechanisms of action, showing higher selectivity towards cancer cells while increasing ibuprofen solubility [56].

### 1.2.3.2. Flurbiprofen

Flurbiprofen ( $C_{15}H_{13}FO_2$ ) (**Figure 1.9**) is a racemic propionic acid and a potent NSAID with strong analgesic, antipyretic and anti-inflammatory effects. Flurbiprofen is a non-specific COX inhibitor that inhibits PG synthesis and consequently reduces pain and inflammation [106,114]. It is current used for chronic inflammatory diseases, like osteoarthritis and rheumatoid arthritis and for mild-to-moderate acute pain [114,115].

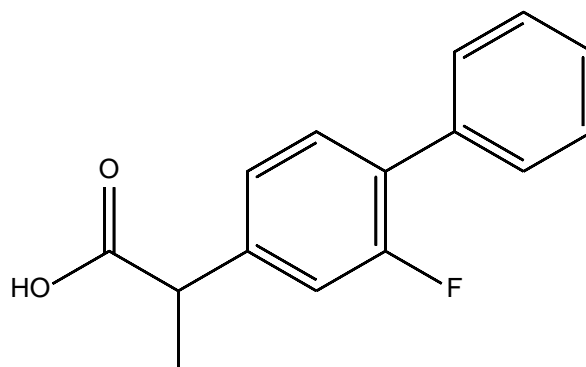


**Figure 1.9.** Flurbiprofen structure.

Flurbiprofen has been described as an anticancer agent, since it present antiproliferative effects due to its anti-inflammatory activity and inhibition of PGs [116,117].

R-flurbiprofen is not cytotoxic *in vitro*, even at concentrations greater than those possible to achieve *in vivo*, since it does not inhibit COX-1 [115,116], however, when combined with S-

flurbiprofen, the ulcerogenicity and toxicity effects of S-flurbiprofen are greatly exacerbated [115].

S-flurbiprofen suppressed inflammatory pain and edema in a rat adjuvant-induced arthritis through the decrease of PGE<sub>2</sub> production [118]. Edema is a consequence of an increase in COX<sub>2</sub>-derivated PGE<sub>2</sub> levels in inflamed tissue that leads to arterial dilatation and increased microvascular permeability, this results in plasmatic extravasation and elevated blood flow that form the edema [119].

Flurbiprofen as already been reported as a THEDES. The combination of flurbiprofen with nicotinamide presented an increase in flurbiprofen solubility. Additionally, an eutectic mixture of caffeine with flurbiprofen also presented an increased solubility rate associated with an enhancement of the flurbiprofen anti-inflammatory effect compared with the pure compound [120,121].

### 1.2.3.3. Ketoprofen

Ketoprofen (C<sub>16</sub>H<sub>14</sub>O<sub>3</sub>) (**Figure 1.10**) is a potent NSAID of the substituted 2-phenylpropionic acid class, that has been clinically used since 1975 in Europe. Ketoprofen has a chiral centre, so two enantiomers exist on the preparations, but only S-enantiomer has pharmacological activities [107,122].

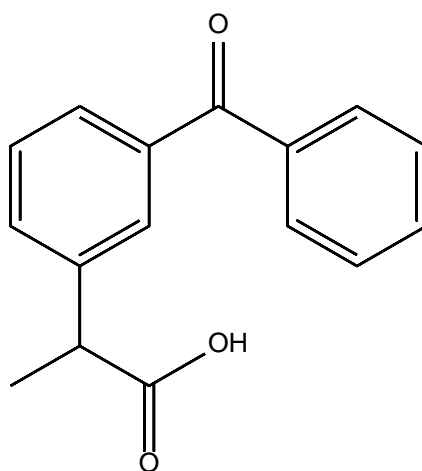


**Figure 1.10.** Ketoprofen structure.

Ketoprofen was studied in numerous animal models, and it has the ability to reduce acute, subacute and chronic inflammation, and showed a 20 times more potent activity than ibuprofen in reducing inflammation in a subacute rat model. Furthermore, it also present potent peripherally acting analgesic effects [122].

Its potent action as anti-inflammatory is a result of its great inhibitory effect on PG synthesis and its strong COX inhibitor capacity [107,122]. In addition, ketoprofen also inhibits the lipoxygenase pathway of the arachidonic acid cascade. This pathway generates noncyclized monohydroxy acids (HETE - 5-Hidroxyeicosatetraenoic acid) and leukotrienes, both responsible for leukocyte migration and activation and leukotrienes also increase vascular permeability (**Figure 1.11**). The inhibition of this pathway reduces cell-mediated inflammation and consequently reduces tissue destruction. Moreover, ketoprofen also inhibits bradykinin, a peptide that mediates pain and inflammation [122].



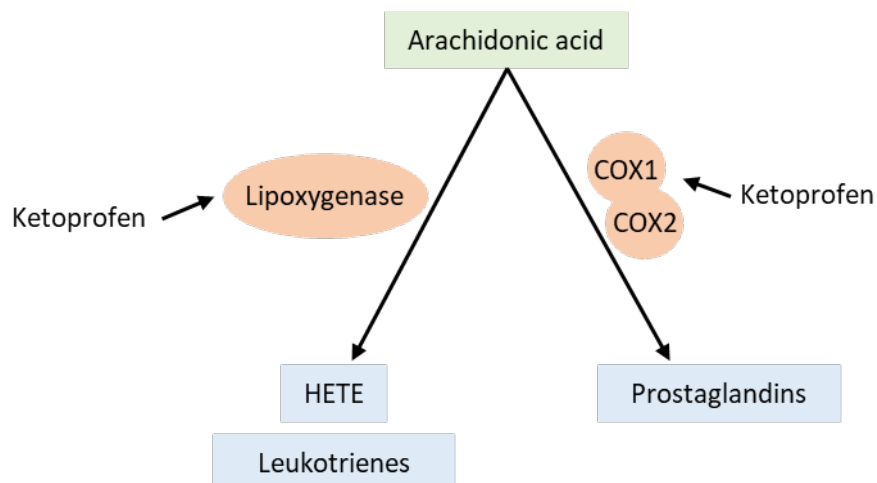


**Figure 1.11.** Ketoprofen acts as anti-inflammatory through the inhibition of COX1 and COX2 and consequent decrease of prostaglandin synthesis, and also through the inhibition of the lipoyxygenase pathway of the arachidonic acid cascade that is responsible for the production of noncyclized monohydroxy acids (HETE) and leukotrienes.

Although the R-enantiomer of ketoprofen is therapeutically inactive, it is responsible for the side effects of ketoprofen that are expressed by gastrointestinal damages and nephrotoxicity, a major cause of morbidity and mortality [107,109]. Actually, ketoprofen is one of the most ulcerogenic NSAIDs, due to its nonselective COX inhibition [109,123]. Because, unlike COX2, COX1 is constitutively expressed in the body and its responsible for kidney and stomach protection against damage and prostaglandin synthesis needed for housekeeping functions [103,104].

As mentioned herein cancer is a major health problem worldwide and is highly associated with inflammation, especially in the case of CRC. Therefore, in this work a mixture of a natural occurring anticancer molecule and an anti-inflammatory drug were combined in a THEDES, in order to create a potential new anticancer pharmaceutical with improved characteristics and that follows the green chemistry metrics. For that, terpenes, such as menthol, linalool and safranal, and NSAIDs, specifically ibuprofen, flurbiprofen and ketoprofen, were combined as a eutectic mixture to evaluate their anticancer activity against CRC and the mechanisms behind their effect.



The main aim of this thesis is to combine NSAIDs with naturally occurring compounds as a THEDES, to evaluate their specific anti-tumour potential against CRC. For that NSAIDs, namely ibuprofen, flurbiprofen and ketoprofen, were combined with terpenes, such as menthol, safranal and linalool, to further proceed with their biological activity assessment. This thesis is a result of a highly interdisciplinary work which involved several scientific areas in order to achieve this main goal.

Within the chemistry area, new THEDES were prepared and physical-chemically characterized by NMR (Nuclear Magnetic Resonance) and POM (Polarized Optical Microscope). After that, with the aim to analyse the potential of these systems as increases of NSAIDs bioavailability, their pharmaceutical properties were evaluated through the assessment of NSAIDs solubility and permeability.

In order to determine the therapeutic window of these THEDES, their effect against normal and cancer cells was evaluated through their cytotoxic and antiproliferative effects. Continue on the biological analysis, the effect of THEDES on inflammation, induction of apoptosis via caspase-3 and membrane integrity were evaluated to understand the mechanisms behind their anticancer activity against CRC. To achieve this aim, some of the protocols were optimized before the performance of the assays.

Part of the work herein described has been presented at two international conferences: Greenering International Conference and International Meeting on DES.



## MATERIALS AND METHODS

### 3.1. THEDES preparation

THEDES were prepared using menthol (Me, ref. W266507-1000, Sigma), safranal (Saf, ref. W338907, Sigma-Aldrich), linalool (Lin, ref. W263516-1KG-K, Sigma), ibuprofen (IBU, ref. B20989, Alfa Aesar), flurbiprofen (Flu, ref. F8514, Sigma-Aldrich) and ketoprofen (Ket, ref. K1751, Sigma-Aldrich). Different eutectic mixtures using these individual compounds were prepared in different molar ratios. THEDES were prepared by heating both components at 50°C, under constant stirring, until a clear liquid was formed. Afterwards, THEDES were left to cool down at room temperature (RT), without stirring. THEDES were prepared right before each assay or were kept at -20 °C until being used.

### 3.2. POM

A drop of THEDES at RT was deposited in a microscope glass slide and observed by a transmission mode of an BX-51 polarized optical microscope (Olympus, Tokyo, Japan) coupled to an Olympus KL2500 LCD cold light source. The images were acquired with a digital camera (Olympus DP73) connected to the microscope, and Olympus Stream Basic 1.9 software (Olympus, Tokyo, Japan) was used to treat the images.

### 3.3. NMR

The NMR analysis was performed in a 400.13 MHz Bruker Avance III (USA). Approximately, 10 mg of THEDES and individual compounds were dissolved in 500  $\mu$ L dimethyl sulfoxide- $d_6$  (DMSO- $d_6$ , ref. D010ES-0050, Euriso-Top) or chloroform- $d$  (ref. D007H-0100, Euriso-Top) in a 5 mm NMR tube.

The assignment of the THEDES and individual compounds signals was done using MestReNova 11.0 software (Mestrelab Research, Spain).  $^1\text{H}$ , 2D-COSY (Correlated Spectroscopy), 2D-HMBC (Heteronuclear Multiple Bond Correlation) and 2D-NOESY (Nuclear Overhauser Effect Spectroscopy) experiments were obtained at 298 K, using tetramethylsilane (TMS -  $\text{Me}_4\text{Si}$ ) as chemical shift reference in the  $^1\text{H}$  NMR experiments ( $\delta$  TMS = 0 ppm). Chemical shifts were expressed in ppm. All the experiments were performed when the systems were in equilibrium and no changes in their properties were observed.

### 3.4. Solubility Assessment

The solubility measurements were performed using the NSAIDs in powder form, in THEDES form and as a physical mixture. An excess of NSAIDs in the three forms were added to 1 mL of PBS (Sigma Aldrich, St. Louis, MO, USA) and put on a bath at 37 °C (LSB 12 Aqua Pro, Grant, United Kingdom) and stirred during 72 h. 600 µL of sample were retrieved from the aqueous phase. Then, the samples were filtered using a hydrophilic PTFE syringe filter with a 0.22 µm pore size (Filter Lab, Barcelona, Spain). At least three replicates were performed. The NSAIDs solubility was quantified by high-performance liquid chromatography (HPLC), using a Thermo Scientific Finnigan Surveyor (Thermo Scientific, Waltham, MA, USA), equipped with a quaternary pump, solvent degasser, auto sampler and column oven, coupled to a UV-VIS detector (Accela, Thermo Scientific, USA). The column used was a Eclipse XDB - C18 with 5 µm particle size, pore size 100 Å, L × I.D. 250 mm × 4.6 mm (Agilent, USA) and the column was maintained at 30 °C. The chromatographic separation was performed using a mobile phase of 50 mM KH<sub>2</sub>PO<sub>4</sub> (pH 4.2): acetonitrile = 50:50, v/v. The volume injected was 10 µL at a flow rate of 1 mL/min with the absorbance of the solutions measured at 220 nm for IBU and 254 nm for Ket and Flu. The procedure was performed adapting the protocol described by L. Ascar *et al.* [124]. For quantification, a calibration curve was made using the respective NSAIDs as standards.

### 3.5. Permeability studies

Permeability assessment was performed using glass diffusion Franz cells (PermeGear, USA) with an 8 mL receptor compartment and an effective mass transfer area of 1 cm<sup>2</sup>. It was used a polyethersulphone (PES-U) hydrophilic membrane, with 25 mm of diameter, 150 µm thickness and 0.45 µm pore size (ref. 15406-25-N, Sartorius Stedim Biotech, Germany), which was placed between the donor compartment and the receptor compartment and held with a clamp. The receptor compartment was filled with 8 mL of PBS and air bubbles formed below the membrane were removed by carefully tilting the Franz cells for the air bubbles to escape through the sampling arm. Then, the NSAIDs in powder form or as a THEDES was added to the donor compartment along with 2 mL of PBS, obtaining a total concentration of 2.5-3 mg/mL. At different time points (10 min and hourly from 1 to 8 h) 400 µL were retrieved from the receptor compartment and replaced with the same volume of fresh PBS. The experience was conducted at 37 °C under constant stirring at 200 rpm using a magnetic bar to eliminate the boundary layer effect. At least three replicates were performed. The determination of the NSAID diffused was performed by HPLC, as described for the solubility assay (Section 3.4).

The cumulative mass of API that pass to the receptor compartment was determine considering the replacement of the aliquots with fresh PBS and the dilution associated with it. The permeability (*P*) of the NSAIDs was calculated using equation 3.1:

$$-\ln\left(1 - \frac{2C_t}{C_0}\right) = \frac{2A}{V} \times P \times t \quad 3.1$$

Where  $C_t$  is the concentration (mol/L) in the receptor compartment at time  $t$  (h),  $C_0$  is the initial concentration (mol/L) in the donor compartment,  $A$  is the effective area of mass transfer (cm<sup>2</sup>),  $V$  is the total volume in both compartments (cm<sup>3</sup>), and  $P$  is the permeability (cm/s) [58,125].

Fick's first law of diffusion enables further the determination of the NSAIDs' diffusion coefficient ( $D$ ) through the membrane using the derived equation 3.2:

$$D = \frac{V_1 \times V_2}{V_1 + V_2} \times \frac{h}{A} \times \frac{1}{t} \ln \left( \frac{C_f - C_i}{C_f - C_t} \right) \quad 3.2$$

Where  $D$  is the diffusion coefficient (cm<sup>2</sup>/s);  $C_f$  and  $C_i$  are the final and initial concentration (mol/L) in the receptor compartment and  $C_t$  is the concentration in the receptor compartment at time  $t$  (h).  $V_1$  and  $V_2$  are the volume in the donor and receptor compartment (cm<sup>3</sup>) respectively,  $h$  is the thickness of the membrane (cm) and  $A$  is the effective area of mass transfer (cm<sup>2</sup>) [58,126].

The partition coefficient ( $K_d$ ) is a measurement of the solubility of the solute in the membrane and is calculated according to equation 3.3:

$$K_d = \frac{P \times h}{D} \quad 3.3$$

Where  $P$  is the permeability (cm/s),  $h$  is the membrane thickness (cm) and  $D$  is the diffusion coefficient (cm<sup>2</sup>/s) [125].

### 3.6. Cell Culture and sub-culturing

HT29 cell line (Deutsche Sammlung von Mikroorganismen und Zellkulturen (DSMZ), Germany) and Caco-2 cell line (Deutsche Sammlung von Mikroorganismen und Zellkulturen (DSMZ), Germany), two immortalized human colorectal adenocarcinoma cell lines, were used for this study. HT29 cells were maintained in Gibco Roswell Park Memorial Institute (RPMI, Corning, USA) 1640 medium with phenol red, supplemented with 10 % (v/v) of heat-inactivated fetal bovine serum (FBS, Corning, USA) and 1 % (v/v) of penicillin-streptomycin (PS, Corning, USA). Caco-2 cells were maintained in Dulbecco's Modification Eagle's Medium (DMEM, Corning, USA) with phenol red, supplemented with 10 % (v/v) of FBS and 1 % (v/v) PS. Cell cultures were routinely grown as a monolayer in a 75 cm<sup>2</sup> culture flasks (Falcon, Corning, USA) until reach 80-90 % of optical confluence in a humidified atmosphere, at 37 °C with 5 % of CO<sub>2</sub>. Afterwards, sub-culturing was achieved by detaching cells from the T-flask through the addition of trypsin (ref. 25-050-CI, Corning, USA) for approximately 10 min at 37 °C. Then, sub-culturing medium (culture medium with 10 % FBS and 1 % PS) was added to neutralize trypsin effect. Thereafter cells were centrifuge (601900066, Z 206, Hermle, Germany) at 200g for 10 min, supernatant was discarded by tube inversion, and cells were resuspended in 3 mL of sub-culturing medium. After that, cells were counted in a Neubauer hemocytometer using Trypan Blue dye (Corning, USA) in order to

differentiate living cells from dead cells, (according to **Figure 3.1**) and cell concentration was calculated using the equation 3.4:

$$[\text{Cells}] = \frac{\text{number of cells counted}}{\text{number of squares}} \times \text{DF} \times 10^4 \quad 3.4$$

Where  $[\text{Cells}]$  is the cells concentration (cells/ml) and  $\text{DF}$  is the dilution factor. The calculated cell concentrations were used for further cell assays.

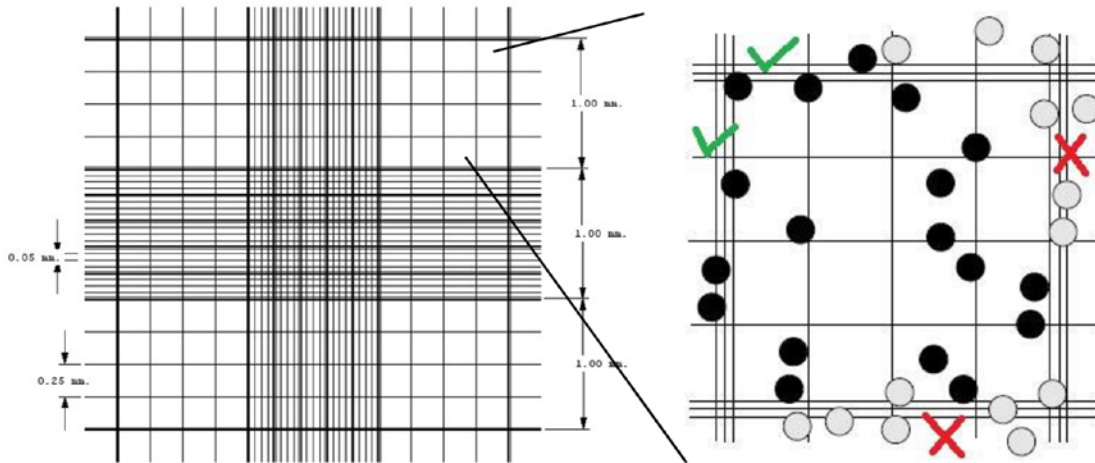


**Figure 3.1.** Hemocytometer chamber scheme for cell counting.

### 3.7. Cell Thawing

Cells were thawed in a 37 °C bath, with gentle agitation, then 9 mL of cell sub-culturing medium was added. Both living and dead cells were counted, as previous described (Section 3.6), and cell viability was accessed using equation 3.5. Cells were cultured with at least 60 % of cell viability. Cells were then transferred to a 25 cm<sup>2</sup> T-Flask (Falcon, Corning, USA) to ensure quality cell culture recovery.

$$\text{cell viability} = \frac{[\text{live cells}]}{[\text{live cells}] + [\text{dead cells}]} \times 100 \quad 3.5$$

### 3.8. Cell Freezing

HT29 and Caco-2 cell cultures were frozen after reaching 80-90 % as a confluence monolayer in an 150 cm<sup>2</sup> T-Flask. The detachment of cells was done as previous described in the sub-culturing procedure (Section 3.6). Afterwards, cells suspensions were resuspended in freezing culture medium (prepared according to **Table 3.1**). Cells were then counted, as described before (Section 3.6), and cell concentration was determined according to equation 3.4. Knowing the cell concentration value, the amount of freezing culture medium and DMSO cryoprotectant agent (ref. 25-950-CQC, Corning, USA) was calculated in order to reach 1 mL per cryovial with 2x10<sup>6</sup> cells/mL.



Freezing medium with DMSO and cell suspension was kept on ice during the transfer of cell to the cryovials. The cryovials were then store in a CoolCell freezing container (432002, Corning, USA) for 24 h at -80 °C, which allows a slow cooling rate (1°C/min) to minimize damage due to osmotic imbalance and intracellular ice crystal formation.

**Table 3.1.** Freezing culture medium and cryoprotectant agent volume to freeze HT29 and Caco-2 cell lines.

Cell lines	Freezing culture medium	Cryoprotectant agent (CPA) - DMSO	Freezing temperature
HT29	RPMI + 10 % FBS	10 %	-80 °C for short to middle term storage or -196 °C for long term storage
Caco-2	DMEM + 10 % FBS	10 %	

With this protocol, it was possible to create a cell bank. For that, factory stock cells were sub-culture and, after reaching a stable behaviour and optimal optical confluence, were frozen according to this protocol.

### 3.9. Cell viability assessment

In a preliminary approach to evaluate the realistic anticancer effect of a drug, it is important to choose the appropriate cellular model. There are more than 70 CRC cell lines described that depending on their genetic background, represent different types of CRC. The most used cell lines are Caco-2, COLO 320, HCT15, HCT116, HT29 and SW480 [127]. For this study HT29 and Caco-2 colonic cell lines were used.

HT29 (**Figure 3.2**) is a human colon adenocarcinoma cell line isolated from a primary tumour of a 44 years old Caucasian female in 1964. These cells are extensively used to study the biologic aspects of human cancers [128]. In the presence of glucose and serum these cells present an undifferentiated phenotype, like in cancer [128,129].

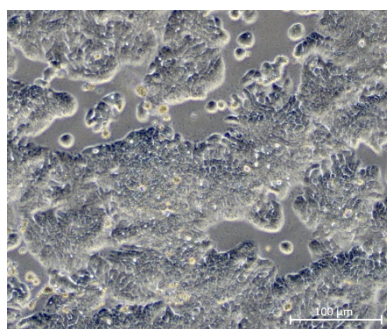


**Figure 3.2.** HT29 cell line in culture.

Caco-2 cell line (**Figure 3.3**) is also a human colon adenocarcinoma cell line originated from a human colon carcinoma, that when cultured in the presence of glucose and serum and after 7 days of seeding, lead to a cell's monolayer growth with characteristics similar to mature enterocytes. This cell model can mimic the intestinal barrier and can be used to evaluate transport properties [129,130]. Therefore, these cells are widely used as a model of normal intestine cells.

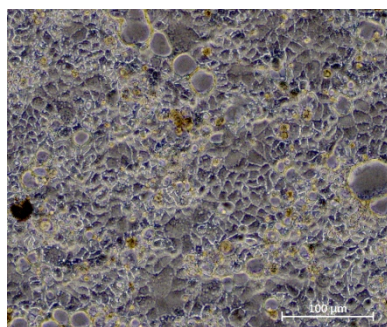


**Figure 3.3.** Caco-2 cell line in culture.

To access cell viability, MTS (3-(4,5-dimethylthiazol-2-yl)-5-(3-carboxymethoxyphenyl)-2-(4-sulfophenyl)-2H-tetrazolium) viability agent was used, since it is an *in vitro* cytotoxicity assay easy to use, economic, precise, rapid, sensitive, with high accuracy and reproducibility. This assay is based on the conversion of this tetrazolium salt into a coloured formazan by mitochondrial dehydrogenase enzymes in viable cells. Thus, the amount of formazan produced is directly proportional to the number of living cells and can be measured at 490 nm [131].

### 3.9.1. Cytotoxicity Assay

Cytotoxicity effect of THEDES and individual compounds was evaluated in confluent Caco-2 cells. For that, cells were seeded into 96-well plates (Falcon, Corning, USA) at a density of  $2 \times 10^5$  cells/mL and allowed to grow for 7 days, with medium renewal every 48 h. At day 7, cells were incubated with different concentrations of the samples diluted in sub-culture medium or just sub-culture medium (controls). After 24 h, cells were washed twice with PBS (Sigma-Aldrich, USA) and cell viability was assessed using MTS (16 %) (CellTiter 96® AQueous One Solution Cell Proliferation Assay, PROMG3581, Promega, USA) in a dilution of 1:10 in assay culture medium (DMEM+0,5 % FBS). Cell viability was measured after 3 h by UV-vis spectroscopy at 490 nm in a microplate reader (HH35L2019044, Victor Nivo 3S, Perkin Elmer, USA). At least three replicates were performed in triplicate. The results are expressed in percentage of living cells relatively to the control and the effective concentration values ( $EC_{50}$  - concentration necessary to decrease 50 % of cell viability) were obtained from dose-response curve fit using software GraphPad Prism 8.0 (GraphPad Software, California).

### 3.9.2. Antiproliferative Assay

Antiproliferative effect of THEDES and individual compounds was evaluated in HT29 cells. For that, cells were seeded at a density of  $1 \times 10^5$  cells/mL in 96-well culture plates (Falcon, Corning, USA). After 24 h cells were exposed to different concentrations of the samples diluted in sub-culture medium or just sub-culture medium (controls). 24 h later, cells were washed twice with PBS and MTS (16 %) was added to all the wells in a dilution of 1:10 in assay culture medium (RPMI+0,5 % FBS). Cell viability was measured after 3 h by UV-vis spectroscopy at 490 nm in a microplate reader (HH35L2019044, Victor Nivo 3S, Perkin Elmer). At least three replicates were performed in triplicate. The results are expressed in percentage of living cells relatively to the control and effective concentration values ( $EC_{50}$  - concentration

necessary to decrease 50 % of cell viability) were obtained from a dose-response curve fit using GraphPad Prism 8.0 software.

### 3.10. Lactate Dehydrogenase (LDH) Release

The effects of THEDES on membrane integrity were evaluated through the release of LDH to extra cellular medium.

LDH is a cytoplasmatic enzyme responsible for the conversion of lactate into pyruvate coupled with the reduction of  $\text{NAD}^+$  to NADH. LDH is only released to the extra cellular medium when membranes collapse, so when LDH crosses the damage membrane to the extracellular medium it becomes available to quantify through the conversion of lactate to pyruvate with the release of NADH [132].

In 1973, Babson and Babson described a colorimetric assay to measure LDH release, in which the reduction of  $\text{NAD}^+$  to NADH is coupled to the reduction of tetrazolium salt in the presence of an intermediate electron carrier, that originates an orange formazan dye [133] (Figure 3.4).

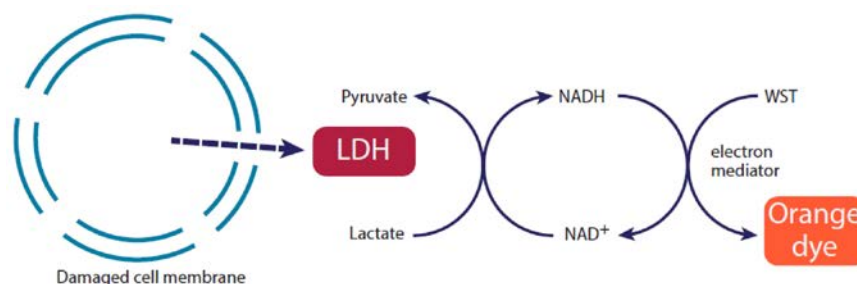


**Figure 3.4.** Colorimetric reaction to measure LDH release. LDH is responsible for the conversion of lactate in pyruvate coupled with the reduction of  $\text{NAD}^+$  to NADH. The NADH will reduce the water-soluble tetrazolium salt (WST) in the presence of an electron mediator, originating an orange formazan dye.

Hence, LDH-Cytox™ Assay Kit (426401, Biologend, San Diego, California, USA) was used, accordingly to the manufacturer.

Firstly, cell density was tested to determine the optimum number of cells, for that cells were seeded at sequential concentrations (from an initial cell suspension with  $5 \times 10^5$  cells/ml, and using concentrations within the range of  $2,5 \times 10^5$  to  $3,9 \times 10^3$  cell/ml) in a 96-well culture plate with RPMI medium supplemented with 5 % FBS (LDH medium). 100  $\mu\text{L}$  of the cell suspension was added to the first well after adding 100  $\mu\text{L}$  of LDH medium to each well, and sequential dilutions were performed in the plate. The 2-fold serial dilution was done in triplicate for the Hight Control (death control) and in triplicate for the Low Control (live control). The plate was incubated for 24h in a 37 °C incubator.

To test the THEDES systems, some modifications were made to the protocol. Briefly, 100  $\mu\text{L}$  of cell suspension with  $2.5 \times 10^5$  cells/ml of sub-culturing medium was added to each well of the 96-well plate and incubate for 24 h at 37 °C in the incubator. The medium was discarded by plate inversion and 100  $\mu\text{L}$  of LDH medium was added to the “High Control”, “Low Control” and “Background Control” (without cells) wells. Additionally, 100  $\mu\text{L}$  of a 2-fold serial dilution of the tested compounds was performed in the LDH medium until

reaching seven different concentrations. At least two replicates were performed in triplicate for all the dilutions. Furthermore, the plate was incubated for 24 h at 37 °C.

The LDH measurement was done by adding 10 µL of Lysis Buffer to the High Control wells and incubate 30 min at 37 °C. When THEDES were tested, after the incubation with the Lysis Buffer, cells supernatants were transferred to clear bottom 96-well plate. Thereafter, 100 µL of Working Solution was added to each well and incubated at room temperature for 20 min, and the absorbance was measured at 490 nm, in a microplate reader (HH35L2019044, Victor Nivo 3S, Perkin Elmer).

Before the optimized protocol described above, some different approaches were tested, such as i) using different cell concentrations ( $3.13 \times 10^4$  or  $2.5 \times 10^5$  cells/ml) and volume (50 or 100 µL), ii) apply different incubation times (10, 15 and 20 min), iii) test only the EC50 concentrations of the test compounds, or iv) measure the absorbance of the control before the addition of the test compounds.

The results are expressed in percentage of LDH released in comparison to the "High Control" and "Low Control", calculated using the equation 3.6.

$$\text{LDH released (\%)} = \frac{\text{Abs}(\text{Test Substance}) - \text{Abs}(\text{"Low Control"})}{\text{Abs}(\text{"High Control"}) - \text{Abs}(\text{"Low Control"})} \times 100 \quad 3.6$$

## 3.11. Anti-inflammatory Potential Assessment

### 3.11.1. Intracellular ROS Production

DCFH-DA (dichlorofluorescein-diacetate) is the most widely used probe to detect oxygen species. DCFH-DA crosses the cell membrane and is hydrolysed enzymatically by intracellular esterases to nonfluorescent DCFH (dichlorofluorescein), which is retained in the cell. When in the presence of ROS, DCFH is oxidized to fluorescent dichlorofluorescein (DCF) (**Figure 3.5**). The fluorescence emitted by the DCF is directly proportional to the concentration of ROS and can be measured in a microplate reader or by flow cytometry [134,135].

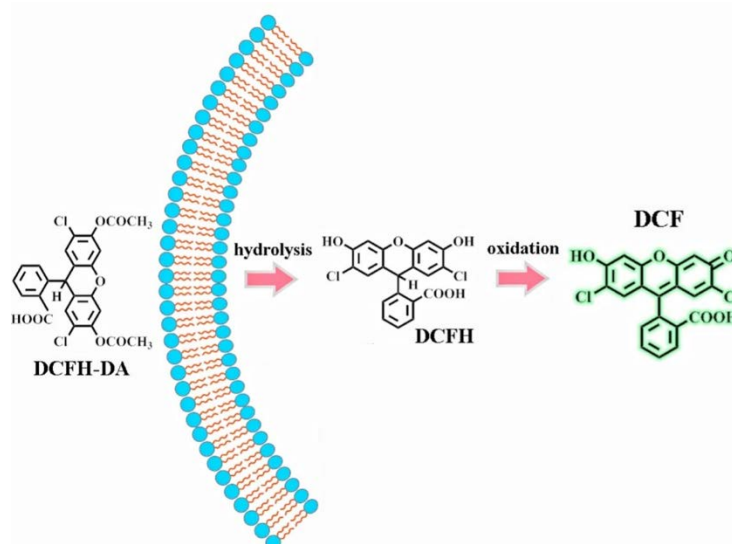


**Figure 3.5.** DCFH-DA reaction for detection of ROS. DCFH-DA crosses the cell membrane where it is hydrolyzed by esterases originating DCFH. Then, DCFH reacts with ROS and is oxidated to the fluorescent DCF (Adapted from [136]).

To access the effects of THEDES on ROS production, HT29 cells were seeded in a 24-well plate at a density of  $1.52 \times 10^5$  cells/mL. After 24 h cells were exposed to THEDES and their individual compounds diluted in sub-culture medium, or sub-culture medium alone (control), during 1h. Then, the culture medium was removed, and cells were washed twice with PBS.

To quantify the presence of ROS, 600  $\mu$ L of DCFH-DA in a 25  $\mu$ M concentration was added to each well for 1 h. Fluorescence was measured in a microplate reader (HH35L2019044, Victor Nivo 3S, Perkin Elmer) applying an excitation wavelength of 480 nm and an emission wavelength of 530 nm. At least three replicates were performed in triplicate.

### 3.11.2. NO Production

To access the effects of THEDES on NO production, HT29 cells were seeded in a 24-well plate at a density of  $1.52 \times 10^5$  cells/ml. After 24 h cells were exposed to THEDES and their corresponding individual compounds diluted in sub-culture medium or sub-culture medium alone (control). To measure the amount of NO produced, a Griess reagent-based kit (ab234044, Abcam, Cambridge, United Kingdom) was used. After 24h of exposure to the compounds, 100  $\mu$ L of the supernatants was recovered to a new 96-well plate without cell treatment. Firstly, 80  $\mu$ L of Nitrite assay buffer was added, followed by 10  $\mu$ L of Griess reagent I and 10  $\mu$ L of Griess reagent II, and incubation at room temperature during 10 min. The background control wells were prepared with 90  $\mu$ L of nitrite assay buffer and 10  $\mu$ L of Griess Reagent I. Absorbance was measured at 540 nm, in a microplate reader (HH35L2019044, Victor Nivo 3S, Perkin Elmer).

Before the optimized protocol described above, some different approaches were tested, such as i) expose cells only 1h to the compounds, ii) discard the supernatant and lyse the cells with 100  $\mu$ L of ice cold Nitrite Assay Buffer (with or without mechanical detachment of cells), putting them next on ice for 10 min, then centrifuge at 13 000 rpm for 5 min and recover the

supernatant to perform the assay, or iii) inducing inflammation with 600  $\mu$ M de AAPH (2,2'-azobis(2-amidinopropane) dihydrochloride) or 10 mM of H<sub>2</sub>O<sub>2</sub> for 1h.

### 3.11.3. IL-8 ELISA

A sandwich enzyme-linked immunosorbent assay (ELISA) was performed to quantify the amount of IL-8 produced by cells after being exposed to the THEDES and individual compounds (**Figure 3.6**). The sandwich ELISA consists on the use of two antibodies, a capture antibody and a detection antibody. First, the capture antibody is fixed on the plate, then, to avoid unspecific binding, a blocking buffer solution is added to block the remaining protein-binding sites. After that, the samples in study are added to the wells of the coated plate followed by the addition of the detection antibody. Then, streptavidin-horse radish peroxidase (HRP) is added to the plate. Streptavidin is a protein that binds to biotin of the biotinylated detection antibody, coupled to an HRP enzyme. When the substrate (3,3',5,5'-Tetramethylbenzidine - TMB) is added, the HRP oxidizes the substrate, and a blue colour is originated. Then the stop solution is added, acidifying the medium, which leads to the formation of a yellow colour.

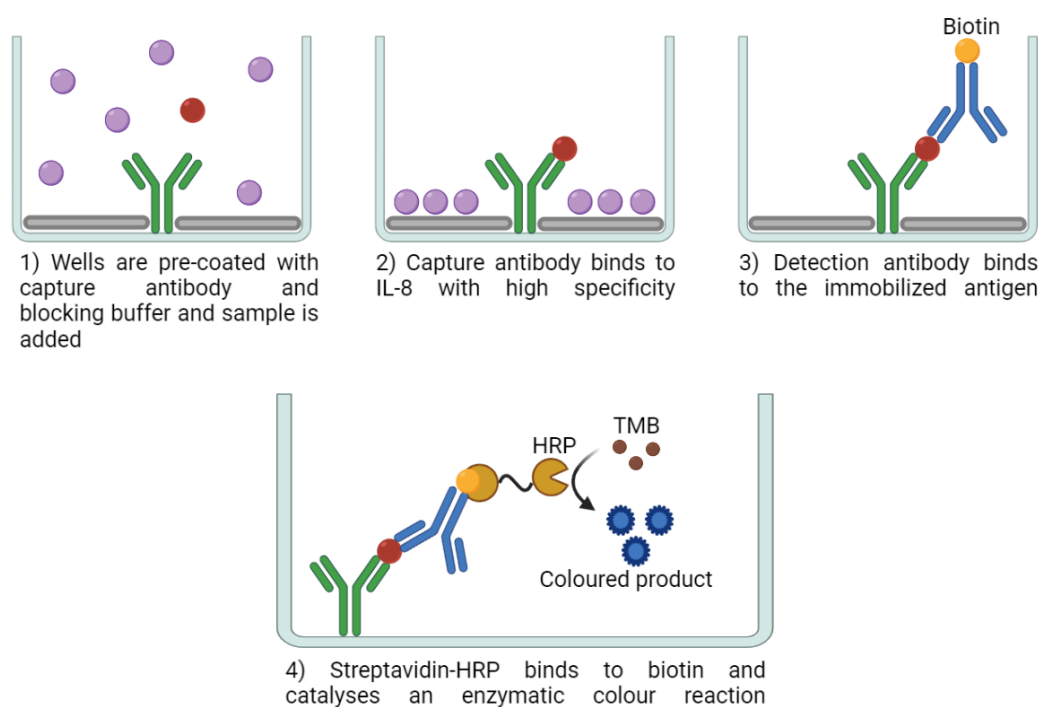


**Figure 3.6.** Sandwich ELISA method. First the plate wells are coated with capture antibody and blocking buffer to avoid unspecific protein bindings. After the coating the samples are added to the wells. Secondly, the IL-8 binds specifically to the capture antibody. Thirdly, the biotinylated detection antibody is added and binds to the immobilized IL-8. Finally, streptavidin-HRP binds to the biotin and catalyses an enzymatic colour reaction, originating a blue solution. Image created with BioRender.com.

For that, cells were seeded at  $2 \times 10^6$  cells/mL for 24h and then exposed to THEDES and their respective individual compounds diluted in assay culture medium, or assay culture medium alone (control) during 24 h. At least three replicates were performed. Then, the supernatants were recovered to Eppendorfs, frozen in liquid nitrogen and stored at -80 °C until the ELISA assay.

The ELISA assay was performed according to the manufacturer (900-T18, Peprotech by Tebu-bio). First, the ELISA plates (Nunc-Immuno MaxiSorp™ F96 flat-bottom, M5785, Thermo Fisher Scientific, EUA) were exposed to 100 µL of 0.125 µg/mL of capture antibody overnight. Then, the liquid was removed by plate inversion, and the plates were washed four times with 300 µL of wash buffer (0.05 % Tween-20 (P7949-100ML, Sigma, EUA) in DPBS (Dulbecco's phosphate-buffered saline) 1x (14200075, Gibco, US)). After, plates were incubated with 300 µL of Block Buffer (1 % BSA (Bovine serum albumin) (A7030-0010, Sigma, EUA) in DPBS 1x) for 1 h at RT in the dark. Then, the liquid was removed by plate inversion, and the plates were washed four times with 300 µL of wash buffer. Afterwards, 100 µL of the biological samples or of the calibration curve samples in triplicate were added, and incubated at RT and in the dark for 2 h. Then, the liquid was removed by plate inversion, and the plates were washed four times with 300 µL of wash buffer. Next, 100 µL of 0.25 µg/mL of detection antibody was added to each well, and incubated at RT in the dark for 2 h. After that, the liquid was removed by plate inversion, and the plates were washed four times with 300 µL of wash buffer. Following that, 100 µL of 0.1 µg/mL of streptavidin-HRP was added to each well, and the plates were incubated 30 min at RT in the dark. After that, the liquid was removed by plate inversion, and the plates were washed four times with 300 µL of wash buffer. Then, 100 µL of substrate solution (TMB, 421501, BioLegend, EUA) was added to each well, and incubated for 20 min at RT. Finally, 100 µL of stop solution was added to each well and absorbance was measured at 450 nm and 620 nm, in a microplate reader (HH35L2019044, Victor Nivo 3S, Perkin Elmer).

### **3.11.3.1. Bradford**

The Bradford assay is a simple, fast and sensitive method used to quantify the total protein concentration. This assay was reported by Bradford in 1976 and depends on the binding of the dye Coomassie Brilliant Blue G-250 to the proteins. This dye exists in two color forms, where the red form is converted into the blue form when the dye binds to the protein. Therefore, the amount of protein can be estimated by measuring the amount of dye in the blue form at 595 nm [137].

To quantify the total amount of protein produced by cells after being exposed to the THEDES and individual compounds, the Bradford assay was performed. The concentration of proteins produced by cells is necessary in order to normalize the ELISA results to the total protein synthesis.

First, a calibration curve of BSA was prepared by diluting a 2 mg/mL stock into 1 mg/mL, 0.8 mg/mL, 0.6 mg/mL, 0.4 mg/mL, 0.2 mg/mL and 0 mg/mL in water. Secondly, the test samples were diluted in a 1:2 dilution factor. Then, 5 µL of each test sample and calibration curve samples in triplicate was pipetted to a 96-well plate. After that, 250 µL of Bradford reagent (B6916, Sigma-Aldrich, EUA) was added to the samples and incubated for 30 min at RT in the dark. Finally, the absorbance was measured at 595 nm, in a microplate reader (HH35L2019044, Victor Nivo 3S, Perkin Elmer).

### 3.12. Caspase-3 Activity

To evaluate THEDES potential to activate apoptosis via caspase-3 pathway, HT29 cells were seeded in a 24-well plate at a density of  $1.52 \times 10^5$  cells/mL for 24 h. Then, cells were exposed to THEDES and their individual compounds diluted in sub-culture medium or sub-culture medium alone (control) during 24h. At least three replicates were performed. After that period, the culture medium was removed, and cells were washed twice with PBS.

In order to stain living and death cells, NucView®488 and MitoView™633 Apoptosis Assay Kit (Biotium, USA) was used. This assay is based on the fluorescence of two dyes, NucView 488 Caspase-3 Substrate and MitoView 633 mitochondrial membrane potential dye. NucView 488 detects caspase-3 activity within intact cells without inhibiting apoptosis. NucView 488 is a fluorogenic DNA dye substrate and a DEVD substrate moiety. The substrate, that are nonfunctional and non-fluorescent, crosses the plasm membrane where it is cleaved by caspase-3, releasing a high affinity DNA dye. This free dye migrates to the nucleus and stain the DNA with green fluorescence. MitoView 633 is a far-red fluorescent cell membrane permeable dye that becomes fluorescent by accumulating in mitochondria. Mitochondrial staining is dependent on mitochondrial membrane potential, therefore, death cells that lost their mitochondrial membrane potential show much lower staining than healthy cells.

Staining was performed by adding 200  $\mu$ L/well of assay culture medium containing 1  $\mu$ L of NucView®488 and 1  $\mu$ L of MitoView™633 to cells for 2h at 37 °C. Cells were then washed with PBS and re-suspended in 200  $\mu$ L/well of PBS for fluorescence microscopy observation (Zeiss, Axio Vert A1, Germany) with a Colibri 7 (Zeiss, Germany) light source. Cells were subjected to an excitation and emission wavelengths of 631 nm and 650 nm, respectively for MitoView™633, and excitation wavelength of 500 nm and emission wavelength of 520 nm for NucView®488.

### 3.13. Statistical Analysis

The statistical analysis was carried out using GraphPad Prism 8.0 (GraphPad Software, California). All data are expressed as mean  $\pm$  Standard Deviation (SD) and significant differences were calculated comparing the different compounds with the control. P-values smaller than 0.05 were considered statistically significant (confidence interval of 95 %). To analyse significant differences, different statistical tests were used. First the normality of the results was tested using the Shapiro-Wilk test. When the results followed a normal distribution One-Way ANOVA was used to perform the comparisons following Dunnett or Tukey multiple comparison test. On the other hand, when results did not correspond to a normal distribution Kruskal-Wallis test was used.



## RESULTS AND DISCUSSION

### 4.1. THEDES Preparation

THEDES are a combination of two or more components, containing an API, that, in a specific molar ratio, present a lower melting point than its individual elements. In order to produce THEDES combining terpenes and NSAIDs, different molar ratios were tested to evaluate which ones are liquid at RT. The results are presented in **Table 4.1**.

**Table 4.1.** Different THEDES prepared. <sup>a</sup> Valour retrieved from [138]

THEDES		Molar Ratio	Visual aspect at RT
Terpene	NSAID		
Me	IBU	3:1	Liquid <sup>a</sup>
Saf	IBU	1:1	Solid
		2:1	Solid
		3:1	Liquid
		4:1	Liquid
		8:1	Liquid
Me	Flu	3:1	Liquid
		4:1	Liquid
		8:1	Liquid
Lin	Flu	3:1	Solid
		4:1	Liquid
		8:1	Liquid
Me	Ket	3:1	Liquid
		4:1	Liquid
		8:1	Liquid
Lin	Ket	3:1	Liquid
		4:1	Liquid
		8:1	Liquid

Me:IBU (3:1) was selected for further analysis since this molar ratio was already reported as a liquid at RT, as a IBU solubility and permeability enhancer, and was associated with antiproliferative activity [58,60].

Since the aim of this work is to evaluate the effect of different combinations of anti-inflammatory drugs with terpenes, it was chosen a similar molar ratio among the different systems for comparison purposes. The 8:1 molar ratio was not selected since at this ratio the amount of terpene is so high that could overcome the effect of the anti-inflammatory agent. Given that Lin:Flu (3:1) is solid at room temperature, the molar ratio 4:1 was selected for all systems. Except for Me:IBU where a 3:1 ratio was chosen according to its previous report and directly compared with Saf:IBU (3:1).

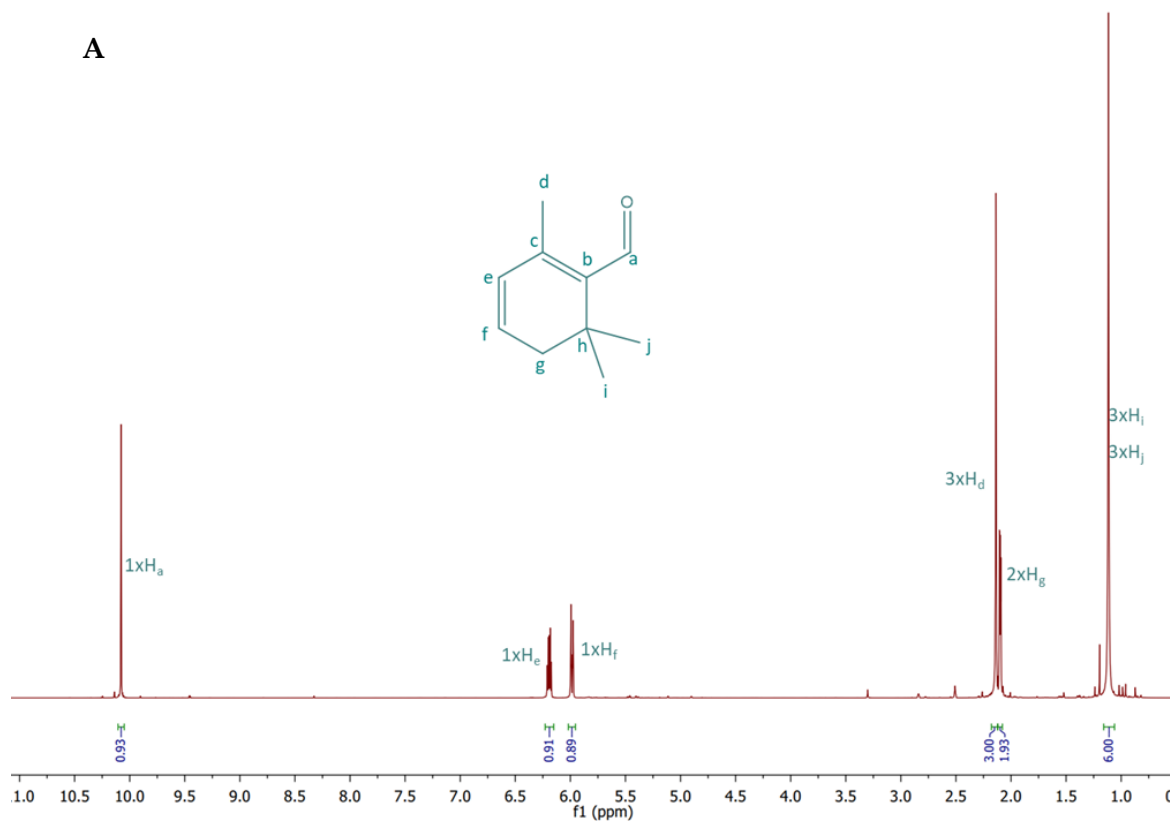
From the different prepared THEDES, Saf:IBU (3:1), Saf:IBU (4:1) Me:Flu (4:1), Lin:Flu (4:1), Me:Ket (4:1) and Lin:Ket (4:1) were chosen for further work since they are liquids at RT. Moreover, all these THEDES are also liquids at body temperature, a critical feature for the biological assays and further therapeutic applications.

## 4.2. NMR Studies

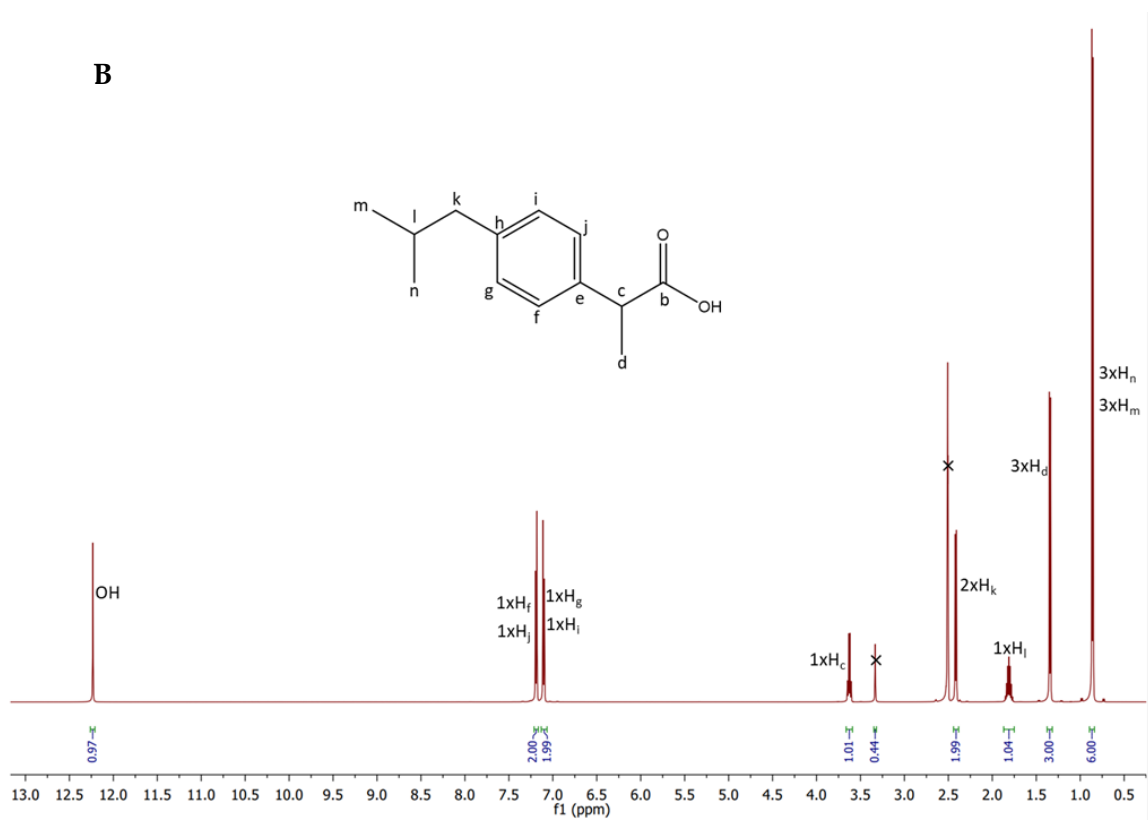
DES are combinations of two or more components, that, in a specific molar ratio, present a lower melting point than its individual elements. This phenomenon may be attributed to the charge delocalization resultant of the hydrogen bonding between a HBD and a HBA [3,47,48]. The H-bond is a result of a charge transfer between a HBA and a HBD that can be detected by Fourier transform infrared spectroscopy (FTIR) and NMR [48].

To characterize the THEDES in study and verify possible intermolecular interactions, usually assigned to DES, NMR spectroscopy was performed for the individual compounds (**Figure 4.1**) and the prepared THEDES (**Figure 4.2**).

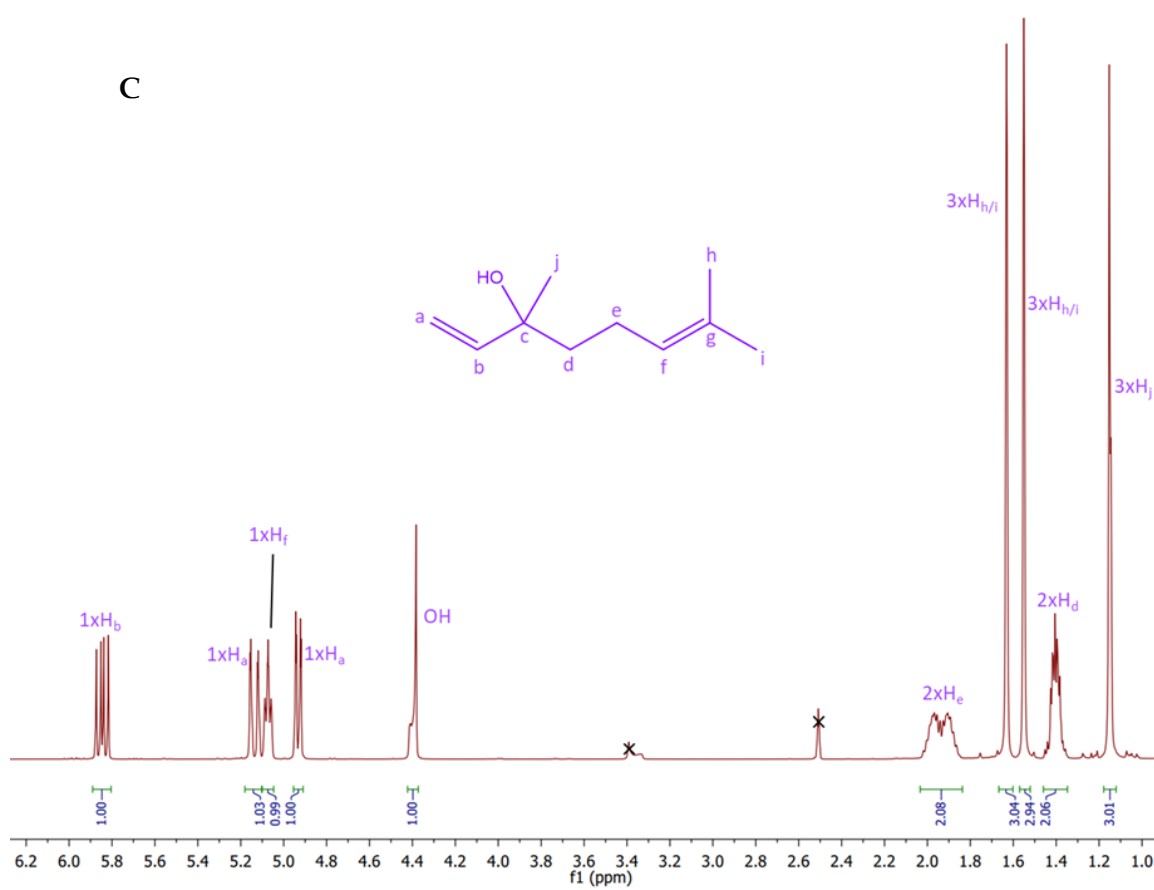
A



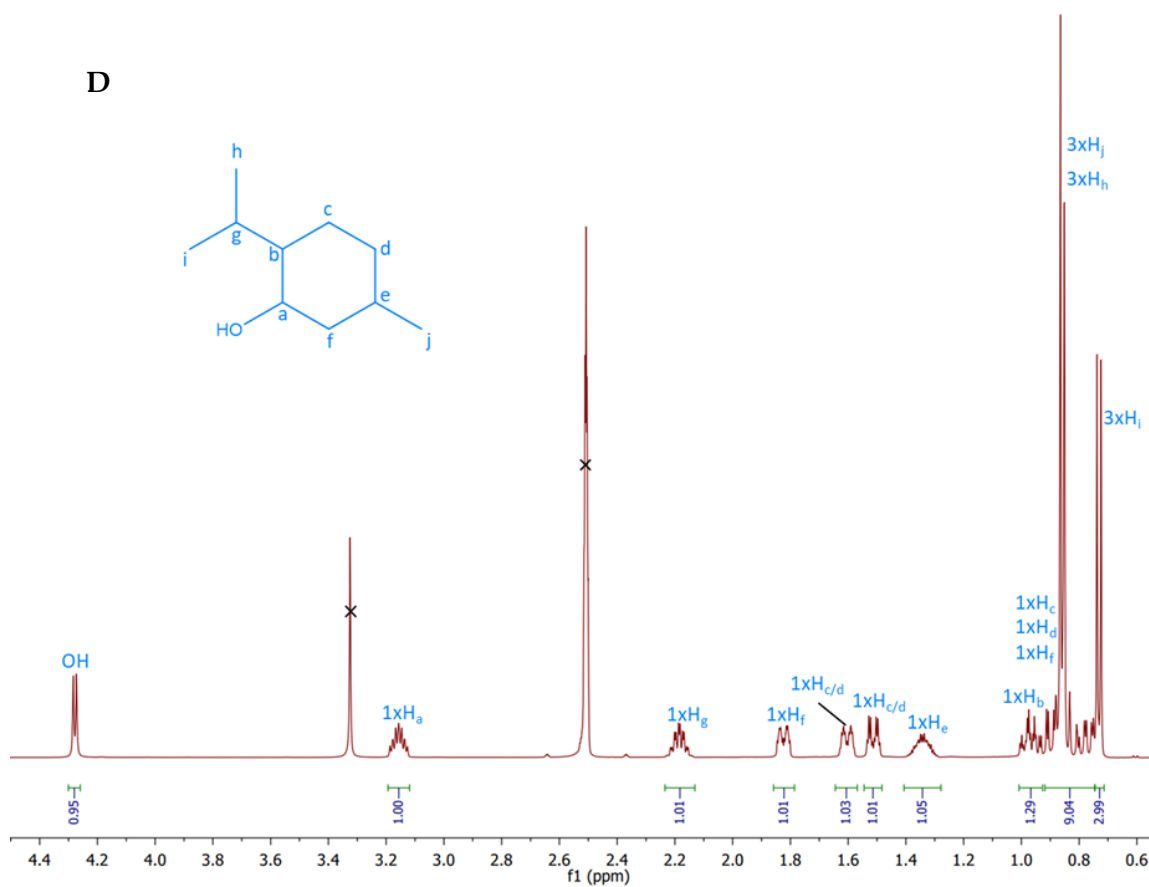
B

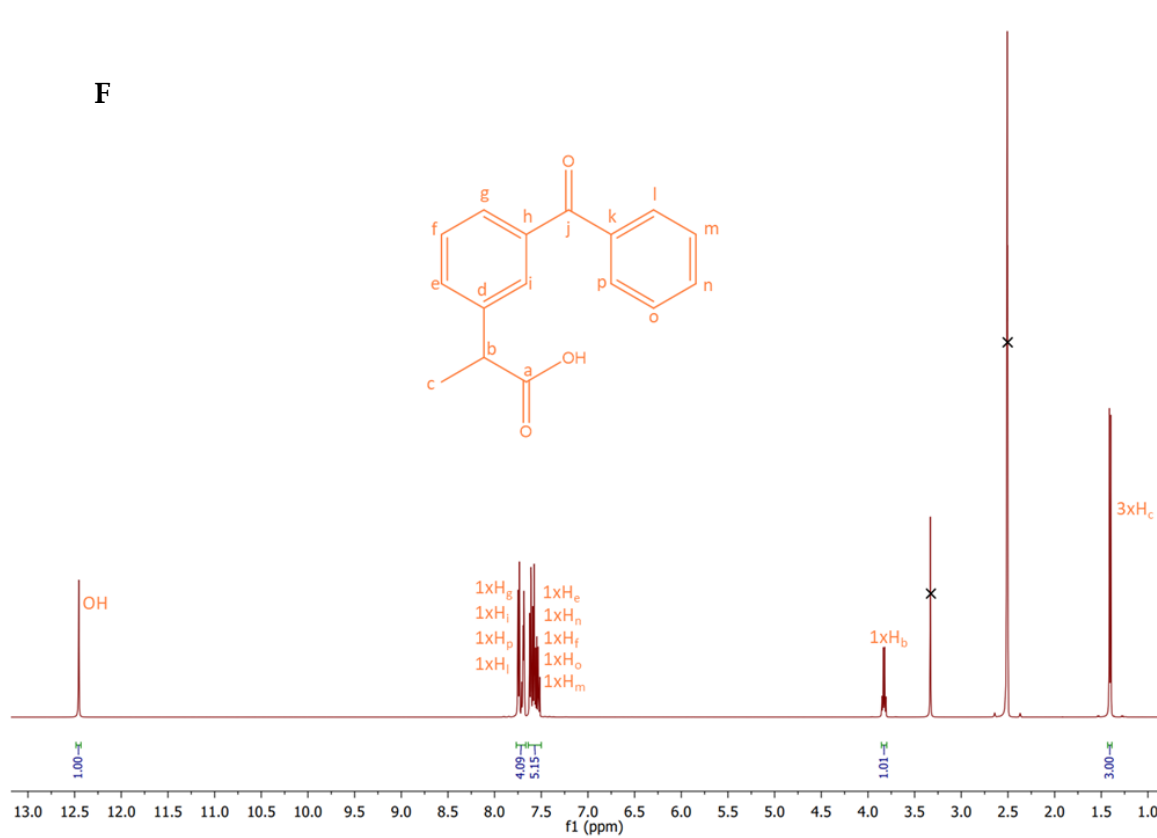
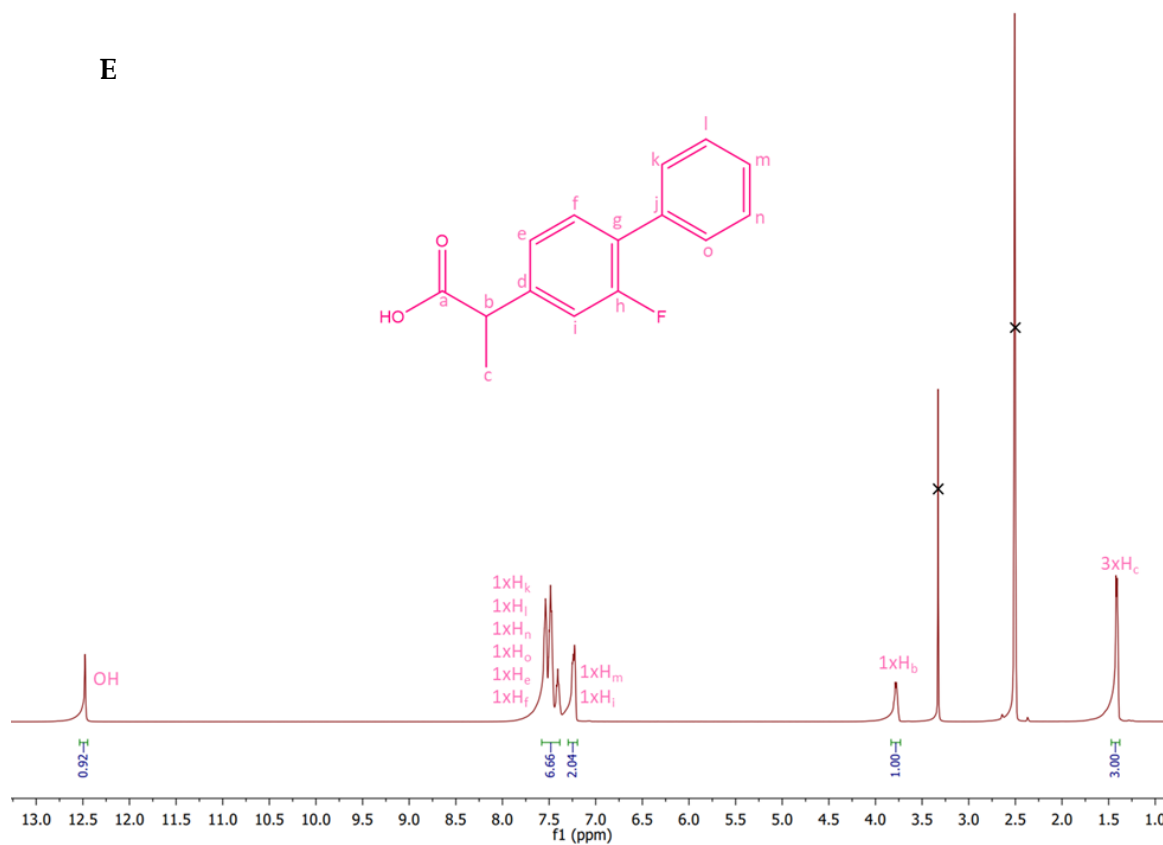


C

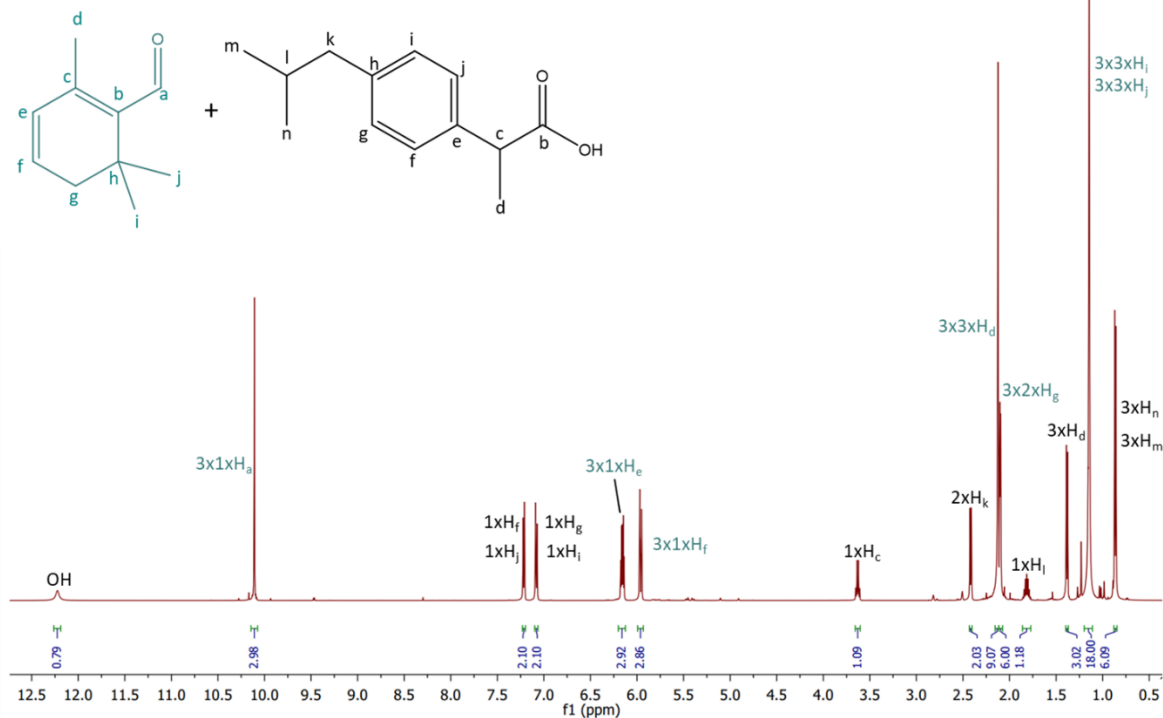
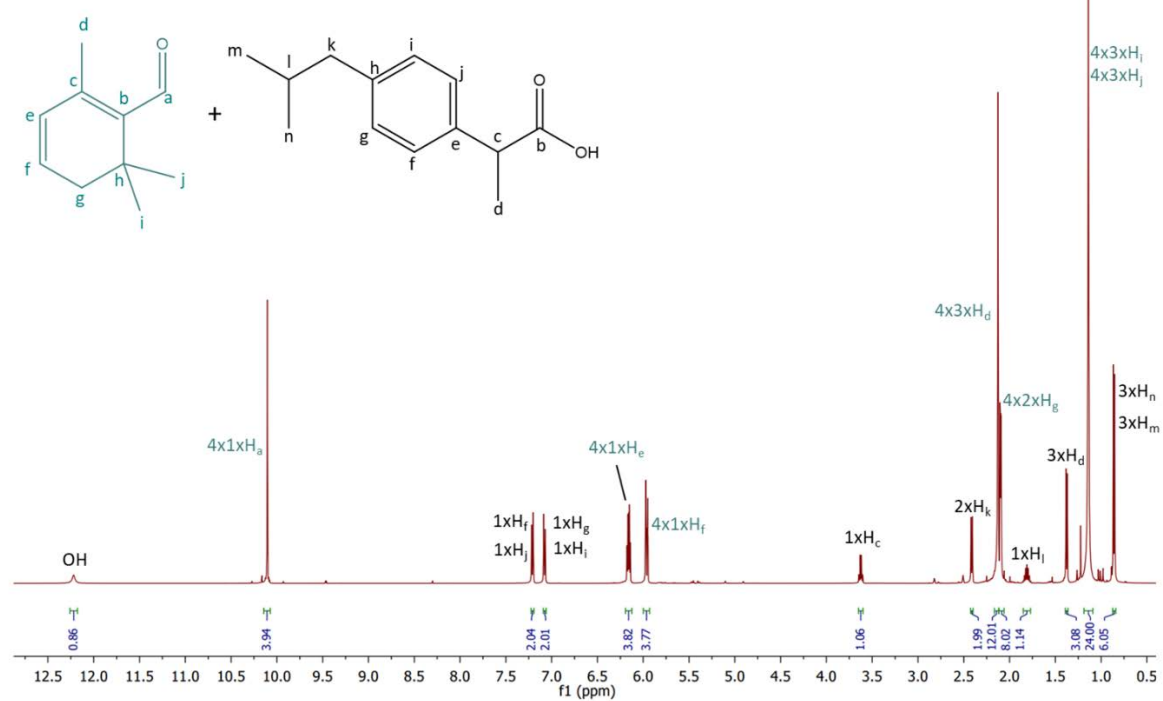


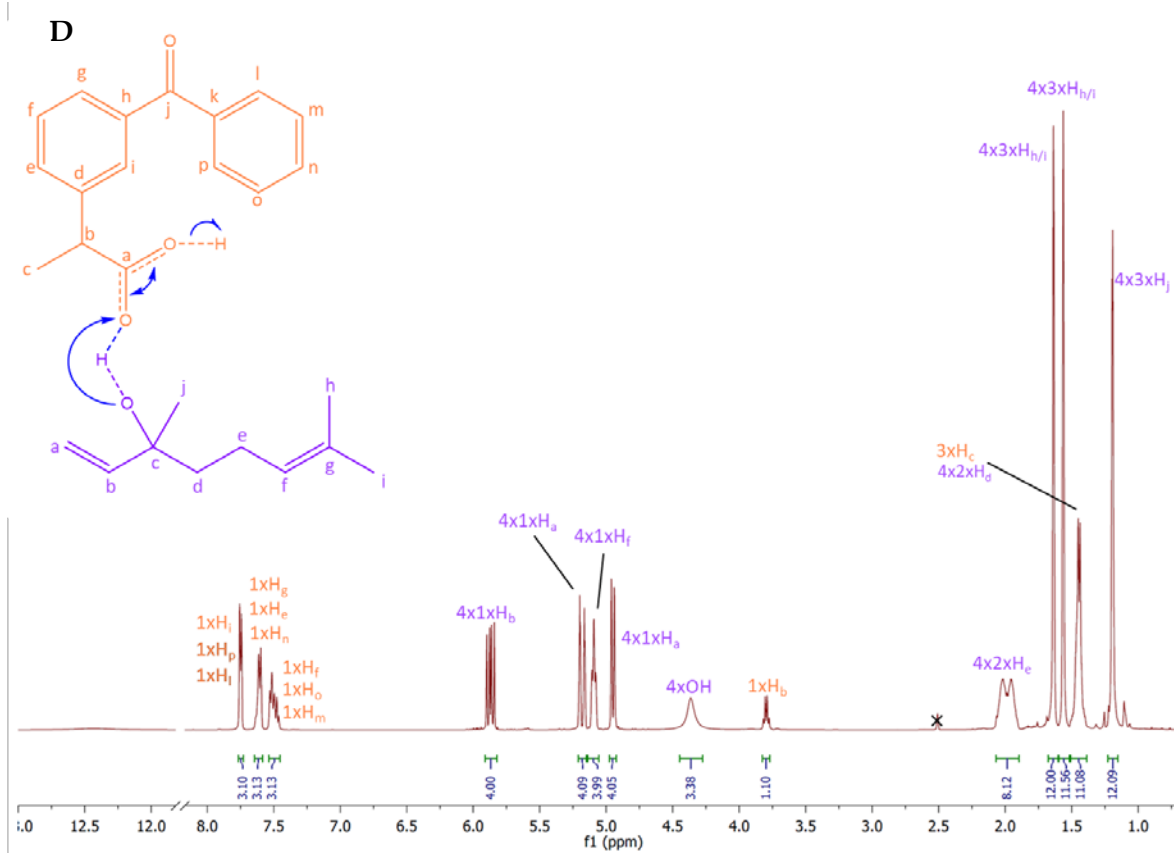
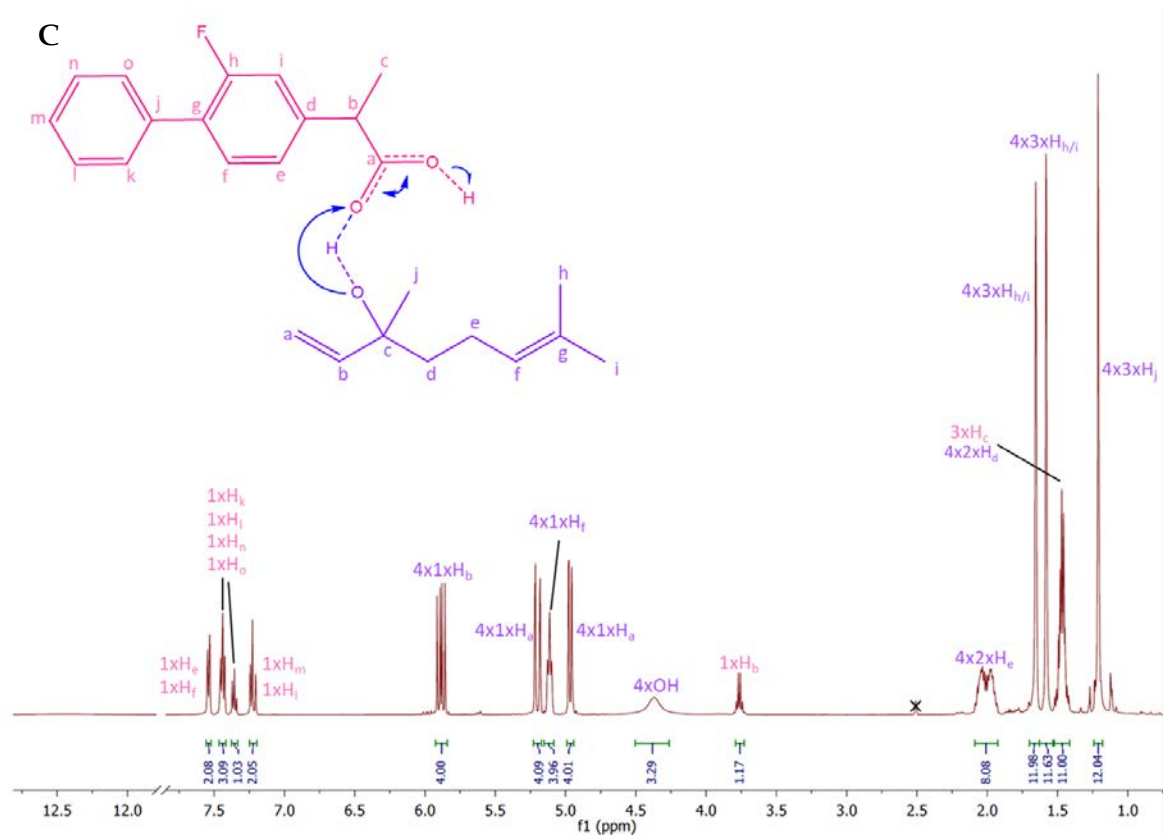
D





**Figure 4.1.** <sup>1</sup>H NMR spectra and pick assignment of (A) IBU, (B) Saf, (C) Lin, (D) Me, (E) Flu and (F) Ket. Samples prepared in DMSO-d<sub>6</sub>.

**A****B**



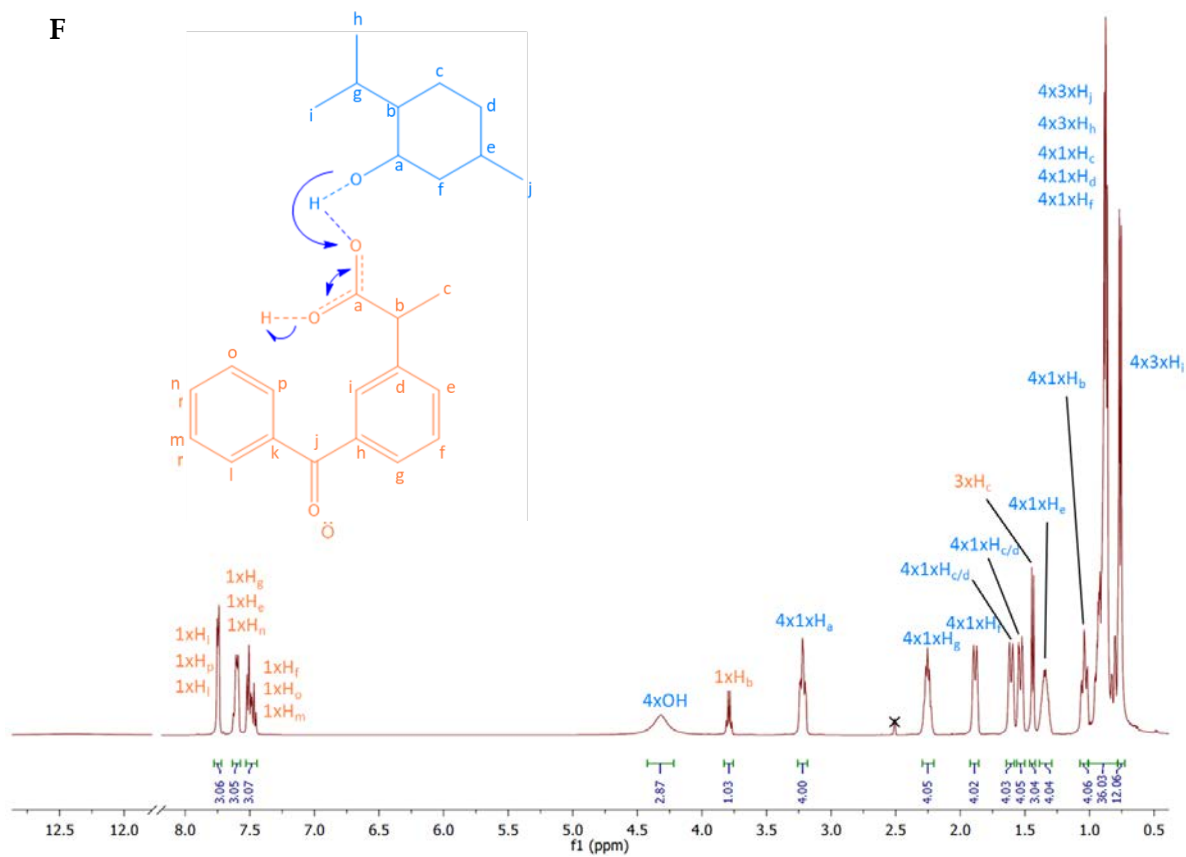
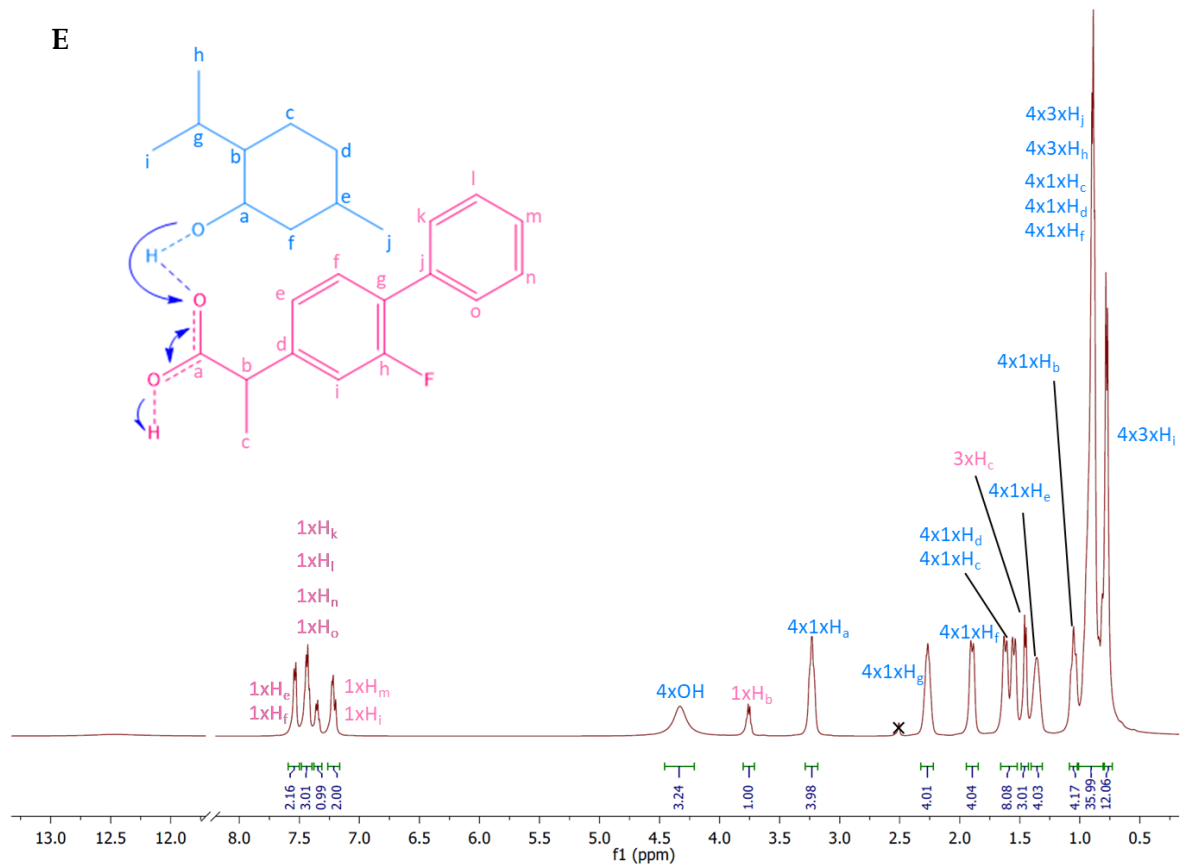


**Figure 4.2.** <sup>1</sup>H NMR spectra and signal assignment of THEDES (A) Saf:IBU (3:1), (B) Saf:IBU (4:1) (C) Lin:Flu (4:1), (D) Lin:Ket (4:1), (E) Me:Flu (4:1) and (F) Me:Ket (4:1). Samples prepared in DMSO-d<sub>6</sub>.



NMR is a technique commonly used to determine the presence of a concrete compound, analyse their purity, confirm mixture molar ratio and evaluate interactions (type of interactions and atoms involved) [50,52].

Looking at the individual compounds spectra it is possible to confirm their purity, since the spectra present in **Figure 4.1** for Saf, IBU, Lin, Me, Flu and Ket are in accordance with the previous reported in literature [60,138–141]. Additionally, it is possible to confirm THEDES molecular ratio since the signal integral values of the systems spectra increases proportionally to the molar ratio of the formulations (**Figure 4.2**).

The assignment of the signals was achieved by comparison with reported spectra, and also with HMBC spectra performed for all THEDES in study (**Figure A.1** of the Supplementary Information) and one homonuclear COSY obtained for Me:Flu (4:1) (**Figure A.2** of the Supplementary Information). Results present in the Supplementary Information.

Moreover, the existence of hydrogen bonding interactions can be verified in the spectra of Lin:Flu (4:1), Lin:Ket (4:1), Me:Flu (4:1) and Me:Ket (4:1). That is supported by the differences on the chemical signals of the Me and Lin hydroxyl group (-OH), that isolated is a multiple ( $\delta = 4.28$  ppm and  $\delta = 4.39$  ppm, respectively) (**Figure 4.1**), while in THEDES spectrum became a large singlet with  $\delta = 4.32$  ppm (**Figure 4.2**). This alteration in the spectra is an hallmark of hydrogen-bound interactions [142]. Furthermore, it is possible to observe a suppression of the signals corresponding to IBU, Flu and Ket's -OH when in THEDES form (**Figure 4.2**), which is also an indicative of the potential establishment of hydrogen bound interactions between the compounds in THEDES formulations.

The NMR analysis for Me:IBU (3:1) was well described by Eduardo Silva *et al.*, where the hydrogen interactions between Me and IBU are present, and suggest the formation of a DES [60].

These observations strongly indicate that hydrogen bond interactions are established between the Me or Lin hydroxyl groups, as hydrogen bond donors, and the Flu and Ket hydroxyl groups, as hydrogen bond acceptors. To additionally support these conclusions,  $^1\text{H}$ - $^1\text{H}$ -NOESY spectroscopy was performed (**Figure 4.3** and **Figure A.3** of the Supplementary Information), where physical proximity between the -OH groups of the THEDES' compounds was observed.

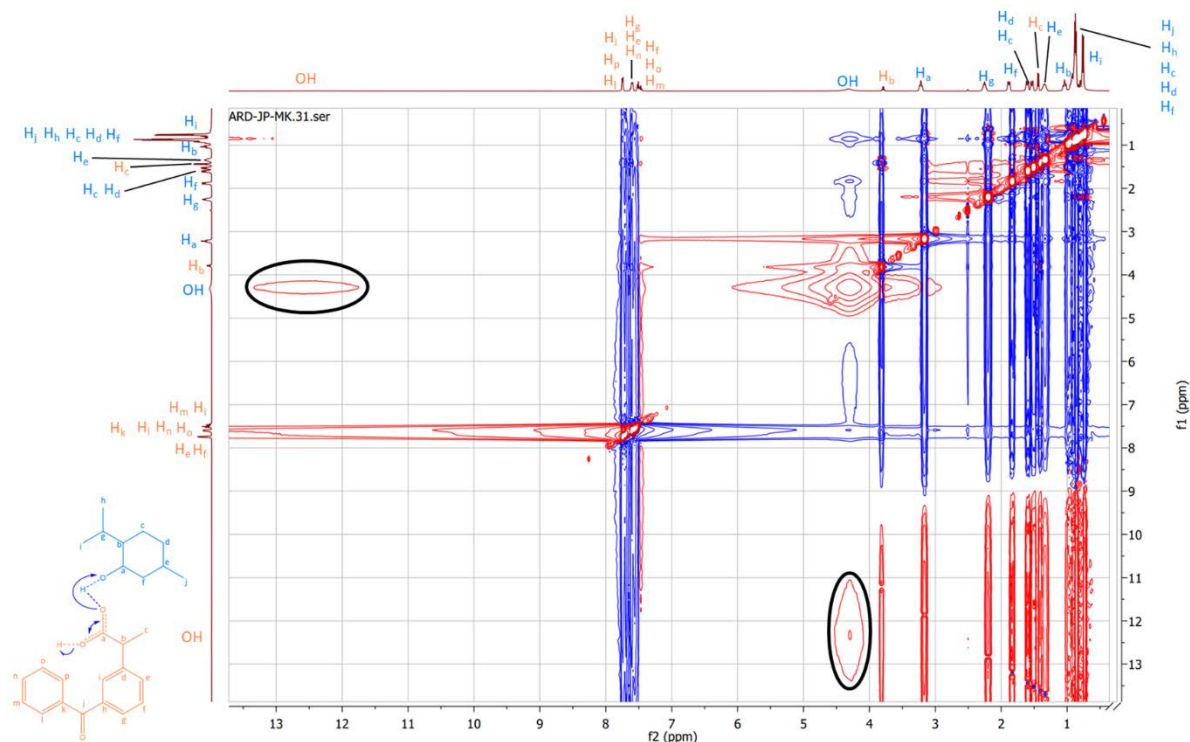


**Figure 4.3.** NOESY NMR spectra, signal assignment and interactions assignment of THEDES Me:Ket (4:1). Samples prepared in DMSO-d<sub>6</sub>.

For Saf:IBU (3:1) and Saf:IBU (4:1) these interactions are, however, not observed. Other interactions may occur, such as Van der Waals interactions. Additionally, it has already been reported eutectic systems that did not show interactions observed by NMR spectroscopy, but it was verified that its bioactivity was different comparing with its physical mixture, hence complying with the hypothesis that the THEDES are more than a physical mixture of two components [56]. Therefore, Saf:IBU-based systems need to be further analyzed in the future.

### 4.3. POM

Morphological characterization of THEDES was performed with POM. [52]. Eutectic mixtures were observed under polarized light that allows the detection of crystals. This provide an indication of an homogeneous and amorphous mixture [52].

The results obtained are present on **Figure 4.4**, and it is observable for all THEDES a black image, which reveals an amorphous and homogeneous liquid. This indicates a successful production of THEDES since no solid-like crystals are present, as expected for an eutectic mixture [143,144].

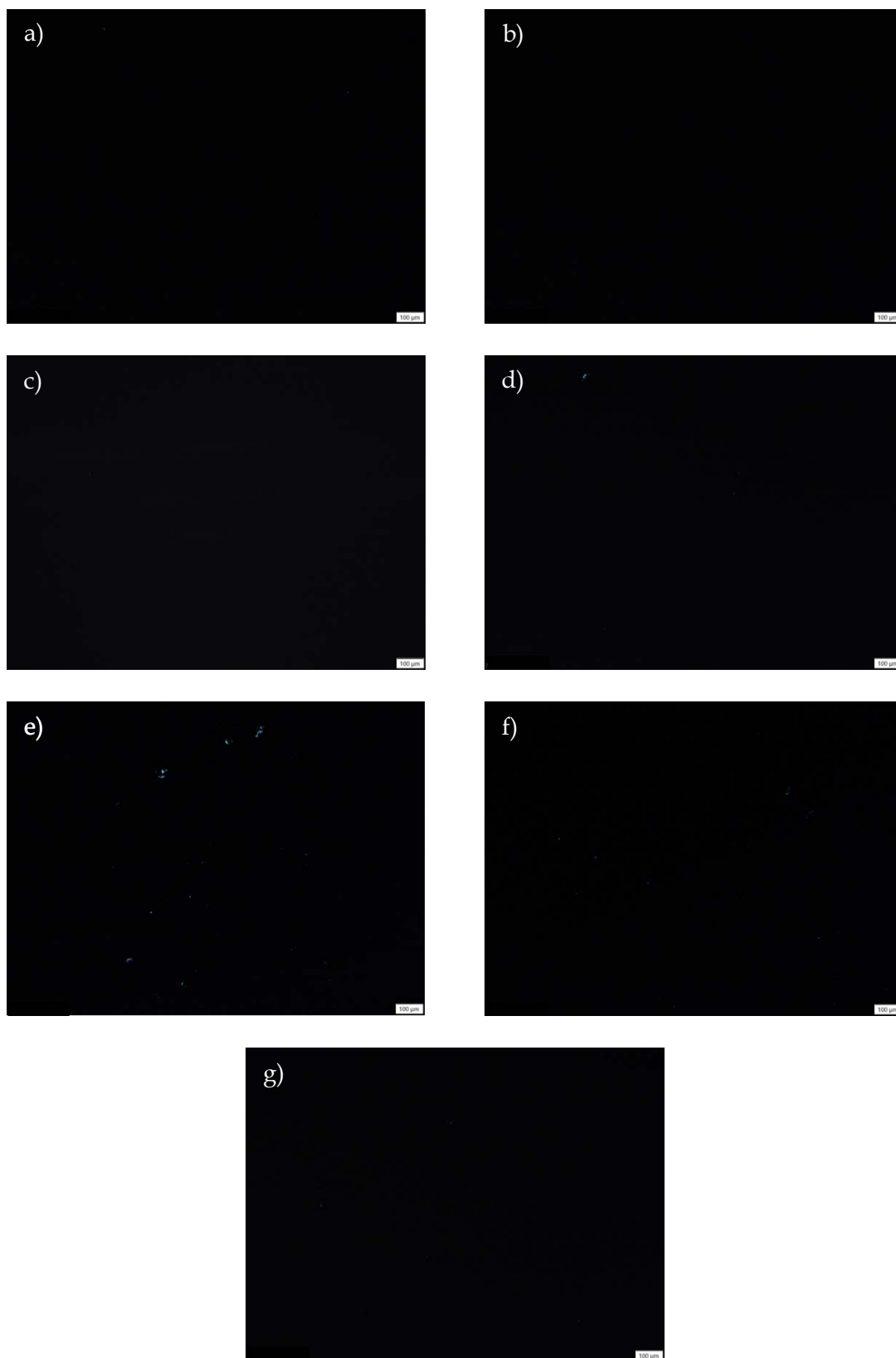


**Figure 4.4.** POM results obtained for a) Lin:Flu (4:1), b) Lin:Ket (4:1), c) Me:Flu (4:1), d) Me:Ket (4:1), e) Saf:IBU (3:1), f) Saf:IBU (4:1) and g) Me:IBU (3:1).

The main advantages of having an amorphous structure, is the absence of polymorphisms and the possibility to increase API solubility and permeability, since there is

a physical and morphologic change of the compound. Thus, these eutectic systems have been reported for drug bioavailability and transdermal delivery enhancement [52,54,58]. All these features, especially the amorphous structure obtained, are important for the pharmaceutical field and the development of more efficient drugs.

#### 4.4. NSAIDs Solubility and Permeability Assessment

NSAID efficacy as a therapeutic agent is highly dependent on its bioavailability. This is defined by its capacity to be soluble in physiological medium, and to be able to permeate tissues and cells membranes considering its administration route and the specific target. The maximum therapeutic efficacy occurs when these compounds present maximum permeability and solubility at the site of absorption [52,54,145].

Since DES are known to increase solubility and permeability of poorly soluble molecules, with reports on API's solubility and permeability improvement in PBS at 37 °C (physiologically-like condition) [52,54,58], it was hypothesized that eutecticity of combinations of NSAIDs with terpenes would promote the bioavailability enhancement. The quantitative determination of solubility and permeability was performed and the results are present on **Figure 4.5** and **Table 4.2** and **Figure 4.6** and **Table 4.3**, respectively.

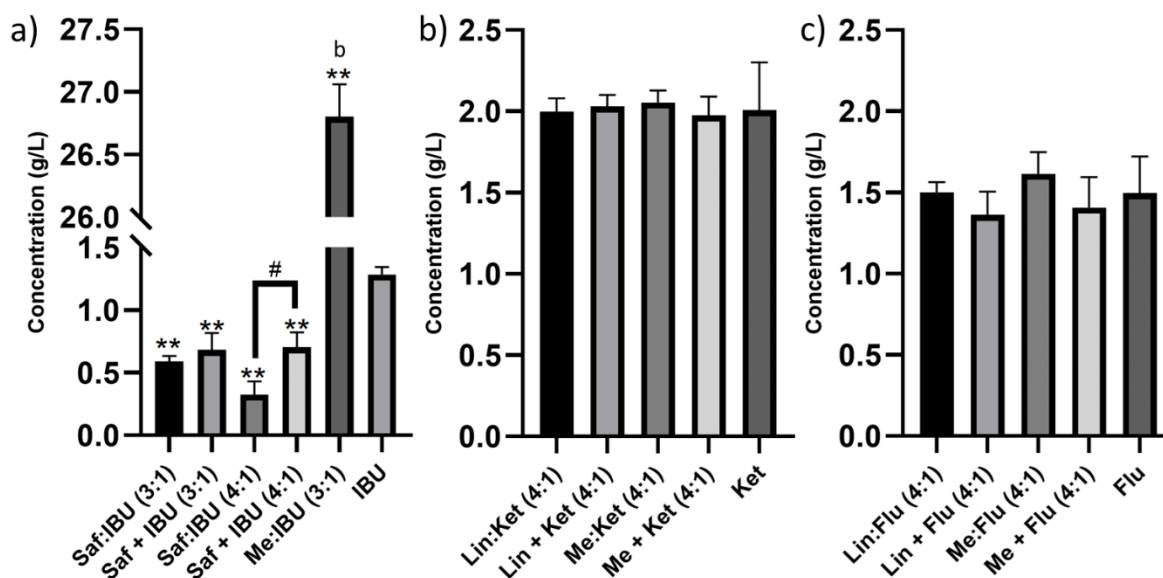


**Figure 4.5.** Solubility results obtained for the NSAIDs in pure form, in THEDES form and as a physical mixture. a) Solubility results for IBU and IBU containing systems. b) Solubility results for Ket and Ket containing systems. c) Solubility results for Flu and Flu containing systems. Results were performed in triplicate. <sup>b</sup> Valour retrieved from [58]. Data indicated as mean + SD (Standard deviation). \* $p < 0.05$  and \*\* $p < 0.01$ . "##" - statistical significance compared with the control. "#" - statistical significance between different conditions.

**Table 4.2.** Solubility results obtained for NSAIDs in pure form, in THEDES form and as a physical mixture. Results were performed in triplicate. Data indicated as mean + SD. <sup>b</sup> Valour retrieved from [58].

Solubility (g/L)		Solubility (g/L)	
IBU	1.28 ± 0.06	Ket	2.01 ± 0.30
Saf:IBU (3:1)	0.60 ± 0.04	Lin:Ket (4:1)	2.00 ± 0.08
Saf+IBU (3:1)	0.68 ± 0.14	Lin+Ket (4:1)	2.03 ± 0.07
Saf:IBU (4:1)	0.32 ± 0.11	Me:Ket (4:1)	2.06 ± 0.07
Saf+IBU (4:1)	0.70 ± 0.12	Me+Ket (4:1)	1.97 ± 0.12
Me:IBU (3:1)	26.80 ± 2.62 <sup>b</sup>		

Solubility (g/L)	
Flu	1.50 ± 0.22
Lin:Flu (4:1)	1.50 ± 0.06
Lin+Flu (4:1)	1.36 ± 0.14
Me:Flu (4:1)	1.62 ± 0.13

The solubility results show that despite being in a eutectic formulation, Lin:Ket, Me:Ket, Lin:Flu and Me:Ket, the respective NSAIDs solubility was not affected when compared with the APIs in powder. Additionally, Me:IBU (3:1) were capable to increase IBU solubility by 21x, in contrast to Saf-based THEDES that decreased IBU solubility.

The decreased in IBU solubility in the Saf-based THEDES seems to be related with the presence of safranal, since the physical mixtures also reveal an IBU solubility decrease. Interestingly, a difference in solubility between Saf:IBU (4:1) and its physical mixture is observable, which can indicate that Saf:IBU (4:1) acts as a different entity and not just a mixture of the two compounds.

Permeability was evaluated using a glass diffusion Franz cells with a PES-U membrane. Franz diffusion cells are a model used to assess skin permeability, since they enable the assessment of the relationship between skin, drug and formulation. These cells can be prepared with human or animal skin or with synthetic membranes when biological membranes are not available. The most used type of synthetic membranes are quality control membranes, called porous membranes, because of their porosity character. The FDA (Food and Drug Administration) has defined that porous synthetic membranes are appropriate to use for epithelial-like tissues formulation performance assessment, since they act as a support and are not rate-limiting barriers for drugs [146]. The porous membrane that we selected was PES-U that is a hydrophilic synthetic membrane, very stable in terms of oxidation, temperature and hydrolysis and with good mechanical properties and high flux [146–149]. However, it also presents a relative hydrophobic character [147], which can give it an amphipathic behaviour, mimicking better the cell membrane and the passive transport (diffusion of drug across tissue barriers and cell membrane [150]) through the plasm membrane.

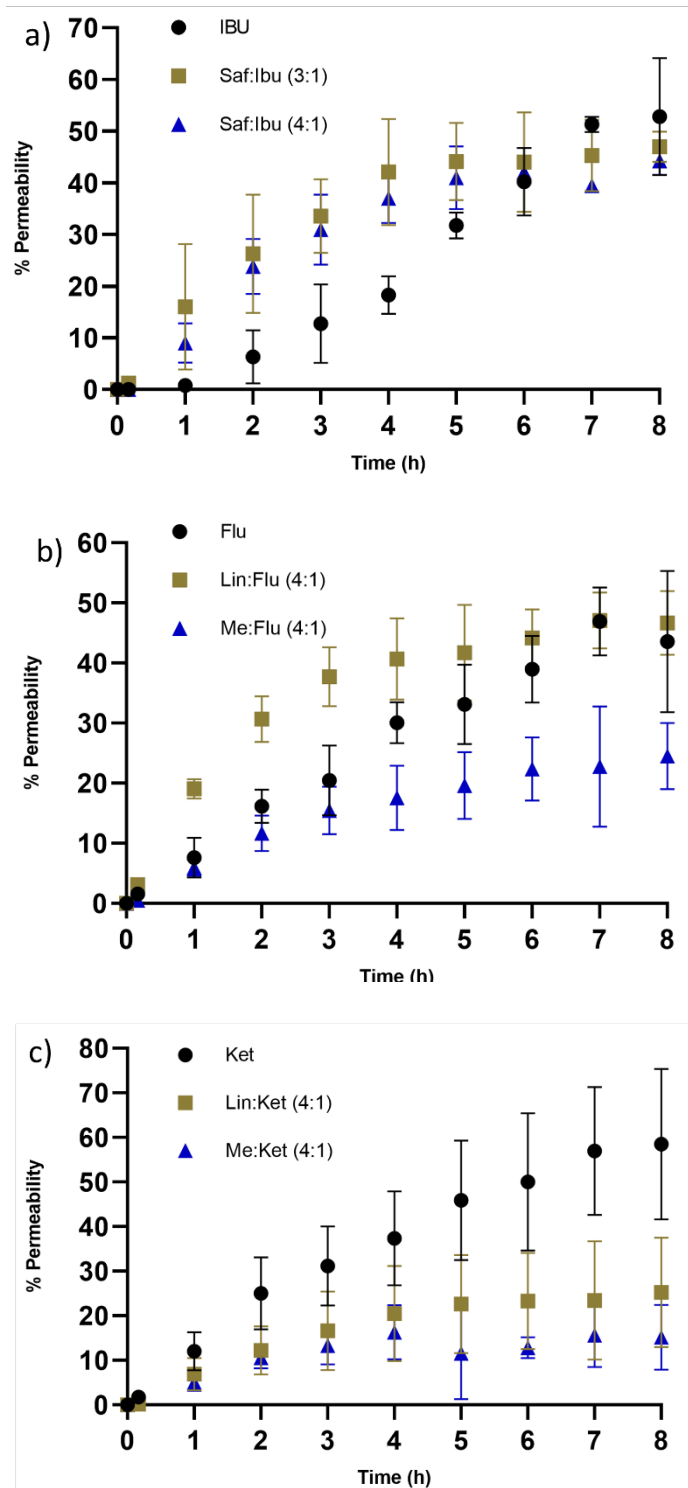


**Figure 4.6.** Permeability results obtained for the NSAIDs in pure form and in THEDES form. a) Permeability results for IBU and IBU containing systems. b) Permeability results for Ket and Ket containing systems. c) Permeability results for Flu and Flu containing systems. Results were performed in triplicate. Data indicated as mean + SD.

**Table 4.3.** Permeability results and diffusion coefficients obtained for the NSAIDs in pure form and in THEDES form. Results were performed in triplicate. Data indicated as mean + SD. <sup>b</sup> Valour retrieved from [58].

	Permeability (10 <sup>5</sup> cm s <sup>-1</sup> )	Diffusion coefficient (10 <sup>6</sup> cm <sup>2</sup> s <sup>-1</sup> )		Permeability (10 <sup>5</sup> cm s <sup>-1</sup> )	Diffusion coefficient (10 <sup>6</sup> cm <sup>2</sup> s <sup>-1</sup> )
IBU	3.52 ± 0.26	1.30 ± 0.22	Ket	6.40 ± 0.45	3.53 ± 0.26
Saf:IBU (3:1)	8.14 ± 0.73	3.41 ± 0.46	Lin:Ket (4:1)	3.54 ± 0.10	4.01 ± 0.85
Saf:IBU (4:1)	6.21 ± 0.43	3.11 ± 0.73	Me:Ket (4:1)	2.80 ± 0.06	3.24 ± 0.41
Me:IBU (3:1)	14.00 ± 1.53 <sup>b</sup>	4.32 ± 0.34 <sup>b</sup>			

	Permeability (10 <sup>5</sup> cm s <sup>-1</sup> )	Diffusion coefficient (10 <sup>6</sup> cm <sup>2</sup> s <sup>-1</sup> )
Flu	4.59 ± 0.20	2.86 ± 0.83
Lin:Flu (4:1)	8.08 ± 0.76	5.59 ± 0.18
Me:Flu (4:1)	2.80 ± 0.11	3.11 ± 0.40

Although solubility results did not show significant differences, except for Me:IBU (3:1), in the case of permeability the results show a different behaviour. Me:IBU (3:1) continues to be the THEDES with a greater capacity to increase IBU bioavailability, since it increases both IBU solubility and permeability. In contrast, Saf:IBU (3:1) and Saf:IBU (4:1), which did not show any differences in the solubility comparatively to the API alone, are able to increase IBU permeability (**Figure 4.6a** and **Table 4.3**).

Moreover, Me:IBU (3:1), Saf:IBU (3:1) and Saf:IBU (4:1) also increased the diffusion coefficients (**Table 4.3**) when compared with IBU in pure form, meaning that there is a faster diffusion of IBU through the membrane [143]. The diffusion coefficient correlates the amount of API diffused with time, therefore, higher diffusion coefficients mean faster diffusion of the API through the membrane [58].

In the case of Flu (**Figure 4.6b** and **Table 4.3**), Lin:Flu (4:1) had the capacity to increase Flu permeability and the diffusion coefficient, however, Me:Flu (4:1) was not able to increase Flu permeability, there is only a small increase on the diffusion coefficient, not statistically significant.

Although no increase in solubility were previously observed for Saf:IBU (3:1), Saf:IBU (4:1) and Lin:Flu (4:1), in terms of permeability the scenario changes, most likely due to the fact that terpenes are skin penetration-enhancing agents [63], allowing a greater permeability despite the maintenance or slight decrease of the solubilization capacity.

Looking at Ket permeability (**Figure 4.6c** and **Table 4.3**), THEDES present lower Ket permeability when compared to the pure compound, yet, in the case of Lin:Ket (4:1) a little non-significant increase of the diffusion coefficient is observable.

IBU that showed the lower solubility followed by Flu and then Ket, that was the most soluble, is the most permeable in THEDES formulations and Ket has shown no increase in its

permeability. This suggests that more lipophilic compounds are more permeable, as already reported by Vaishali Pade and Salomon Stavchansky [145].

Although, among terpenes, Me is known to be the most effective penetration enhancer [63,68], it seems that in our THEDES it is only capable to increase IBU permeability (Me:IBU (3:1)). For the other NSAIDs Lin seems to be a better penetration enhancer. In addition, for IBU, Safranal appears to be also a good penetration enhancer (**Table 4.3**).

The results obtained for IBU, Ket and Flu solubility and permeability are consistent with results previous reported [58,151–153], and variations can be related with differences in the membrane used, buffer media, quantification method and/or temperature at which the assay was performed.

With the results obtained for solubility and permeability we can fit the THEDES within the biopharmaceutical classification system (BCS). BCS is a classification system provided by FDA to serve as guideline to predict intestinal absorption. Drugs are classified in four classes, class I contain drugs that have high permeability and solubility, class II drugs have low solubility and high permeability, class III drugs present high solubility and low permeability, and class IV drugs are low soluble and permeable [52]. Initially IBU, Ket and Flu were classified as class II APIs, meaning that they have low solubility and high intestine membrane permeability [58,154,155], unfortunately when combined in the THEDES form in study, the API still belongs to the class II, meaning that they need more than 250 mL to dissolve the hights recommended dose reported by World Health Organization (WHO) and present permeability results above  $6 \times 10^{-6}$  (cm s<sup>-1</sup>) [155,156]. Me:IBU (3:1) is the exception, because it increases both solubility and permeability, meaning that this THEDES can be classified as a class I biopharmaceutic [58], which is a great improvement for the biopharmaceutical field.

## 4.5. THEDES Cytotoxicity and Antiproliferative Effects

In order to evaluate the safety/toxicity, determine the anticancer potential, and assess the optimal dosage of THEDES as potential therapeutic agents, *in vitro* cell models were used. For that, it was necessary to test THEDES effect on cell viability towards two different cell lines, one representing normal intestine epithelial cells and the other colorectal cancer cells. This allows to investigate THEDES selectivity towards cancer cells and predict possible side-effects on non-target cells [59,157].

In this work, MTS cell viability assay was used in two different approaches. In the case of cytotoxicity, Caco-2 was used to assess the effect of THEDES on cell viability of normal intestine cells. This assay considers these cells as a confluent monolayer in the stationary phase of the cell growth curve. Thus, providing an indication of THEDES safety/toxicity. In the case of the antiproliferative assay, HT29 was used to evaluate THEDES effect on CRC cells proliferation, considering cells while they are in the log phase. Therefore, providing an indication of THEDES cytotoxicity towards cancer cells.

The results obtained for THEDES cytotoxicity and antiproliferative activity is present on **Table 4.4**. **Table 4.4** also presents the selectivity index (SI), which is a parameter calculated to express the efficacy of a therapeutic agent to inhibit a particular target while not compromising normal cells viability. This means that it reveals the therapeutic window



between antiproliferative activity and cytotoxic side effects, as a result of the ratio between the cytotoxicity and the antiproliferative effect of THEDES [51].

**Table 4.4.** Cytotoxicity and antiproliferative results obtained for THEDES and corresponding individual compounds. The results are expressed in terms of EC<sub>50</sub> and corresponding selectivity indexes. Results were obtained from three independent experiments performed in triplicate. <sup>c</sup> Values retrieved from [60]. <sup>d</sup> Value retrieved from [56]. NC - Not calculated. Data indicated as mean ± SD.

THEDES/Compounds	EC <sub>50</sub> (mM)		Selectivity Index
	Cytotoxicity	Antiproliferative	
Saf:IBU (3:1)	4.82 ± 1.48	0.85 ± 0.25	5.67
Saf:IBU (4:1)	5.87 ± 1.33	0.77 ± 0.27	7.62
Me:IBU (3:1)	8.92 ± 1.39 <sup>c</sup>	4.30 ± 0.71 <sup>c</sup>	2.53
Me:Ket (4:1)	0.97 ± 0.33	1.55 ± 0.45	0.63
Me:Flu (4:1)	1.46 ± 0.43	1.38 ± 0.48	1.06
Lin:Ket (4:1)	2.30 ± 0.69	3.89 ± 0.50	0.59
Lin:Flu (4:1)	2.37 ± 0.43	2.05 ± 0.33	1.16
IBU	2.89 ± 0.06 <sup>d</sup>	3.90 ± 1.12	0.74
Ket	9.44 ± 4.28	8.14 ± 0.97	1.16
Flu	7.26 ± 2.27	NC	-
Saf	0.029 ± 0.064	1.35 ± 0.50	0.02
Me	5.09 ± 0.73 <sup>c</sup>	4.31 ± 0.63 <sup>c</sup>	1.18
Lin	0.70 ± 0.41	NC	-

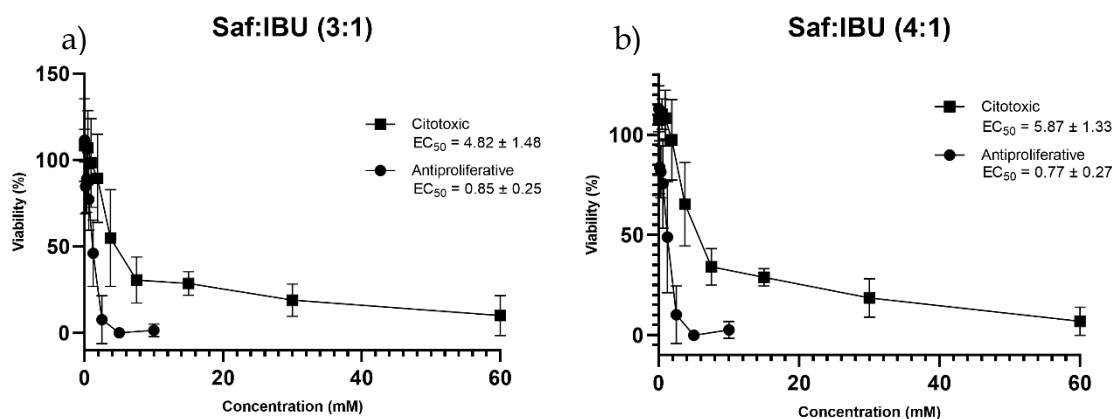


**Figure 4.7.** Cytotoxicity and antiproliferative viability curves obtained after Caco-2 and HT29 cells, respectively, had been exposed to different concentrations of a) Saf:IBU (3:1) and b) Saf:IBU (4:1).  $EC_{50}$  results indicated in the graphics. Results were expressed relatively to the control as the mean  $\pm$  SD of three independent experiments performed in triplicate.

Saf:IBU (4:1), Saf:IBU (3:1) and Me:IBU (3:1) are the THEDES with greater selectivity index (SI), respectively (**Table 4.4**). As an illustrative example, **Figure 4.7** represents the cytotoxicity and antiproliferative curves where the differences can be clearly observed. Therefore, the concentrations needed by Saf:IBU (4:1), Saf:IBU (3:1) and Me:IBU (3:1) to kill 50 % of cancer cells ( $EC_{50}$  - effective concentration) do not affect in a great extend normal intestine cells, due to a more specific action towards cancer cells.

The other THEDES, Me:Ket (4:1), Me:Flu (4:1), Lin:Ket (4:1) and Lin:Flu (4:1) (**Table 4.4**), also show antiproliferative effects in a dose-dependent manner but, in the same extent, also present cytotoxicity against Caco-2 cell line. Meaning that at the concentrations that these THEDES exercise their antiproliferative effect may also cause cell death in normal cells, not exhibiting a selectivity action for cancer cells and hence no therapeutic window can be defined for these systems.

Flu and Lin antiproliferative activities were not possible to calculate due to a deep decrease in cell viability as can be seen in **Figure A.4c** and **Figure A.4d** of the Supplementary Information, respectively.

It has been described that cell cytotoxicity is dependent on DES viscosity, concentration, pH, composition, and respective interaction of the individual compound with the different functional groups present on cell surface, and cell line requirements [59,144,158,159].

In order to evaluate if the antiproliferative and cytotoxic effect of THEDES was related with only one of the compounds or both, the individual compounds were dissolved separately in culture medium. Looking at the results obtained for the individual compounds, it is possible to see a very different action when compared with the same compounds in THEDES form. Most of them did not reveal a specific action against cancer cells, being toxic for both cell lines at the same extend. This suggests that when combined as a eutectic formulation these compounds represent a new entity with a different character and enhanced properties, being different from a simple mixture of the compounds. This can be explained by a synergetic or additive effect between the compounds, as previous reported [59,144,159], thus resulting in a more acute and selectivity action against cancer cells. Additionally, hydrogen bonding

between HBD and HBA affects both the system physical properties and chemical structure and, therefore, it could explain why the concentration of the individual compounds is not the only factor affecting cytotoxicity [51].

The decrease in cell viability in a THEDES concentration manner could also be related with a gradual decrease in pH, due to higher amounts of terpenes and NSAIDs, which do not have the optimal pH for mammalian cell (pH = 7-7.4). Additionally, higher THEDES concentration increases the viscosity of the media that can also affect cell viability, by influencing intracellular activity, like protein-protein interactions, transport of solutes and macromolecules, and signalling transduction [144,158].

Moreover, in the case of Me:IBU (3:1) the antiproliferative effect seems to be mostly associated with the presence of Me, which is in agreement with the fact that HBD as a significant role in the cytotoxic profile of the DES, maybe due to its greater effect on the acidity of the THEDES [158,159].

Menthol can act as anti-cancer agent dependently or independently of the presence of TRPM8. In the case of HT29 cells, it seems that they display loss of expression of TRPM Ca<sup>2+</sup> channels [160], therefore, probably Me acts in a TRPM8 independent way. In the case of Caco-2 cells the action of Me seems to be dose-dependent, since Caco-2 cells express TRPM8 and its activation by Me increases proliferation [70].

One possible mechanism proposed for the induction of cell death was described by Cornmell *et al.* that reported hydrophobic ionic liquids accumulation in cell membranes by interacting with negatively charged groups. This interaction may lead to the penetration of the negatively charged groups into the cytoplasm, compromising membrane integrity, through the increase of cell membrane permeability and fluidity, and consequent cell death [161].

The reason for Saf:IBU (3:1), Saf:IBU (4:1) and Me:IBU (3:1) specific action towards cancer cells may be due to membrane phospholipids constitution, since they are formed by a specific ratio of different functional groups (carboxyl, phosphate and amino groups) that differ from cell to cell. The proportion of these functional groups limits or increases the entry and rate of passage of extracellular elements, such as THEDES, to the cytoplasm. These proportional differences regulate the diffusion of THEDES and their effect on cellular machinery [158]. Moreover, the existence of different cell surface receptors, intracellular retention transport, drug uptake mechanisms or cancer rapidly dividing cells can also influence the effect of the THEDES [92,95].

## 4.6. LDH Release

Cell membrane integrity is fundamental for cell survival and could be the target of DES, inducing this way cell death [59]. Hence, cell membrane integrity was measured through the release of LDH to the extracellular medium.

Following a colorimetric assay to measure LDH release, the results obtained for the LDH release, after cells being exposed to different concentrations of the most promising THEDES previously described (Saf:IBU (3:1), Saf:IBU (4:1) and Me:IBU (3:1)), are present on **Figure 4.8**.

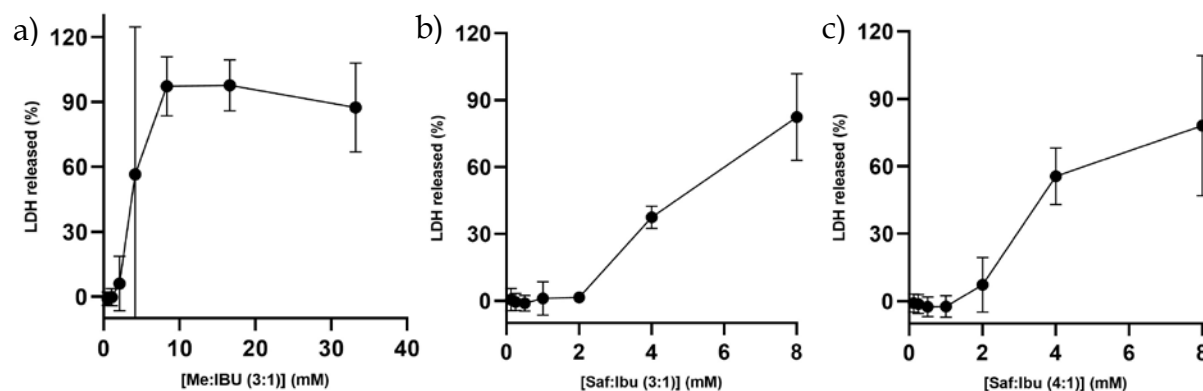


**Figure 4.8.** LDH released by HT29 cell line after being exposed to different concentrations of a) Me:IBU (3:1), b) Saf:IBU (3:1) and c) Saf:IBU (4:1). Results were obtained from three independent experiments performed in duplicate. Data indicated as mean  $\pm$  SD.

The results reveal that at Saf-based THEDES  $EC_{50}$  (Saf:IBU (3:1) 0.85 mM and Saf:IBU (4:1) 0.77 mM) the disruption of the cellular membrane is not the primary cause for their HT29 cell death, since only at much higher concentrations LDH release is observable. In contrast, when considering the results obtained for Me:IBU (3:1), it seems that it disrupts cellular membrane at  $EC_{50}$  value (4.30 mM) thus being a leading mechanism responsible for cell death.

From the observed LDH released to the extracellular medium, due to the disruption of HT29 cellular membrane, it is possible to see that different combinations of terpenes with NSAIDS exert different effects in cell viability. This means different pathways to reduce cancer cells proliferation may be involved, revealing the tailor-made therapeutic opportunities of eutectic systems.

## 4.7. THEDES Anti-inflammatory Effects

Inflammation is characterized by an increase of the production of ROS and RNS, that normally are produced to fight infections, but in tumour context they react and cause more mutations in proliferating cells, giving rise to point and structural mutations that result in higher malignancies, like angiogenesis [16,22]. Therefore, it is important to control the inflammation state to reduce cancer proliferation.

The THEDES in study are formed by a terpene (anticancer agent) and a NSAID (anti-inflammatory agent), thus, these systems have a double function, being capable to target cancer cells and control the inflammation originated during cancer development.

In order to evaluate the anti-inflammatory effects of the most promising THEDES previously described the presence/absence of intra ROS and NO were evaluated as well as the presence of the inflammatory marker IL-8.

### 4.7.1. Intracellular ROS e NO

To evaluate the production of intra ROS and the effect of the THEDES in controlling ROS production, cells were exposed to the most promising THEDES and their individual compounds, in order to evaluate if the intra ROS production was affected. HT29 cells are known for having elevated stress basal levels, presenting high levels of ROS production [162].

The results obtained for Saf:IBU (3:1), Saf:IBU (4:1) and Me:IBU (3:1), and their respective individual compounds are present on **Figure 4.9** and **Figure 4.10**.

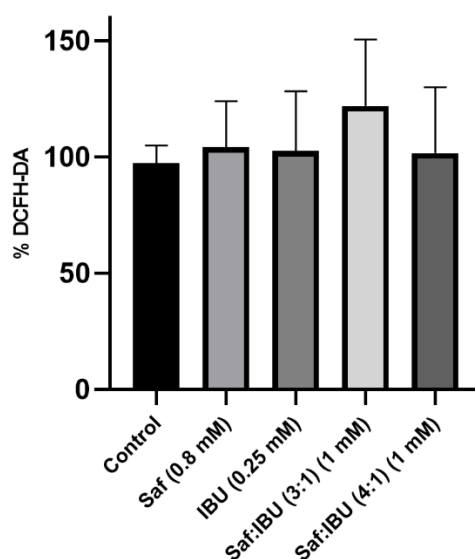


**Figure 4.9.** Intra ROS results obtained for the Saf:IBU (3:1) and Saf:IBU (4:1) in THEDES form and the respective individual compounds at the same concentration present in THEDES. Results were obtained from three independent experiments performed in triplicate. Data indicated as mean  $\pm$  SD.

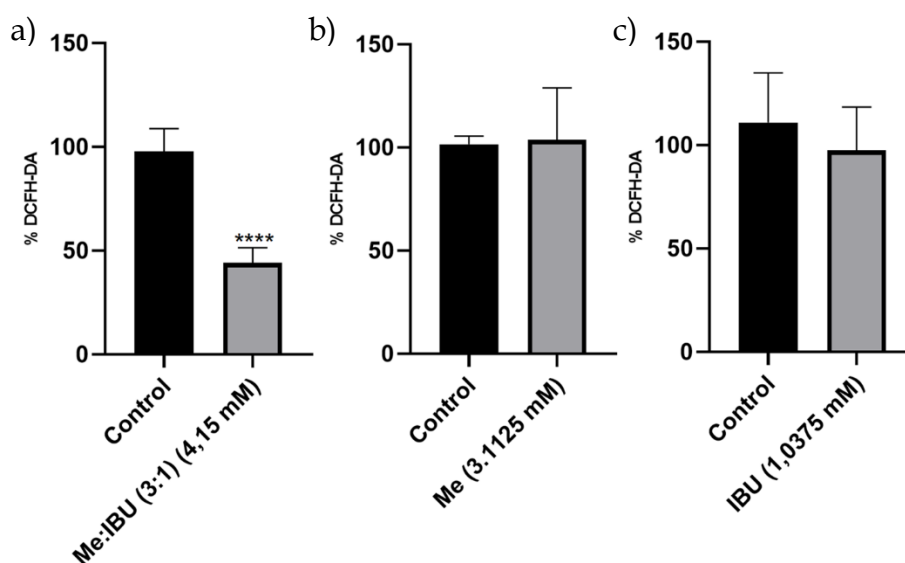


**Figure 4.10.** Intra ROS results obtained for the a) Me:IBU (3:1) in THEDES form and the respective individual compounds [b) Me and c) IBU] at the same concentration present in THEDES. Results were obtained from three independent experiments performed in triplicate. Data indicated as mean + SD. \*\*\*\* $p < 0.0001$ , as the statistical significance compared with the control.

Looking at **Figure 4.9**, Saf, IBU, Saf:IBU (3:1) and Saf:IBU (4:1) do not seem to influence ROS production at the concentrations tested. These concentrations correspond to the  $EC_{50}$  value of the THEDES, and to the corresponding individual compounds concentration. Therefore, Saf:IBU-based THEDES do not seem to act as anti-inflammatories and antiproliferative agents through ROS pathway. Suggesting that may act through other pathways previously reported for safranal, such as influencing NO production, induce cell cycle arrest,

apoptosis, inhibition of DNA and RNA synthesis, inhibition of tubulin assembly or interaction with topoisomerase II, inhibiting DNA repair [92,95,97,99,100].

In the case of Me:IBU (3:1) (**Figure 4.10**), it seems that this system have a role in diminishing intracellular ROS production to half, indicating a possible role as anti-inflammatory. Looking at the individual compounds, they do not influence ROS production, which highlights once more the difference between the individual compound action and their action in THEDES form.

Me:IBU (3:1) and the individual compounds were tested in different plates due to the high volatility, and consequent evaporation, of Me that influenced the results of the neighbouring wells, hence, the results are present in individual graphics (**Figure 4.10**).

In the case of assessing the influence of THEDES on NO production, the Griess method was applied. The results obtained did not reveal NO species. This assay is based on the reduction of nitrites to nitrogen oxide by Griess Reagent I (sulfanilamide), under acidic conditions, forming a diazonium salt that reacts with Griess Reagent II (N-(1 - naphthyl)ethylenediamine dihydrochloride), forming a stable purple azo dye that can be measure at 540 nm [163,164]. This method is very used due to its simplicity and rapidity [165]. However, there are many barriers to measure NO production, like low concentration, short half-life of NO and high reactivity with other molecules. Additionally, Griess method does not measure nitrate levels, only nitrite, being necessary an extra reduction step. Moreover, under the acidic conditions that this method is performed the formation of S-nitroso compounds from nitrites and reduced thiols is favoured, reducing the amount of nitrites available to react with Griess reagent [164,166]. From the absence of NO in the results obtained it can be hypothesized the inexistence of these reactive oxygen species production, or it can be due to lack of sensitivity of this method.

Other methods can be used, like the one described by Andreas Nussler *et al.* that allows the detection of nitrite and/or nitrate in a much sensitive range, based on the reaction of nitrites with 2,3-Diaminonaphthalene (DAN), under acidic conditions, to generate a fluorescent product [167]. Another method is based on GC-MS (gas chromatography coupled with mass spectroscopy) that allows an accurate measure of nitrites and nitrates since it uses stable isotope-labelled analogues of the anions as internal standards [165].

#### 4.7.2. IL-8 Measurement

To access the effect of Saf:IBU (3:1), Saf:IBU (4:1), Me:IBU (3:1) and the respective individual compounds on the expression of IL-8, an inflammatory marker, a sandwich ELISA was performed.

In order to quantify the amount of IL-8 present in the samples, a calibration curve with pure IL-8 was prepared and the best adjustment to the points was calculated. The calibration curves obtained for each plate are present on **Figure A.6** of the Supplementary Information.

Since the amount of protein produced by each cell is different, the results obtained for the quantification of IL-8 were normalized to the total amount of protein. To quantify the total amount of protein in the samples, a Bradford assay was performed.

In order to evaluate quantitatively the amount of protein in each sample, a calibration curve of BSA was prepared for each plate as present on **Figure A.7** of the Supplementary Information.

The results obtained for the IL-8 quantification by ELISA after normalization to the total amount of protein are present on **Figure 4.11**.

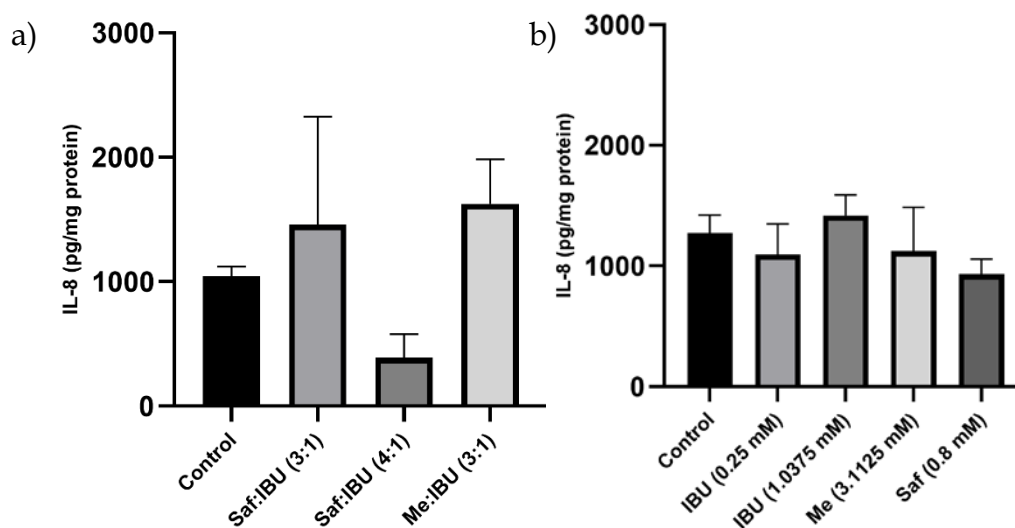


**Figure 4.11.** Concentration of IL-8 (pg/mg protein) after 24h of exposure to a) THEDES Saf:IBU (3:1), Saf:IBU (4:1) and Me:IBU (3:1) and to the respective individual compounds (b). Results were performed in triplicate. Data indicated as mean + SD.

In **Figure 4.11** it is possible to observe the results for the IL-8 concentration obtained from an experiment performed in triplicate. In the case of the individual compounds (**Figure 4.11b**) no significant differences are observed, suggesting that the individual compounds at these concentrations do not influence IL-8 production, and consequently do not affect cells inflammatory state. For the other THEDES (Saf:IBU (3:1) and Me:IBU (3:1)) (**Figure 4.11a**) no differences are observed compared with the control, suggesting no influences on the IL-8 production. Furthermore, although a decrease in Saf:IBU (4:1) is apparently observed (**Figure 4.11a**), which could mean a decrease on IL-8 expression and therefore a decrease of the inflammatory environment, from the statistical analysis no significant differences are observed.

Knowing that all the compounds, terpenes and NSAIDs, have been reported as presenting anti-inflammatory properties [68,79,89,105,106,122], and that these results came from only one experiment, further optimizations, such as in compounds concentration range, should be performed.

#### 4.8. Effects of THEDES on Apoptosis via Caspase-3

From the previous observed results, Saf:IBU (3:1), Saf:IBU (4:1) and Me:IBU (3:1) systems are involved in antiproliferative effects against colorectal cancer cells. In order to evaluate if this antiproliferative effect is related with the induction of apoptosis via caspase-3, cells were subjected to an apoptosis assay.

Cells were exposed to the EC<sub>50</sub> concentrations of the most promising THEDES, and to their individual compounds at the respective concentrations present in the THEDES. The results obtained are present in **Figure 4.12**. An induction of apoptosis is clearly observed for the systems in study when compared with the control. This suggests that the main action of THEDES towards cancer cells proliferation is through the induction of apoptosis via caspase-3. Interestingly, in the case of Saf:IBU-based THEDES that did not show any effect regarding intracellular ROS regulation or membrane disruption, it is possible to observe induction of apoptosis via caspase-3 that could be a main via by which these THEDES exercise their antiproliferative action.

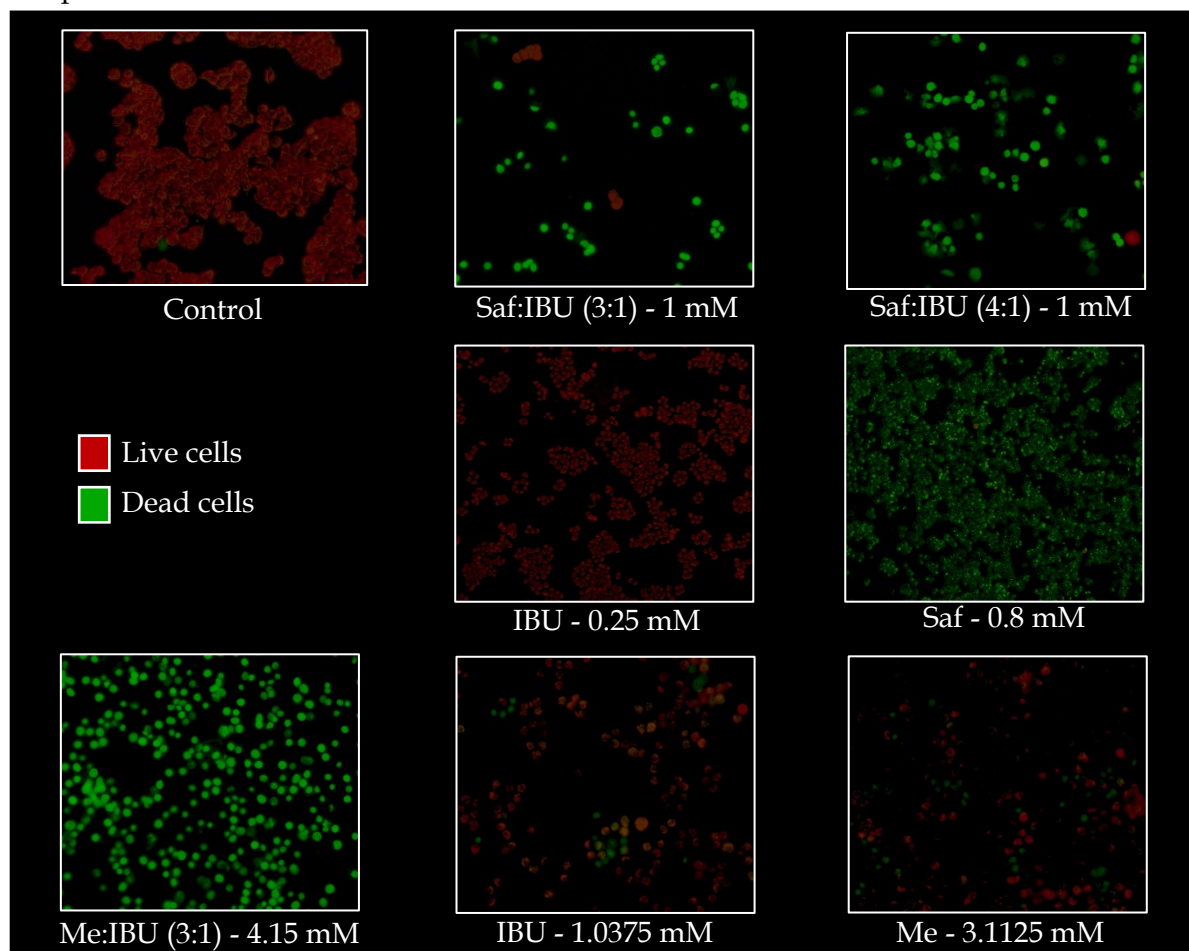


**Figure 4.12.** Results obtained for Saf:IBU (3:1), Saf:IBU (4:1), Me:IBU (3:1) and the respective individual compounds regarding apoptosis via caspase-3.

From these qualitative results, in the case of Saf:IBU (3:1) and Saf:IBU (4:1), it seems that these systems are able to induce apoptosis in cancer cells in a moderate way. Meaning that, if we look at Saf alone it is much more cytotoxic than the corresponding THEDES, and IBU does not induce any cell death via apoptosis at the concentrations studied. Therefore the eutectic systems act in a very different way, apparently equilibrating the induced cytotoxic effect, once more emphasizing the difference between the individual compound action and their action in THEDES form. This is important to reduce the side effects caused by Saf alone, since the main objective of this work is to create a safe patient-compliant therapeutic agent. Safranal has already been previously described as an inducer of apoptosis [93,99,100].



For Me:IBU (3:1) the results are different and more promising since the individual compounds do not induce apoptosis at these concentrations, and only when combined as THEDES are capable of increase cancer cells death. Menthol as already been reported as an inducer of cancer cells apoptosis dependently or independently of TRPM8 presence in a dose dependent manner [68,74]. Moreover, ibuprofen also inhibits cell growth of colon cancer cells through cell cycle block and apoptosis [110].

It is also reported that restoring apoptotic response is the principal mechanism by which NSAIDs prevent CRC. This can occur due to an increase concentration of arachidonic acid, that stimulates the production of ceramide, a potent apoptosis inducer, and alter mitochondrial permeability, causing cytochrome C release and consequent activation of caspase-9 and -3, leading to apoptosis [24,29,103].

Therefore, it seems that when the compounds are in THEDES form there is an increase of the antiproliferative effect via caspase-3, without affecting normal intestine cells.



## CONCLUSIONS

CRC remains as one of the most incident and deathly cancers urging the need for new therapeutic strategies to overcome its high mortality rate. Moreover, this new generation of cancer therapeutics should be a compromise of selectiveness towards the disease, while in compliance with the green chemistry metrics. Hence, the work developed during my master thesis aimed to be a contribution for the development of new THEDES that can act as a selective therapeutic agent against CRC.

For this matter, it was possible to create liquid formulations combining terpenes with NSAIDs. It was proved by NMR that most of the THEDES in study were in fact eutectic systems, due to the physical proximity of the compounds and existence of hydrogen bonding interactions. Specifically, in the case of Saf:IBU (3:1) and Saf:IBU (4:1) this was not verified, nevertheless weaker intermolecular interactions such as Van der Waals can be occurring.

Through POM analysis it was possible to verify the absence of crystals, meaning that we are in the presence of amorphous systems.

In terms of solubility, only Me:IBU (3:1) was capable to increase IBU solubility. In terms of permeability, all IBU-based THEDES increased this API permeability when compared with the pure compound. Additionally, Lin:Flu (4:1) revealed the same trend of increasing Flu permeability.

THEDES impact on cell viability - cytotoxicity and antiproliferative effects - revealed three systems with promising results, by inhibiting cancer cells proliferation without affecting normal intestine cells viability. Me:IBU (3:1), Saf:IBU (3:1) and Saf:IBU (4:1) presented the best selectivity indexes.

To evaluate the hypothetical mechanism behind such selective cytotoxic action towards cancer cells, LDH release, ROS production, IL-8 synthesis and caspase-3 activity were evaluated. LDH release increased in a dose-dependent manner for Me:IBU (3:1), Saf:IBU (3:1) and Saf:IBU (4:1). The Me-based system was able to increase LDH release at the EC<sub>50</sub> concentration, thus, providing evidences that LDH release may be one of the mechanisms behind the antiproliferative action of Me:IBU (3:1).

In the case of ROS production, only Me:IBU (3:1) was able to diminish ROS concentration produced by HT29 cells, indirectly suggesting an anti-inflammatory effect of Me:IBU (3:1). Interestingly, the individual compounds did not influence ROS production at

the tested concentrations, highlighting the difference between a eutectic system and its individual compounds action. In the case of Saf:IBU (3:1) and Saf:IBU (4:1) no alterations were observed in ROS production, meaning that other mechanisms may be behind these systems action.

In terms of IL-8 expression, the preliminary results did not reveal significant alterations. Further work in optimising this assay should be performed.

The three most promising THEDES revealed to be apoptosis inducers via caspase-3, suggesting this may be the main via for its antiproliferative action. In the case of Saf-based THEDES their effect is greater than IBU alone but minor than Saf alone, balancing its toxic effects. Considering Me:IBU (3:1), none of the individual compounds induced apoptosis at the tested concentrations, highlighting again the differences between the individual compounds and the eutectic system.

In conclusion, it was possible to create different THEDES with high value enhanced therapeutic properties, namely increased bioavailability and anticancer specific activity, suggesting lower side effects. Moreover, these results highlight the tailor-made characteristics of DES, since depending on the compounds that constitutes the DES different antiproliferative mechanisms are activated, which could ultimately lead to personalized therapeutics. Lastly, in the current scenario of an ongoing problematic situation related to cancer, along with the worldwide demand for alternative therapies, the claim for therapeutics with less side effects, improved efficacy but less expensive, and environmentally friendlier, has provided the opportunity to eutectics, to win its market share from the established pharmaceutical industry.

## BIBLIOGRAPHY

- [1] Bray F.; Ferlay J.; Soerjomataram I.; Siegel R.L.; Torre L.A.; Jemal A. Global Cancer Statistics 2018: GLOBOCAN Estimates of Incidence and Mortality Worldwide for 36 Cancers in 185 Countries. *CA. Cancer J. Clin.* **2018**, *68* (6), 394–424. doi: 10.3322/caac.21492
- [2] Madia F.; Worth A.; Whelan M.; Corvi R. Carcinogenicity assessment: Addressing the challenges of cancer and chemicals in the environment. *Environ. Int.* **2019**, *128*, 417–29. doi: 10.1016/j.envint.2019.04.067
- [3] Ahmad A.S.; Ormiston-Smith N.; Sasieni P.D. Trends in the lifetime risk of developing cancer in Great Britain: Comparison of risk for those born from 1930 to 1960. *Br. J. Cancer.* **2015**, *112* (5), 943–7. doi: 10.1038/bjc.2014.606
- [4] van de Haar J.; Hoes L.R.; Coles C.E.; Seamon K.; Fröhling S.; Jäger D.; et al. Caring for patients with cancer in the COVID-19 era. *Nat. Med.* **2020**, *26* (5), 665–71. doi: 10.1038/s41591-020-0874-8
- [5] Wilking N.E.; Brådvik G.; Lindgren P.; Christer S.; Jönsson B.; Hofmarcher T. A comparative study on costs of cancer and access to medicines in Europe | *OncologyPRO. J. Clin. Oncol.* **2020**, *38* (15\_suppl), e19051–e19051. doi: 10.1200/JCO.2020.38.15\_suppl.e19051
- [6] Hofmarcher T.; Lindgren P.; Wilking N.; Jönsson B. The cost of cancer in Europe 2018. *Eur. J. Cancer.* **2020**, *129*, 41–9. doi: 10.1016/j.ejca.2020.01.011
- [7] Park J.; Look K.A. Health Care Expenditure Burden of Cancer Care in the United States. *Inq. (United States).* **2019**, *56*, 46958019880696. doi: 10.1177/0046958019880696
- [8] Mariotto A.B.; Enewold L.; Zhao J.; Zeruto C.A.; Robin Yabroff K. Medical care costs associated with cancer survivorship in the United States. *Cancer Epidemiol. Biomarkers Prev.* **2020**, *29* (7), 1304–12. doi: 10.1158/1055-9965.EPI-19-1534
- [9] Ó Céilleachair A.; Costello L.; Finn C.; Timmons A.; Fitzpatrick P.; Kapur K.; et al. Inter-relationships between the economic and emotional consequences of colorectal cancer for patients and their families: A qualitative study. *BMC Gastroenterol.* **2012**, *12*, 62. doi: 10.1186/1471-230X-12-62
- [10] Coyne E.; Frommolt V.; Salehi A. The experience and challenges of rural persons with cancer and their families. *Collegian.* **2019**, *26* (6), 609–14. doi: 10.1016/j.colegn.2019.10.002
- [11] Haraldstad K.; Wahl A.; Andenæs R.; Andersen J.R.; Andersen M.H.; Beisland E.; et al. A systematic review of quality of life research in medicine and health sciences. *Qual. Life Res.* **2019**, *28* (10), 2641–50. doi: 10.1007/s11136-019-02214-9
- [12] Tarar A.H.; Shaloom A. Cancer and Quality of Life: Importance of Gender and Marital Adjustment in Psycho-Social Oncology. *Pak Armed Forces Med J.* **2020**, *70* (3), 734–9.
- [13] Oar A.; Moraes F.Y.; Romero Y.; Ilbawi A.; Yap M.L. Core elements of national cancer control plans: a tool to support plan development and review. *Lancet Oncol.* **2019**, *20* (11), e645–52. doi: 10.1016/S1470-2045(19)30404-8
- [14] Siegel R.L.; Miller K.D.; Jemal A. Cancer statistics, 2020. *CA. Cancer J. Clin.* **2020**, *1–24*. doi: 10.3322/caac.21590

- [15] Hanahan D.; Weinberg R.A. The hallmarks of cancer. *Cell*. **2000**, *100* (1), 57–70.
- [16] Hanahan D.; Weinberg R.A. Hallmarks of cancer: the next generation. *Cell*. **2011**, *144* (5), 646–74. doi: 10.1016/j.cell.2011.02.013
- [17] Helfinger V.; Schröder K. Redox control in cancer development and progression. *Mol. Aspects Med.* **2018**, *63*, 88–98. doi: 10.1016/j.mam.2018.02.003
- [18] Compton C. Cancer Initiation, Promotion, and Progression and the Acquisition of Key Behavioral Traits. In *Cancer: The Enemy from Within*; Springer: Cham, Switzerland, 2020; pp. 25–48. doi: 10.1007/978-3-030-40651-6\_2
- [19] Cooper G.M. The Development and Causes of Cancer. In *The Cell: A Molecular Approach. 6nd edition*; Sinauer Associates: Sunderland (MA), 2013; pp. 713–22.
- [20] Hennings H.; Glick A.B.; Greenhalgh D.A.; Morgan D.L.; Strickland J.E.; Tennenbaum T.; et al. Critical Aspects of Initiation, Promotion, and Progression in Multistage Epidermal Carcinogenesis. *Proc. Soc. Exp. Biol. Med.* **1993**, *202* (1), 1–8. doi: 10.3181/00379727-202-43511A
- [21] Micalizzi D.S.; Farabaugh S.M.; Ford H.L. Epithelial-mesenchymal transition in cancer: Parallels between normal development and tumor progression. *J. Mammary Gland Biol. Neoplasia*. **2010**, *15* (2), 117–34. doi: 10.1007/s10911-010-9178-9
- [22] Coussens L.M.; Werb Z. Inflammation and cancer. *Nature*. **2002**, *420* (6917), 860–867. doi: 10.1038/nature01322
- [23] Singh N.; Baby D.; Rajguru J.; Patil P.; Thakkannavar S.; Pujari V. Inflammation and cancer. *Ann. Afr. Med.* **2019**, *420* (6917), 860–7. doi: 10.4103/aam.aam\_56\_18
- [24] Lasry A.; Zinger A.; Ben-Neriah Y. Inflammatory networks underlying colorectal cancer. *Nat. Immunol.* **2016**, *17* (3), 230–40. doi: 10.1038/ni.3384
- [25] Labianca R.; Beretta G.D.; Kildani B.; Milesi L.; Merlin F.; Mosconi S.; et al. Colon cancer. *Crit. Rev. Oncol. Hematol.* **2010**, *74* (2), 106–33. doi: 10.1016/j.critrevonc.2010.01.010
- [26] Parkin D.M. Global cancer statistics in the year 2000. *Lancet Oncol.* **2001**, *2* (9), 533–43. doi: 10.1016/S1470-2045(01)00486-7
- [27] Terzić J.; Grivennikov S.; Karin E.; Karin M. Inflammation and Colon Cancer. *Gastroenterology*. **2010**, *138* (6), 2101–2114. doi: 10.1053/j.gastro.2010.01.058
- [28] Rhodes J.M.; Campbell B.J. Inflammation and colorectal cancer: IBD-associated and sporadic cancer compared. *Trends Mol. Med.* **2002**, *8* (1), 10–6. doi: 10.1016/S1471-4914(01)02194-3
- [29] Itzkowitz S.H.; Yio X. Inflammation and cancer - IV. Colorectal cancer in inflammatory bowel disease: The role of inflammation. *Am. J. Physiol. - Gastrointest. Liver Physiol.* **2004**, *287* (1), G7–17. doi: 10.1152/ajpgi.00079.2004
- [30] West N.R.; Mccuaig S.; Franchini F.; Powrie F. Emerging cytokine networks in colorectal cancer. *Nat. Rev. Immunol.* **2015**, *15*, 615–29. doi: 10.1038/nri3896
- [31] Pai S.G.; Carneiro B.A.; Mota J.M.; Costa R.; Leite C.A.; Barroso-Sousa R.; et al. Wnt/beta-catenin pathway: Modulating anticancer immune response. *J. Hematol. Oncol.* **2017**, *10* (1), 1–12. doi: 10.1186/s13045-017-0471-6
- [32] Colussi D.; Brandi G.; Bazzoli F.; Ricciardiello L. Molecular pathways involved in colorectal cancer: implications for disease behavior and prevention. *Int. J. Mol. Sci.* **2013**, *14* (8), 16365–85. doi: 10.3390/ijms140816365
- [33] Novellademunt L.; Antas P.; Li V.S.W. Targeting Wnt signaling in colorectal cancer. A review in the theme: Cell signaling: Proteins, pathways and mechanisms. *Am. J. Physiol. - Cell Physiol.* **2015**, *309* (8), C511–21. doi: 10.1152/ajpcell.00117.2015
- [34] Their J.P. Epithelial-mesenchymal transitions in tumor progression. *Nat. Rev. Cancer.* **2002**, *2* (6), 442–54. doi: 10.1038/nrc822
- [35] Ning Y.; Lenz H. Targeting IL-8 in colorectal cancer. *Expert Opin. Ther. Targets.* **2012**, *16* (5), 491–7.
- [36] Rubie C.; Frick V.O.; Pfeil S.; Wagner M.; Kollmar O.; Kopp B.; et al. Correlation of

IL-8 with induction, progression and metastatic potential of colorectal cancer. *World J. Gastroenterol.* **2007**, *13* (37), 4996–5002. doi: 10.3748/wjg.v13.i37.4996

[37] Chambers A.F.; Groom A.C.; MacDonald I.C. Dissemination and growth of cancer cells in metastatic sites. *Nat. Rev. Cancer.* **2002**, *2* (8), 563–72. doi: 10.1038/nrc865

[38] Kalluri R.; Weinberg R.A. The basics of epithelial-mesenchymal transition. *J. Clin. Invest.* **2009**, *119* (6), 1420–8. doi: 10.1172/JCI39104

[39] Anderson E.C.; Hessman C.; Levin T.G.; Monroe M.M.; Wong M.H. The role of colorectal cancer stem cells in metastatic disease and therapeutic response. *Cancers (Basel).* **2011**, *3* (1), 319–39. doi: 10.3390/cancers3010319

[40] Salibasic M.; Pusina S.; Bicakcic E.; Pasic A.; Gavric I.; Kulovic E.; et al. Colorectal Cancer Surgical Treatment, our Experience. *Med. Arch. (Sarajevo, Bosnia Herzegovina).* **2019**, *73* (6), 412–4. doi: 10.5455/medarh.2019.73.412-414

[41] Sun J.; Jiang T.; Qiu Z.; Cen G.; Cao J.; Huang K.; et al. Short-term and medium-term clinical outcomes of laparoscopic-assisted and open surgery for colorectal cancer: A single center retrospective case-control study. *BMC Gastroenterol.* **2011**, 11–85. doi: 10.1186/1471-230X-11-85

[42] De Crignis L.; Slim K.; Cotte E.; Meillat H.; Dupré A. Impact of surgical indication on patient outcomes and compliance with enhanced recovery program for colorectal surgery: A Francophone multicenter retrospective analysis. *J. Surg. Oncol.* **2020**, *122*, 928–33. doi: 10.1002/jso.26097

[43] Flynn D.E.; Mao D.; Yerkovich S.T.; Franz R.; Iswariah H.; Hughes A.; et al. The impact of comorbidities on post-operative complications following colorectal cancer surgery. *PLoS One.* **2020**, *15* (12), e0243995. doi: 10.1371/journal.pone.0243995

[44] Jana S.; Patra K.; Sarkar S.; Jana J.; Mukherjee G.; Bhattacharjee S.; et al. Antitumorigenic potential of linalool is accompanied by modulation of oxidative stress: An in vivo study in sarcoma-180 solid tumor model. *Nutr. Cancer.* **2014**, *66* (5), 835–48. doi: 10.1080/01635581.2014.904906

[45] Yuan H.; Ma Q.; Ye L.; Piao G. The Traditional Medicine and Modern Medicine from Natural Products. *Molecules.* **2016**, *21* (5), 559. doi: 10.3390/molecules21050559

[46] Kudłak B.; Owczarek K.; Namieśnik J. Selected issues related to the toxicity of ionic liquids and deep eutectic solvents – a review. *Environ. Sci. Pollut. Res.* **2015**, *22* (16), 11975–92. doi: 10.1007/s11356-015-4794-y

[47] Anastas P.; Eghbali N. Green Chemistry: Principles and Practice. *Chem. Soc. Rev.* **2010**, *39* (1), 301–12. doi: 10.1039/b918763b

[48] Del Monte F.; Carriazo D.; Serrano M.C.; Gutiérrez M.C.; Ferrer M.L. Deep eutectic solvents in polymerizations: A greener alternative to conventional syntheses. *ChemSusChem.* **2014**, *7* (4), 999–1009. doi: 10.1002/cssc.201300864

[49] Paiva A.; Craveiro R.; Aroso I.; Martins M.; Reis R.L.; Duarte A.R.C. Natural deep eutectic solvents - Solvents for the 21st century. *ACS Sustain. Chem. Eng.* **2014**, *2*, 1063–1071. doi: 10.1021/sc500096j

[50] Hansen B.B.; Spittle S.; Chen B.; Poe D.; Zhang Y.; Klein J.M.; et al. Deep Eutectic Solvents: A Review of Fundamentals and Applications. *Chem. Rev.* **2021**, *121* (3), 1232–85. doi: 10.1021/acs.chemrev.0c00385

[51] Oliveira F.S.N. de; Duarte A.R.C. A look on target-specificity of eutectic systems based on natural bioactive compounds. In *Advances in Botanical Research*; Academic Press Inc.: Cambridge, Massachusetts, United States, 2021; pp. 271–307. doi: 10.1016/bs.abr.2020.09.008

[52] Santos F.; Duarte A.R.C. Therapeutic Deep Eutectic Systems for the Enhancement of Drug Bioavailability. In *Deep Eutectic Solvents for Medicine, Gas Solubilization and Extraction of Natural Substances. Environmental Chemistry for a Sustainable World, vol 56*; Springer: Cham, Switzerland, 2021; pp. 103–29. doi: 10.1007/978-3-030-53069-3\_3

[53] Abbott A.P.; Boothby D.; Capper G.; Davies D.L.; Rasheed R.K. Deep Eutectic

Solvents formed between choline chloride and carboxylic acids: Versatile alternatives to ionic liquids. *J. Am. Chem. Soc.* **2004**, *126* (29), 9142–9147. doi: 10.1021/ja048266j

[54] Zainal-Abidin M.H.; Hayyan M.; Ngoh G.C.; Wong W.F.; Looi C.Y. Emerging frontiers of deep eutectic solvents in drug discovery and drug delivery systems. *J. Control. Release.* **2019**, *316*, 168–95. doi: 10.1016/j.jconrel.2019.09.019

[55] Craveiro R.; Aroso I.; Flammia V.; Carvalho T.; Viciosa M.T.; Dionísio M.; et al. Properties and thermal behavior of natural deep eutectic solvents. *J. Mol. Liq.* **2016**, *215*, 534–40. doi: 10.1016/j.molliq.2016.01.038

[56] Pereira C. V.; Silva J.M.; Rodrigues L.; Reis R.L.; Paiva A.; Duarte A.R.C.; et al. Unveil the Anticancer Potential of Limonene Based Therapeutic Deep Eutectic Solvents. *Sci. Rep.* **2019**, *9* (1). doi: 10.1038/s41598-019-51472-7

[57] Stott P.W.; Williams A.C.; Barry B.W. Transdermal delivery from eutectic systems: Enhanced permeation of a model drug, ibuprofen. *J. Control. Release.* **1998**, *50* (1–3), 297–308. doi: 10.1016/S0168-3659(97)00153-3

[58] Duarte A.R.C.; Ferreira A.S.D.; Barreiros S.; Cabrita E.; Reis R.L.; Paiva A. A comparison between pure active pharmaceutical ingredients and therapeutic deep eutectic solvents: Solubility and permeability studies. *Eur. J. Pharm. Biopharm.* **2017**, *114*, 296–304. doi: 10.1016/j.ejpb.2017.02.003

[59] Hayyan M.; Looi C.Y.; Hayyan A.; Wong W.F.; Hashim M.A. In Vitro and In Vivo Toxicity Profiling of Ammonium-Based Deep Eutectic Solvents. *PLoS One.* **2015**, *10* (2), e0117934.

[60] Silva E.; Oliveira F.; Silva J.M.; Reis R.L.; Duarte A.R.C. Untangling the bioactive properties of therapeutic deep eutectic solvents based on natural terpenes. *Curr. Res. Chem. Biol.* **2021**, *1*, 100003. doi: <https://doi.org/10.1016/j.crchbi.2021.100003>

[61] Paduch R.; Kandefer-Szerszeń M.; Trytek M.; Fiedurek J. Terpenes: Substances useful in human healthcare. *Arch. Immunol. Ther. Exp. (Warsz).* **2007**, *55* (5), 315–27. doi: 10.1007/s00005-007-0039-1

[62] Zwenger S.; Basu C. Plant terpenoids : applications and future potentials. *Biotechnol. Mol. Biol. Rev.* **2008**, *3* (1), 1–7. doi: 10.5897/BMBR

[63] Aqil M.; Ahad A.; Sultana Y.; Ali A. Status of terpenes as skin penetration enhancers. *Drug Discov. Today.* **2007**, *12* (23–24), 1061–7. doi: 10.1016/j.drudis.2007.09.001

[64] Perveen S. Introductory Chapter: Terpenes and Terpenoids. In *Terpenes and Terpenoids*; IntechOpen: London, United Kingdom, 2018. doi: 10.5772/intechopen.79683

[65] Görmer K.; Waldmann H.; Brunsveld L. Lipidation of peptides and proteins. In *Comprehensive Natural Products II: Chemistry and Biology*; Elsevier: Oxford, United Kingdom, 2010; pp. 531–85. doi: 10.1016/b978-008045382-8.00688-2

[66] Williams A.C.; Barry B.W. Penetration enhancers. *Adv. Drug Deliv. Rev.* **2012**, *64*, 128–37. doi: 10.1016/j.addr.2012.09.032

[67] Martins M.A.R.; Silva L.P.; Schaeffer N.; Abranches D.O.; Maximo G.J.; Pinho S.P.; et al. Greener Terpene-Terpene Eutectic Mixtures as Hydrophobic Solvents. *ACS Sustain. Chem. Eng.* **2019**, *7*, 17414–23. doi: 10.1021/acssuschemeng.9b04614

[68] Kamatou G.P.P.; Vermaak I.; Viljoen A.M.; Lawrence B.M. Menthol: A simple monoterpene with remarkable biological properties. *Phytochemistry.* **2013**, *96*, 15–25. doi: 10.1016/j.phytochem.2013.08.005

[69] Liu Z.; Wu H.; Wei Z.; Wang X.; Shen P.; Wang S.; et al. TRPM8: a potential target for cancer treatment. *J. Cancer Res. Clin. Oncol.* **2016**, *142* (9), 1871–81. doi: 10.1007/s00432-015-2112-1

[70] Yee N.S. Roles of TRPM8 ion channels in cancer: Proliferation, survival, and invasion. *Cancers (Basel).* **2015**, *7* (4), 2134–46. doi: 10.3390/cancers7040882

[71] Naziroğlu M.; Çiğ B.; Blum W.; Vizler C.; Buhala A.; Marton A.; et al. Targeting breast cancer cells by MRS1477, a positive allosteric modulator of TRPV1 channels. *PLoS One.*



2017, 12 (6), e0179950. doi: 10.1371/journal.pone.0179950

[72] Koşar P.A.; Nazıroğlu M.; Övey İ.S.; Çiğ B. Synergic Effects of Doxorubicin and Melatonin on Apoptosis and Mitochondrial Oxidative Stress in MCF-7 Breast Cancer Cells: Involvement of TRPV1 Channels. *J. Membr. Biol.* **2016**, *249*, 129–40. doi: 10.1007/s00232-015-9855-0

[73] Simon H.; Haj-Yehia A.; Levi-Schaffer F. Role of reactive oxygen species (ROS) in apoptosis induction. *Apoptosis.* **2000**, *5* (5), 415–8.

[74] Nazıroğlu M.; Blum W.; Jósvey K.; Çiğ B.; Henzi T.; Oláh Z.; et al. Menthol evokes Ca<sup>2+</sup> signals and induces oxidative stress independently of the presence of TRPM8 (menthol) receptor in cancer cells. *Redox Biol.* **2018**, *14*, 439–49. doi: 10.1016/j.redox.2017.10.009

[75] Cavaliere F.; Donno C.; D'Ambrosi N. Purinergic signaling: A common pathway for neural and mesenchymal stem cell maintenance and differentiation. *Front. Cell. Neurosci.* **2015**, *9*, 1–8. doi: 10.3389/fncel.2015.00211

[76] Peana A.T.; Moretti M.D.L. Linalool in essential plant oils: pharmacological effects. In *Botanical medicine in clinical practice*, 2008; pp. 716–24. doi: 10.1079/9781845934132.0716

[77] Lapczynski A.; Letizia C.S.; Api A.M. Addendum to Fragrance material review on linalool. *Food Chem. Toxicol.* **2008**, *46 Suppl 1*, S190–2. doi: 10.1016/j.fct.2008.06.087

[78] Carson C.F.; Riley T. V. Antimicrobial activity of the major components of the essential oil of *Melaleuca alternifolia*. *J. Appl. Bacteriol.* **1995**, *78* (3), 264–9. doi: 10.1111/j.1365-2672.1995.tb05025.x

[79] Peana A.T.; D'Aquila P.S.; Panin F.; Serra G.; Pippia P.; Moretti M.D.L. Anti-inflammatory activity of linalool and linalyl acetate constituents of essential oils. *Phytomedicine.* **2002**, *9* (8), 721–6. doi: 10.1078/094471102321621322

[80] Chang M.Y.; Shen Y.L. Linalool exhibits cytotoxic effects by activating antitumor immunity. *Molecules.* **2014**, *19* (5), 6694–706. doi: 10.3390/molecules19056694

[81] Anjos P.J.C.; Lima A.O.; Cunha P.S.; De Sousa D.P.; Onofre A.S.C.; Ribeiro T.P.; et al. Cardiovascular effects induced by linalool in normotensive and hypertensive rats. *Zeitschrift fur Naturforsch. - Sect. C J. Biosci.* **2013**, *68* (5–6), 181–90. doi: 10.1515/znc-2013-5-603

[82] Cherng J.M.; Shieh D.E.; Chiang W.; Chang M.Y.; Chiang L.C. Chemopreventive effects of minor dietary constituents in common foods on human cancer cells. *Biosci. Biotechnol. Biochem.* **2007**, *71* (6), 1500–4. doi: 10.1271/bbb.70008

[83] Gu Y.; Ting Z.; Qiu X.; Zhang X.; Gan X.; Fang Y.; et al. Linalool preferentially induces robust apoptosis of a variety of leukemia cells via upregulating p53 and cyclin-dependent kinase inhibitors. *Toxicology.* **2010**, *268* (1–2), 19–24. doi: 10.1016/j.tox.2009.11.013

[84] Usta J.; Kreydiyyeh S.; Knio K.; Barnabe P.; Bou-Moughlabay Y.; Dagher S. Linalool decreases HepG2 viability by inhibiting mitochondrial complexes I and II, increasing reactive oxygen species and decreasing ATP and GSH levels. *Chem. Biol. Interact.* **2009**, *180* (1), 39–46. doi: 10.1016/j.cbi.2009.02.012

[85] Srithar G.; Sudha M.; Nalini N. Linalool Exerts Dose Dependent Chemopreventive Effect Against 1, 2-Dimethylhydrazine Induced Rat Colon Carcinogenesis. **2013**, *4* (4), 758–70.

[86] Iwasaki K.; Zheng Y.W.; Murata S.; Ito H.; Nakayama K.; Kurokawa T.; et al. Anticancer effect of linalool via cancer-specific hydroxyl radical generation in human colon cancer. *World J. Gastroenterol.* **2016**, *22* (44), 9765–74. doi: 10.3748/wjg.v22.i44.9765

[87] Sun X. Bin; Wang S.M.; Li T.; Yang Y.Q. Anticancer activity of linalool terpenoid: Apoptosis induction and cell cycle arrest in prostate cancer cells. *Trop. J. Pharm. Res.* **2015**, *14* (4), 619–25. doi: 10.4314/tjpr.v14i4.9

[88] Peana A.T.; Moretti M.D.L. Pharmacological activities and applications of *Salvia sclarea* and *Salvia desoleana* essential oils. *Stud. Nat. Prod. Chem.* **2002**, *26* (PART G), 391–423. doi: 10.1016/S1572-5995(02)80012-6

[89] Samarghandian S.; Borji A. Anticarcinogenic effect of saffron (*Crocus sativus* L.)

and its ingredients. *Pharmacognosy Res.* **2014**, 6 (2), 99–107. doi: 10.4103/0974-8490.128963

[90] Rezaee R.; Hosseinzadeh H. Safranal: From an aromatic natural product to a rewarding pharmacological agent. *Iran. J. Basic Med. Sci.* **2013**, 16 (1), 12–26. doi: 10.22038/ijbms.2013.244

[91] Escribano J.; Alonso G.L.; Coca-Prados M.; Fernández J.A. Crocin, safranal and picrocrocin from saffron (*Crocus sativus* L.) inhibit the growth of human cancer cells in vitro. *Cancer Lett.* **1996**, 100 (1–2), 23–30. doi: 10.1016/0304-3835(95)04067-6

[92] Abdullaev F.I. Cancer Chemopreventive and Tumoricidal Properties of Saffron (*Crocus sativus* L.). *Exp. Biol. Med.* **2002**, 227 (1), 20–5.

[93] Samarghandian S.; Shabestari M.M. DNA fragmentation and apoptosis induced by safranal in human prostate cancer cell line. *Indian J. Urol.* **2013**, 29 (3), 177–83. doi: 10.4103/0970-1591.117278

[94] Samarghandian S.; Boskabady M.H.; Davoodi S. Use of in vitro assays to assess the potential antiproliferative and cytotoxic effects of saffron (*Crocus sativus* L.) in human lung cancer cell line. *Pharmacogn. Mag.* **2010**, 6 (24), 309–14. doi: 10.4103/0973-1296.71799

[95] Naghshineh A.; Dadras A.; Ghalandari B.; Riazi G.H.; Modaresi S.M.S.; Afrasiabi A.; et al. Safranal as a novel anti-tubulin binding agent with potential use in cancer therapy: An in vitro study. *Chem. Biol. Interact.* **2015**, 238, 151–60. doi: 10.1016/j.cbi.2015.06.023

[96] Jabini R.; Ehtesham-Gharaee M.; Dalirsani Z.; Mosaffa F.; Delavarian Z.; Behravan J. Evaluation of the Cytotoxic Activity of Crocin and Safranal, Constituents of Saffron, in Oral Squamous Cell Carcinoma (KB Cell Line). *Nutr. Cancer.* **2017**, 69 (6), 911–9. doi: 10.1080/01635581.2017.1339816

[97] Milajerdi A.; Djafarian K.; Hosseini B. The toxicity of saffron (*Crocus sativus* L.) and its constituents against normal and cancer cells. *J. Nutr. Intermed. Metab.* **2016**, 3, 23–32. doi: 10.1016/j.jnim.2015.12.332

[98] Kanakis C.D.; Tarantilis P.A.; Tajmir-Riahi H.A.; Polissiou M.G. DNA interaction with saffron's secondary metabolites safranal, crocetin, and dimethylcrocetin. *DNA Cell Biol.* **2007**, 26 (1), 63–70. doi: 10.1089/dna.2006.0529

[99] Zhang Y.; Zhao Y.; Guo J.; Cui H.; Liu S. Anticancer activity of safranal against colon carcinoma is due to induction of apoptosis and G2/M cell cycle arrest mediated by suppression of mTOR/PI3K/Akt pathway. *J. B.U.ON.* **2018**, 23 (3), 574–8.

[100] Al-Hrout A.; Chaiboonchoe A.; Khraiwesh B.; Murali C.; Baig B.; El-Awady R.; et al. Safranal induces DNA double-strand breakage and ER-stress-mediated cell death in hepatocellular carcinoma cells. *Sci. Rep.* **2018**, 8 (1), 1–15. doi: 10.1038/s41598-018-34855-0

[101] Chan T.A. Nonsteroidal anti-inflammatory drugs, apoptosis, and colon-cancer chemoprevention. *Lancet Oncol.* **2002**, 3 (3), 166–74. doi: 10.1016/S1470-2045(02)00680-0

[102] Harris R.E.; Beebe-Donk J.; Doss H.; Burr Doss D. Aspirin, ibuprofen, and other non-steroidal anti-inflammatory drugs in cancer prevention: a critical review of non-selective COX-2 blockade (review). *Oncol. Rep.* **2005**, 13 (4), 559–83. doi: 10.3892/or.13.4.559

[103] Mitchell J.A.; Akarasereenont P.; Thiemermann C.; Flower R.J.; Vane J.R. Selectivity of nonsteroidal antiinflammatory drugs as inhibitors of constitutive and inducible cyclooxygenase. *Proc. Natl. Acad. Sci. U. S. A.* **1993**, 90 (24), 11693–7. doi: 10.1073/pnas.90.24.11693

[104] Meade E.A.; Smith W.L.; DeWitt D.L. Differential inhibition of prostaglandin endoperoxide synthase (cyclooxygenase) isozymes by aspirin and other non-steroidal anti-inflammatory drugs. *J. Biol. Chem.* **1993**, 268 (9), 6610–4. doi: 10.1016/S0021-9258(18)53294-4

[105] Kantor T.G. Ibuprofen. *Ann. Intern. Med.* **1979**, 91 (6), 877–82. doi: 10.7326/0003-4819-91-6-877

[106] Davies N.M. Clinical Pharmacokinetics of Flurbiprofen and its Enantiomers. *Clin. Pharmacokinet.* **1995**, 28 (2), 100–14. doi: 10.2165/00003088-199528020-00002

[107] Jamali F.; Brocks D.R. Clinical Pharmacokinetics of Ketoprofen and Its

Enantiomers. *Clin. Pharmacokinet.* **1990**, 19 (3), 197–217. doi: 10.2165/00003088-199019030-00004

[108] Rainsford K.D. Ibuprofen: Pharmacology, efficacy and safety. *Inflammopharmacology.* **2009**, 17 (6), 275–342. doi: 10.1007/s10787-009-0016-x

[109] Henry D.; Lim L.L.Y.; Garcia Rodriguez L.A.; Perez Gutthann S.; Carson J.L.; Griffin M.; et al. Variability in risk of gastrointestinal complications with individual non-steroidal anti-inflammatory drugs: Results of a collaborative meta-analysis. *Br. Med. J.* **1996**, 312 (7046), 1563–6. doi: 10.1136/bmj.312.7046.1563

[110] Janssen A.; Schiffmann S.; Birod K.; Maier T.J.; Wobst I.; Geisslinger G.; et al. P53 Is Important for the Anti-Proliferative Effect of Ibuprofen in Colon Carcinoma Cells. *Biochem. Biophys. Res. Commun.* **2008**, 365 (4), 698–703. doi: 10.1016/j.bbrc.2007.11.051

[111] Matos P.; Oliveira C.; Velho S.; Gonçalves V.; da Costa L.T.; Moyer M.P.; et al. B-Raf (V600E) cooperates with alternative spliced Rac1b to sustain colorectal cancer cell survival. *Gastroenterology.* **2008**, 135 (3), 899–906. doi: 10.1053/j.gastro.2008.05.052

[112] Matos P.; Kotelevets L.; Gonçalves V.; Henriques A.; Zerbib P.; Moyer M.P.; et al. Ibuprofen inhibits colitis-induced overexpression of tumor-related Rac1b. *Neoplasia (United States).* **2013**, 15 (1), 102–11. doi: 10.1593/neo.121890

[113] Melzer C.; Hass R.; Lehnert H.; Ungefroren H. RAC1B: A Rho GTPase with Versatile Functions in Malignant Transformation and Tumor Progression. *Cells.* **2019**, 8 (1), 21. doi: 10.3390/cells8010021

[114] Bethesda (MD): National Institute of Diabetes and Digestive and Kidney Diseases. LiverTox: Clinical and Research Information on Drug-Induced Liver Injury - Flurbiprofen. *NCBI NLM NIH.gov.* **2018**, Flurbiprofen.

[115] Wechter W.J.; Leipold D.D.; Quiggle D.D.; McCracken J.D.; Murray J.; Loughman B.E. R-flurbiprofen (E-7869), a chemopreventive and treatment of cancer. *Inflammopharmacology.* **2000**, 8 (2), 189–206. doi: 10.1163/15685600038224

[116] McCracken J.D.; Wechter W.J.; Liu Y.; Chase R.L.; Kantoci D.; Murray E.D.; et al. Antiproliferative effects of the enantiomers of flurbiprofen. *J. Clin. Pharmacol.* **1996**, 36 (6), 540–5. doi: 10.1002/j.1552-4604.1996.tb05043.x

[117] Bennett A.; Houghton J.; Leaper D.J.; Stamford I.F. Cancer growth, response to treatment and survival time in mice: Beneficial effect of the prostaglandin synthesis inhibitor flurbiprofen. *Prostaglandins.* **1979**, 17 (2), 179–91. doi: 10.1016/0090-6980(79)90037-6

[118] Sugimoto M.; Toda Y.; Hori M.; Mitani A.; Ichihara T.; Sekine S.; et al. Topical Anti-Inflammatory and Analgesic Effects of Multiple Applications of S(+)-Flurbiprofen Plaster (SFPP) in a Rat Adjuvant-Induced Arthritis Model. *Drug Dev. Res.* **2016**, 211 (May), 206–11. doi: 10.1002/ddr.21314

[119] Funk C.D. Prostaglandins and leukotrienes: Advances in eicosanoid biology. *Science (80-. ).* **2001**, 294 (5548), 1871–5. doi: 10.1126/science.294.5548.1871

[120] Varma M.M.; Pandi J.K. Dissolution, solubility, XRD, and DSC studies on flurbiprofen-nicotinamide solid dispersions. *Drug Dev. Ind. Pharm.* **2005**, 31 (4–5), 417–23. doi: 10.1080/03639040500214613

[121] Alshaikh R.A.; Essa E.A.; El Maghraby G.M. Eutexia for enhanced dissolution rate and anti-inflammatory activity of nonsteroidal anti-inflammatory agents: Caffeine as a melting point modulator. *Int. J. Pharm.* **2019**, 563, 395–405. doi: 10.1016/j.ijpharm.2019.04.024

[122] Kantor T.G. Ketoprofen: A Review of Its Pharmacologic and Clinical Properties. *Pharmacotherapy.* **1986**, 6 (3), 93–102.

[123] Rao K.V.N.; Detrisac C.J.; Steele V.E.; Hawk E.T.; Kelloff G.J.; McCormick D.L. Differential activity of aspirin, ketoprofen and sulindac as cancer chemopreventive agents in the mouse urinary bladder. *Carcinogenesis.* **1996**, 17 (7), 1435–8. doi: 10.1093/carcin/17.7.1435

[124] Ascar L.; Ahumada I.; López A.; Quintanilla F.; Leiva K. Nonsteroidal anti-inflammatory drug determination in water samples by HPLC-DAD under isocratic

- conditions. *J. Braz. Chem. Soc.* **2013**, *24* (7), 1160–6. doi: 10.5935/0103-5053.20130150
- [125] Silva J.M.; Duarte A.R.C.; Caridade S.G.; Picart C.; Reis R.L.; Mano J.F. Tailored freestanding multilayered membranes based on chitosan and alginate. *Biomacromolecules*. **2014**, *15* (10), 3817–26. doi: 10.1021/bm501156v
- [126] Chu L.Y.; Li Y.; Zhu J.H.; Wang H.D.; Liang Y.J. Control of pore size and permeability of a glucose-responsive gating membrane for insulin delivery. *J. Control. Release*. **2004**, *97* (1), 43–53. doi: 10.1016/j.jconrel.2004.02.026
- [127] Mouradov D.; Sloggett C.; Jorissen R.N.; Love C.G.; Li S.; Burgess A.W.; et al. Colorectal cancer cell lines are representative models of the main molecular subtypes of primary cancer. *Cancer Res.* **2014**, *74* (12), 3238–47. doi: 10.1158/0008-5472.CAN-14-0013
- [128] Martínez-Maqueda D.; Miralles B.; Recio I. HT29 cell line. In *The Impact of Food Bioactives on Health: In Vitro and Ex Vivo Models*, 2015; pp. 113–24. doi: 10.1007/978-3-319-16104-4\_11
- [129] Rousset M. The human colon carcinoma cell lines HT-29 and Caco-2: Two in vitro models for the study of intestinal differentiation. *Biochimie*. **1986**, *68* (9), 1035–40. doi: 10.1016/S0300-9084(86)80177-8
- [130] Sambuy Y.; De Angelis I.; Ranaldi G.; Scarino M.L.; Stamatii A.; Zucco F. The Caco-2 cell line as a model of the intestinal barrier: Influence of cell and culture-related factors on Caco-2 cell functional characteristics. *Cell Biol. Toxicol.* **2005**, *21* (1), 1–26. doi: 10.1007/s10565-005-0085-6
- [131] Malich G.; Markovic B.; Winder C. The sensitivity and specificity of the MTS tetrazolium assay for detecting the in vitro cytotoxicity of 20 chemicals using human cell lines. *Toxicology*. **1997**, *124* (3), 179–92. doi: 10.1016/S0300-483X(97)00151-0
- [132] Vanderlinde R.E. Measurement of total lactate dehydrogenase activity. *Ann. Clin. Lab. Sci.* **1985**, *15* (1), 13–31.
- [133] Babson A.L.; Babson S.R. Kinetic colorimetric measurement of serum lactate dehydrogenase activity. *Clin. Chem.* **1973**, *19* (7), 766–9. doi: 10.1093/clinchem/19.7.766
- [134] Kalyanaraman B.; Darley-Usmar V.; Davies K.J.A.; Dennery P.A.; Forman H.J.; Grisham M.B.; et al. Measuring reactive oxygen and nitrogen species with fluorescent probes: Challenges and limitations. *Free Radic. Biol. Med.* **2012**, *52* (1), 1–6. doi: 10.1016/j.freeradbiomed.2011.09.030
- [135] Wang H.; Joseph J.A. Quantifying cellular oxidative stress by dichlorofluorescein assay using microplate reader. *Free Radic. Biol. Med.* **1999**, *27* (5–6), 612–6. doi: 10.1016/S0891-5849(99)00107-0
- [136] Yu D.; Zha Y.; Zhong Z.; Ruan Y.; Li Z.; Sun L.; et al. Improved detection of reactive oxygen species by DCFH-DA: New insight into self-amplification of fluorescence signal by light irradiation. *Sensors Actuators, B Chem.* **2021**, *339*, 129878. doi: 10.1016/j.snb.2021.129878
- [137] Bradford M.M. A Rapid and Sensitive Method for the Quantitation of Microgram Quantities of Protein Utilizing the Principle of Protein-Dye Binding. *Anal. Biochem.* **1976**, *72*, 248–54. doi: 10.1016/j.cj.2017.04.003
- [138] Ma, Xu; Fang, Liang; Guo, Jianpeng; Zhao, Nanxi; He Z. Effect of Counter-Ions and Penetration Enhancers on the Skin Permeation of Flurbiprofen. *J. Pharm. Sci.* **2010**, *99* (4), 1826–37. doi: 10.1002/jps
- [139] Li X.; Zhou G.J.; Chu G.H.; Lin X.F.; Wang J.L.; Shen K.; et al. Fabrication of size-controllable mPEG-decorated microparticles conjugating optically active ketoprofen based on self-assembly of amphiphilic random copolymers. *J. Appl. Polym. Sci.* **2013**, *127* (4), 3242–8. doi: 10.1002/app.37756
- [140] Khayyat S.; Elgendy E. Safranal epoxide – A potential source for diverse therapeutic applications. *Saudi Pharm. J.* **2018**, *26* (1), 115–9. doi: 10.1016/j.jsps.2017.10.004
- [141] Tao R.; Wang C.Z.; Kong Z.W. Antibacterial/antifungal activity and synergistic interactions between polyprenols and other lipids isolated from Ginkgo Biloba L. leaves.

*Molecules*. **2013**, *18* (2), 2166–82. doi: 10.3390/molecules18022166

[142] Silva E.; Oliveira F.; Silva J.M.; Matias A.; Reis R.L.; Duarte A.R.C. Optimal design of thedes based on perillyl alcohol and ibuprofen. *Pharmaceutics*. **2020**, *12* (11), 1–17. doi: 10.3390/pharmaceutics12111121

[143] Santos F.; Leitão M.I.P.S.; Duarte A.R.C. Properties of therapeutic deep eutectic solvents of L-arginine and ethambutol for tuberculosis treatment. *Molecules*. **2018**, *24* (1), 55. doi: 10.3390/molecules24010055

[144] Silva J.M.; Reis R.L.; Paiva A.; Duarte A.R.C. Design of Functional Therapeutic Deep Eutectic Solvents Based on Choline Chloride and Ascorbic Acid. *ACS Sustain. Chem. Eng.* **2018**, *6* (8), 10355–63. doi: 10.1021/acssuschemeng.8b01687

[145] Fade V. Link between drug absorption solubility and permeability measurements in Caco-2 cells. *J. Pharm. Sci.* **1998**, *87* (12), 1604–7. doi: 10.1021/js980111k

[146] Ng S.F.; Rouse J.; Sanderson D.; Eccleston G. A Comparative study of transmembrane diffusion and permeation of ibuprofen across synthetic membranes using franz diffusion cells. *Pharmaceutics*. **2010**, *2* (2), 209–23. doi: 10.3390/pharmaceutics2020209

[147] Zhao C.; Xue J.; Ran F.; Sun S. Modification of polyethersulfone membranes - A review of methods. *Prog. Mater. Sci.* **2013**, *58* (1), 76–150. doi: 10.1016/j.pmatsci.2012.07.002

[148] Chang-sheng Z.; Ting L.; Zhong-ping L.; Li-ping C.; Jia H. An Evaluation of a Polyethersulfone Hollow Fiber Plasma Separator by Animal Experiment. *Artif. Organs*. **2001**, *25* (1), 60–3. doi: 10.1046/j.1525-1594.2001.025001058.x

[149] Dizge N.; Soydemir G.; Karagunduz A.; Keskinler B. Influence of type and pore size of membranes on cross flow microfiltration of biological suspension. *J. Memb. Sci.* **2011**, *366* (1–2), 278–85. doi: 10.1016/j.memsci.2010.10.010

[150] Keogh J.P. Membrane Transporters in Drug Development. In *Advances in Pharmacology*; Elsevier Inc., 2012; pp. 1–42. doi: 10.1016/B978-0-12-398339-8.00001-X

[151] Faassen F.; Vromans H. Biowaivers for oral immediate-release products: Implications of linear pharmacokinetics. *Clin. Pharmacokinet.* **2004**, *43* (15), 1117–26. doi: 10.2165/00003088-200443150-00004

[152] Ceschel G.C.; Maffei P.; Borgia S.L. Correlation between the transdermal permeation of ketoprofen and its solubility in mixtures of a pH 6.5 phosphate buffer and various solvents. *Drug Deliv. J. Deliv. Target. Ther. Agents*. **2002**, *9* (1), 39–45. doi: 10.1080/107175402753413163

[153] Chandran S.; Roy A.; Saha R.N. Effect of pH and formulation variables on in vitro transcorneal permeability of flurbiprofen: A technical note. *AAPS PharmSciTech*. **2008**, *9* (3), 1031–7. doi: 10.1208/s12249-008-9139-4

[154] Shohin I.E.; Kulinich J.I.; Ramenskaya G. V; Abrahamsson B.; Kopp S.; Langguth P.; et al. Biowaiver Monographs for Immediate-Release Solid Oral Dosage Forms : Ketoprofen. *J. Pharm. Sci.* **2012**, *101* (10), 3593–603. doi: 10.1002/jps

[155] Tsume, Yasuhiro; M Mudie, Deanna; Langguth, Peter; E Amidon, Greg; L Amidon G. The Biopharmaceutics Classification System: Subclasses for in vivo predictive dissolution (IPD) methodology and IVIVC. *Eur. J. Pharm. Sci.* **2014**, *57*, 152–63. doi: 10.1016/j.ejps.2014.01.009.The

[156] Lindenbergh M.; Kopp S.; Dressman J.B. Classification of orally administered drugs on the World Health Organization Model list of Essential Medicines according to the biopharmaceutics classification system. *Eur. J. Pharm. Biopharm.* **2004**, *58* (2), 265–78. doi: 10.1016/j.ejpb.2004.03.001

[157] Constant S.; Huang S.; Wiszniewski L.; Mas C. Colon Cancer: Current Treatments and Preclinical Models for the Discovery and Development of New Therapies. In *Drug Discovery, H. El-Shemy, Ed. InTech*, 2013. doi: 10.5772/53391

[158] Hayyan M.; Mbous Y.P.; Looi C.Y.; Wong W.F.; Hayyan A.; Salleh Z.; et al. Natural deep eutectic solvents: cytotoxic profile. *Springerplus*. **2016**, *5* (1), 913. doi: 10.1186/s40064-016-

[159] Hayyan M.; Hashim M.A.; Al-Saadi M.A.; Hayyan A.; AlNashef I.M.; Mirghani M.E.S. Assessment of cytotoxicity and toxicity for phosphonium-based deep eutectic solvents. *Chemosphere*. **2013**, 93 (2), 455–9. doi: 10.1016/j.chemosphere.2013.05.013

[160] Pérez-Riesgo E.; Gutiérrez L.G.; Ubierna D.; Acedo A.; Moyer M.P.; Núñez L.; et al. Transcriptomic analysis of calcium remodeling in colorectal cancer. *Int. J. Mol. Sci.* **2017**, 18 (5), 922. doi: 10.3390/ijms18050922

[161] Cornmell R.J.; Winder C.L.; Tiddy G.J.T.; Goodacre R.; Stephens G. Accumulation of ionic liquids in *Escherichia coli* cells. *Green Chem.* **2008**, 10 (8), 836–41. doi: 10.1039/b807214k

[162] Huang H.; Aladelokun O.; Ideta T.; Giardina C.; Ellis L.M.; Rosenberg D.W. Inhibition of PGE 2/EP4 receptor signaling enhances oxaliplatin efficacy in resistant colon cancer cells through modulation of oxidative stress. *Sci. Rep.* **2019**, 9 (1), 4954. doi: 10.1038/s41598-019-40848-4

[163] Dirsch V.M.; Stuppner H.; Vollmar A.M. The griess assay: Suitable for a bio-guided fractionation of anti-inflammatory plant extracts? *Planta Med.* **1998**, 64 (5), 423–6. doi: 10.1055/s-2006-957473

[164] Granger D.L.; Taintor R.R.; Boockvar K.S.; Hibbs Jr. J.B. Measurement of nitrate and nitrite in biological samples using nitrate reductase and Griess reaction. *Methods Enzymol.* **1996**, 268, 142–51.

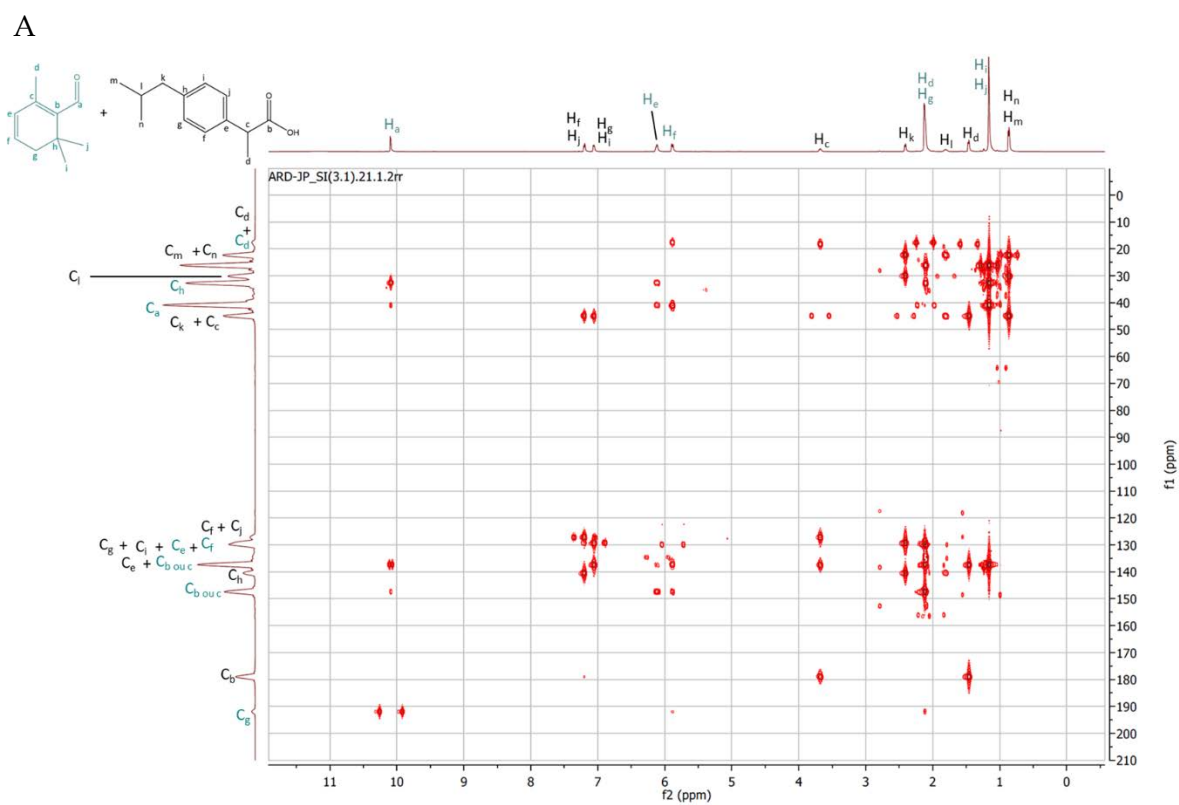
[165] Tsikas D.; Gutzki F.M.; Rossa S.; Bauer H.; Neumann C.; Dockendorff K.; et al. Measurement of nitrite and nitrate in biological fluids by gas chromatography-mass spectrometry and by the griess assay: Problems with the griess assay - Solutions by gas chromatography-mass spectrometry. *Anal. Biochem.* **1997**, 244 (2), 208–20. doi: 10.1006/abio.1996.9880

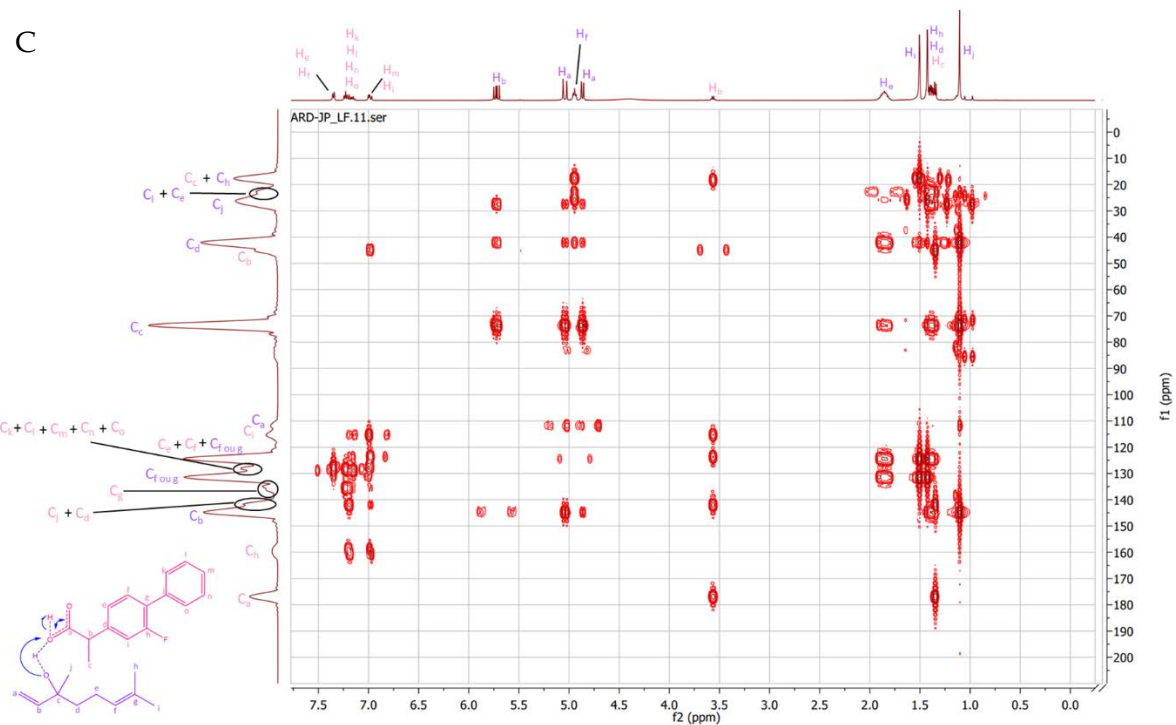
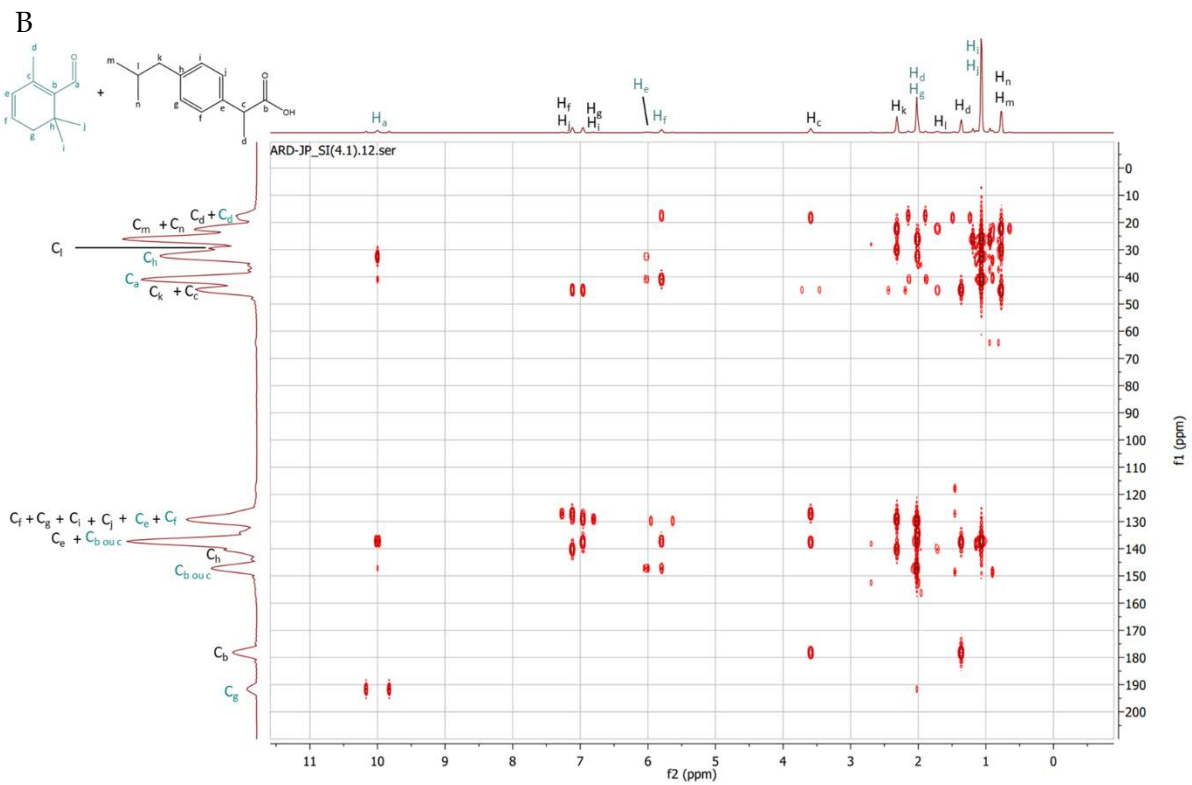
[166] Guevara I.; Iwanejko J.; Dembińska-Kieć A.; Pankiewicz J.; Wanat A.; Anna P.; et al. Determination of nitrite/nitrate in human biological material by the simple Griess reaction. *Clin. Chim. Acta.* **1998**, 274 (2), 177–88. doi: 10.1016/S0009-8981(98)00060-6

[167] Nussler A.K.; Glanemann M.; Schirmeier A.; Liu L.; Nüssler N.C. Fluorometric measurement of nitrite/nitrate by 2,3-diaminonaphthalene. *Nat. Protoc.* **2006**, 1 (5), 2223–6. doi: 10.1038/nprot.2006.341

## SUPPLEMENTARY INFORMATION

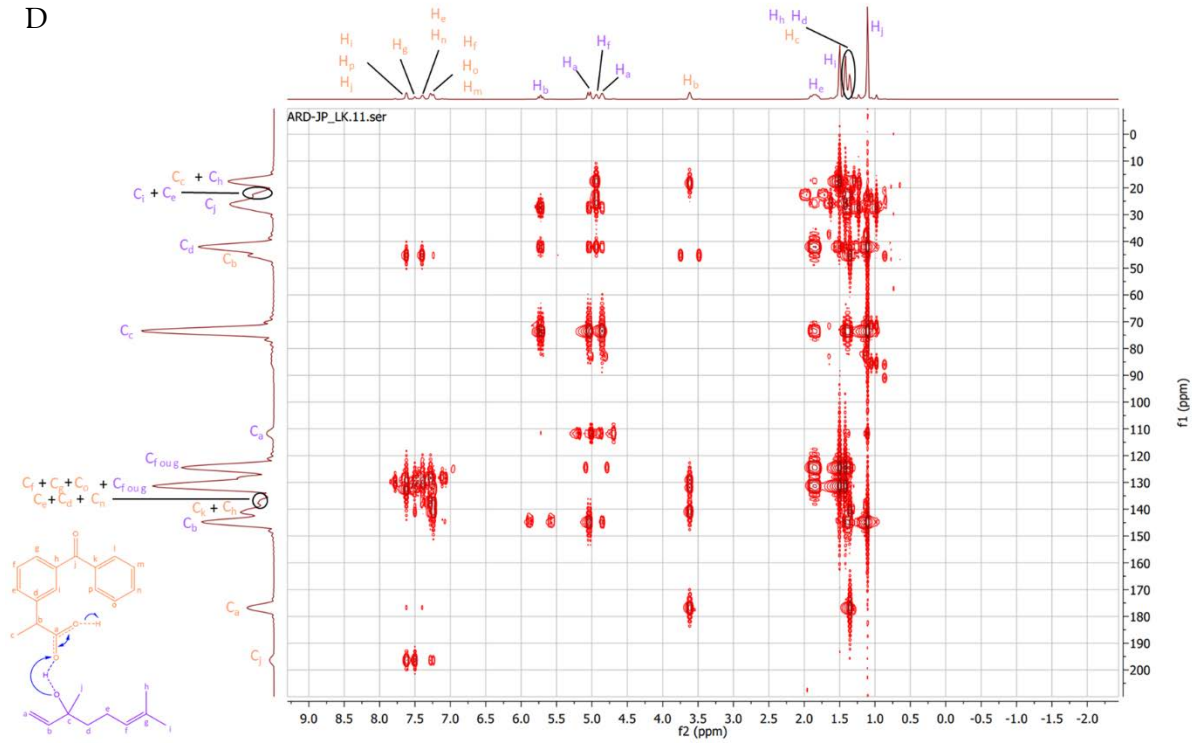
## A.1. NMR Studies



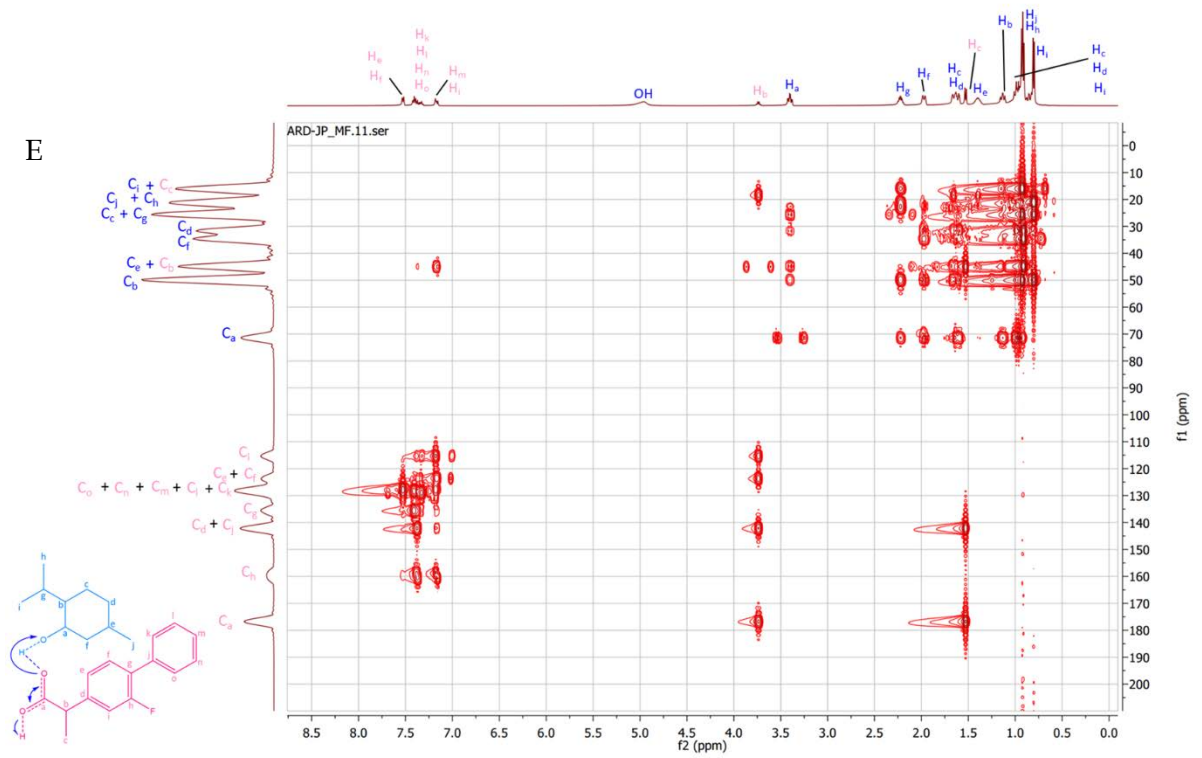




D



E



F

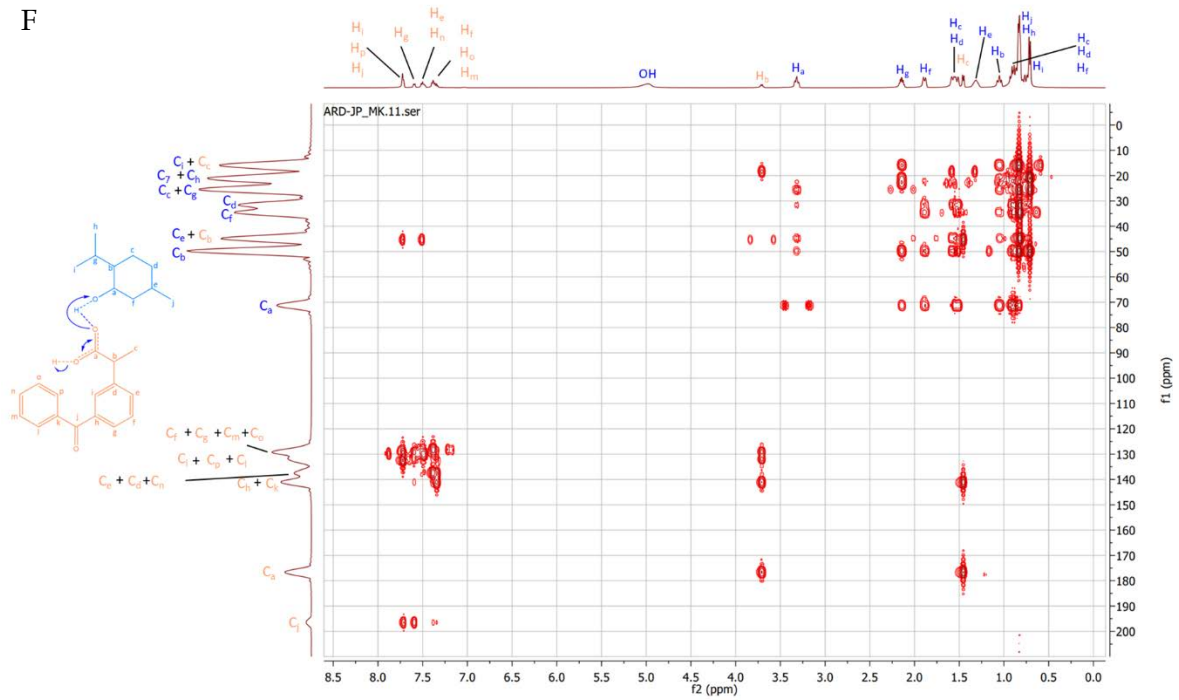


**Figure A.1.** HSQC NMR spectra and signal assignment of THEDES (A) Saf:IBU (3:1), (B) Saf:IBU (4:1) (C) Lin:Flu (4:1), (D) Lin:Ket (4:1), (E) Me:Flu (4:1) and (F) Me:Ket (4:1). Samples prepared in chloroform-d.

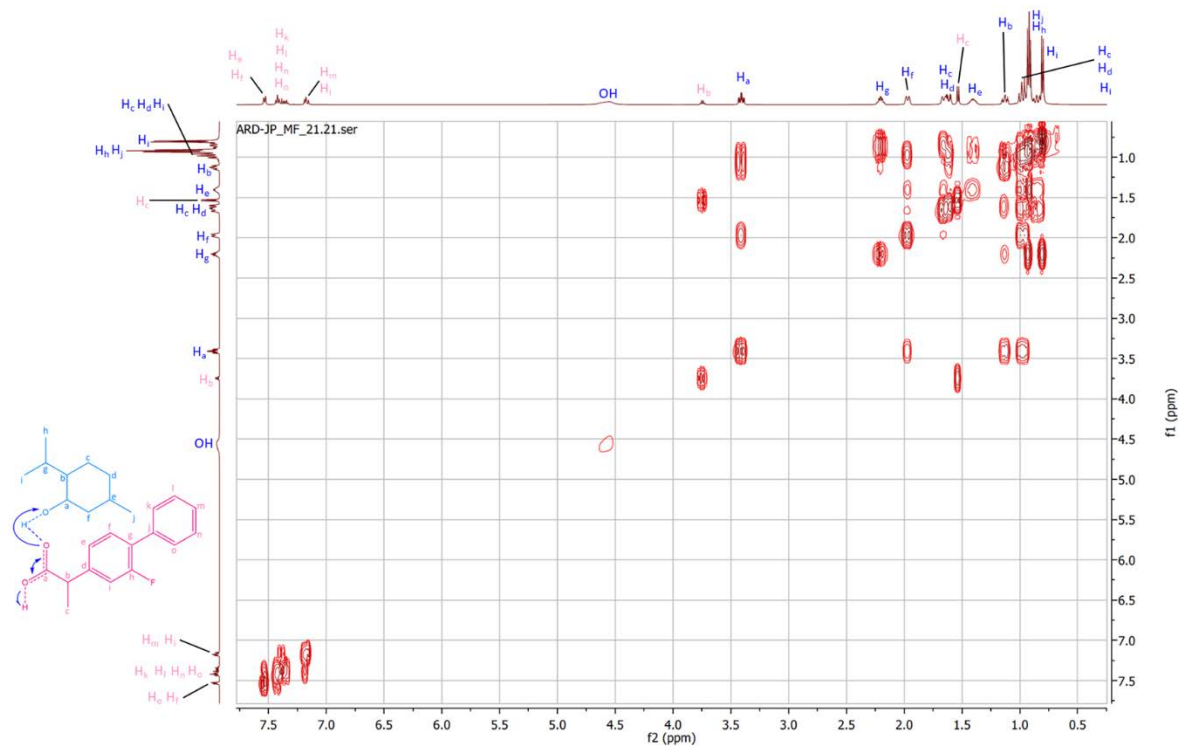
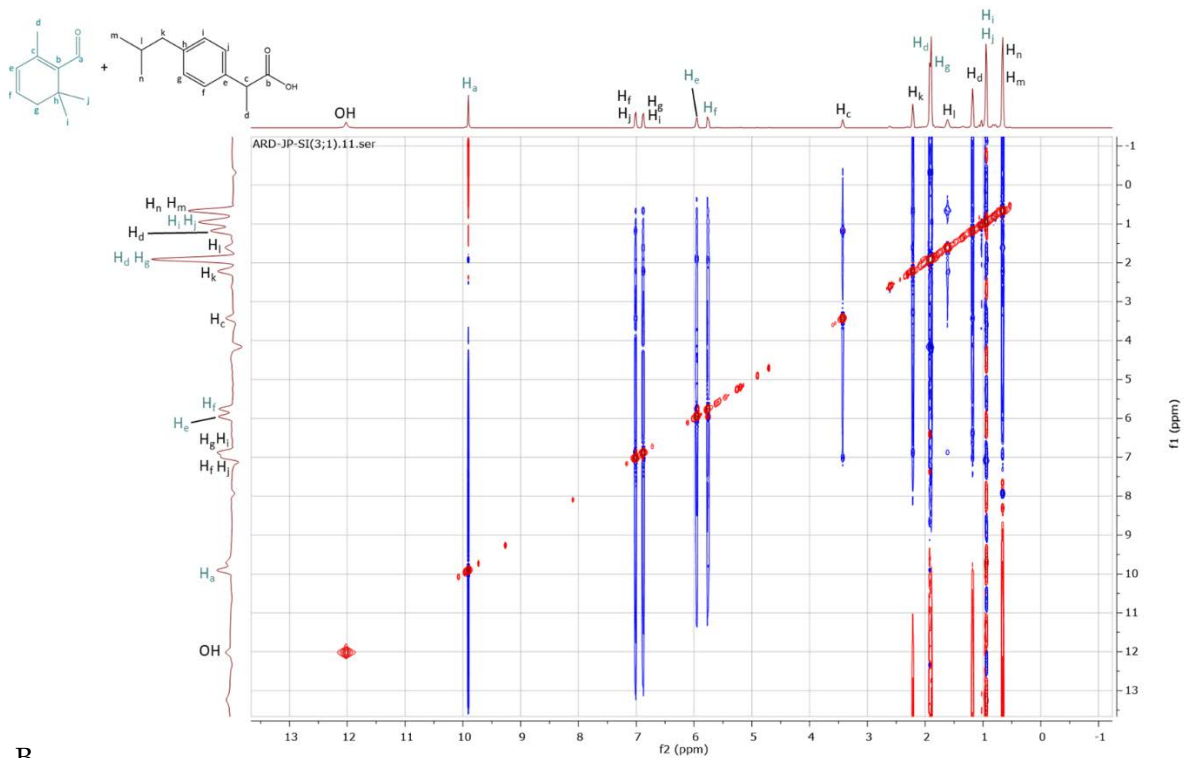
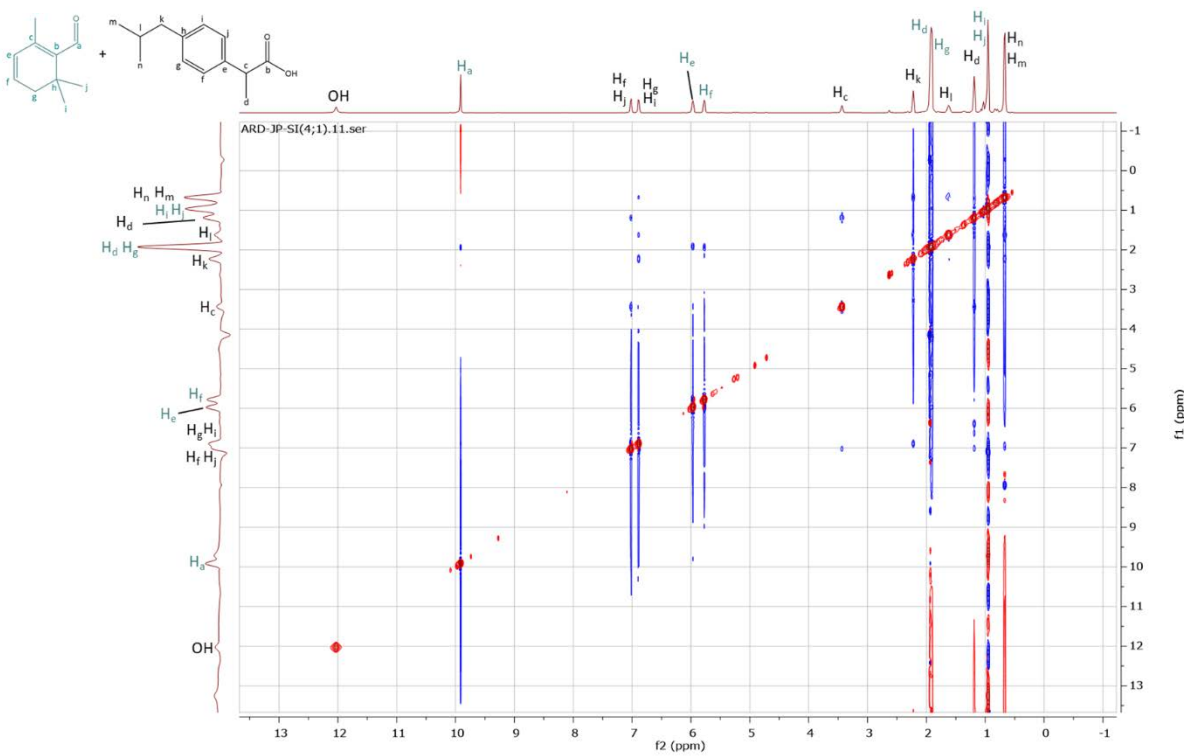


**Figure A.2.** COSY NMR spectra and signal assignment of THEDES Me:Flu (4:1). Sample prepared in chloroform-d.

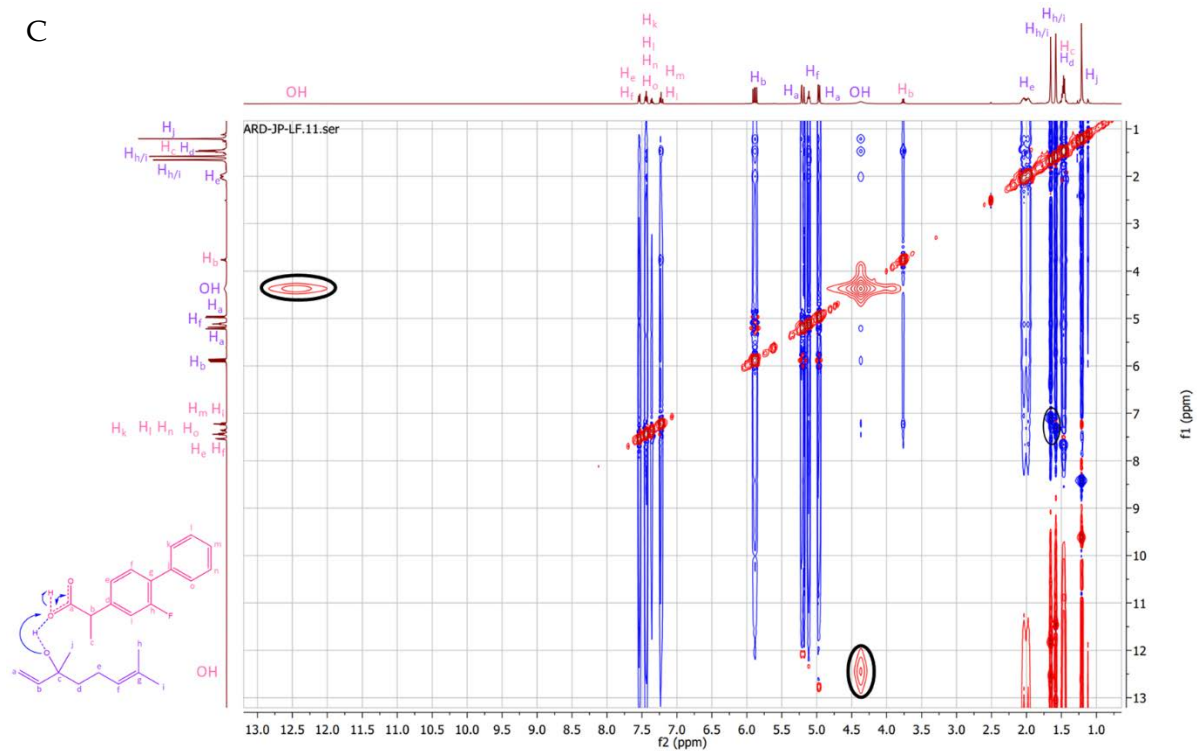
A



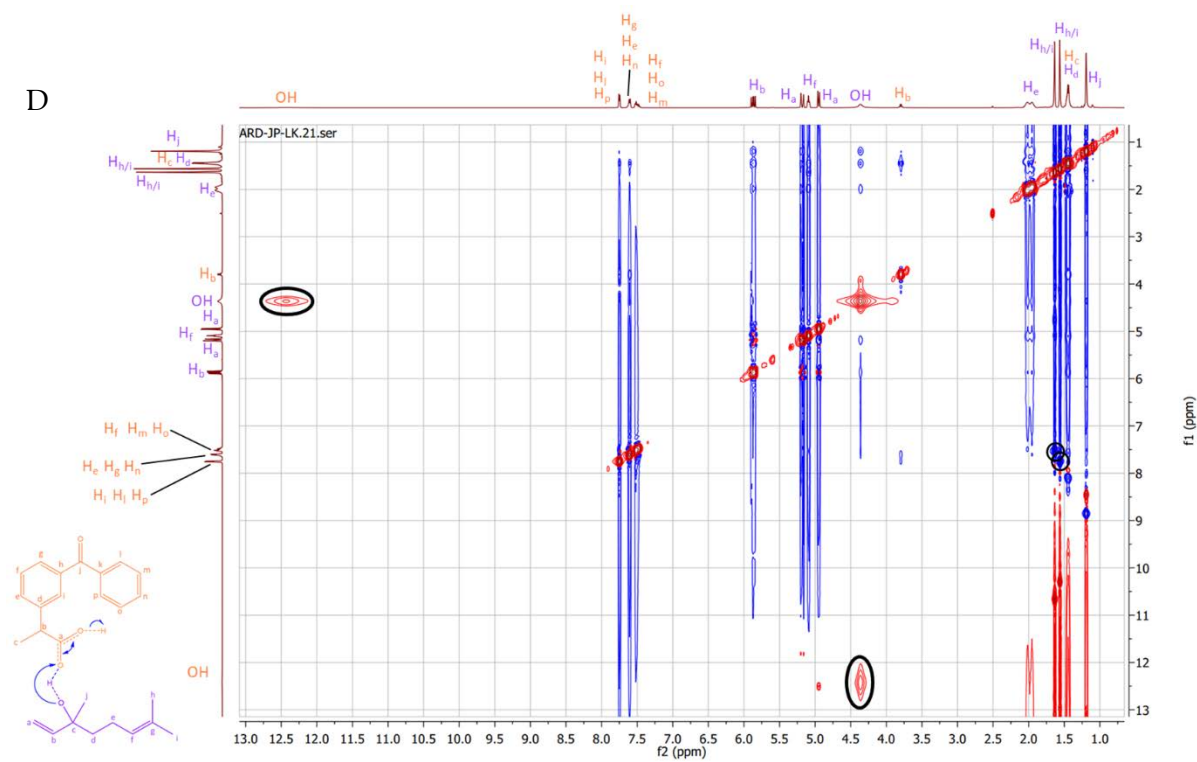
B



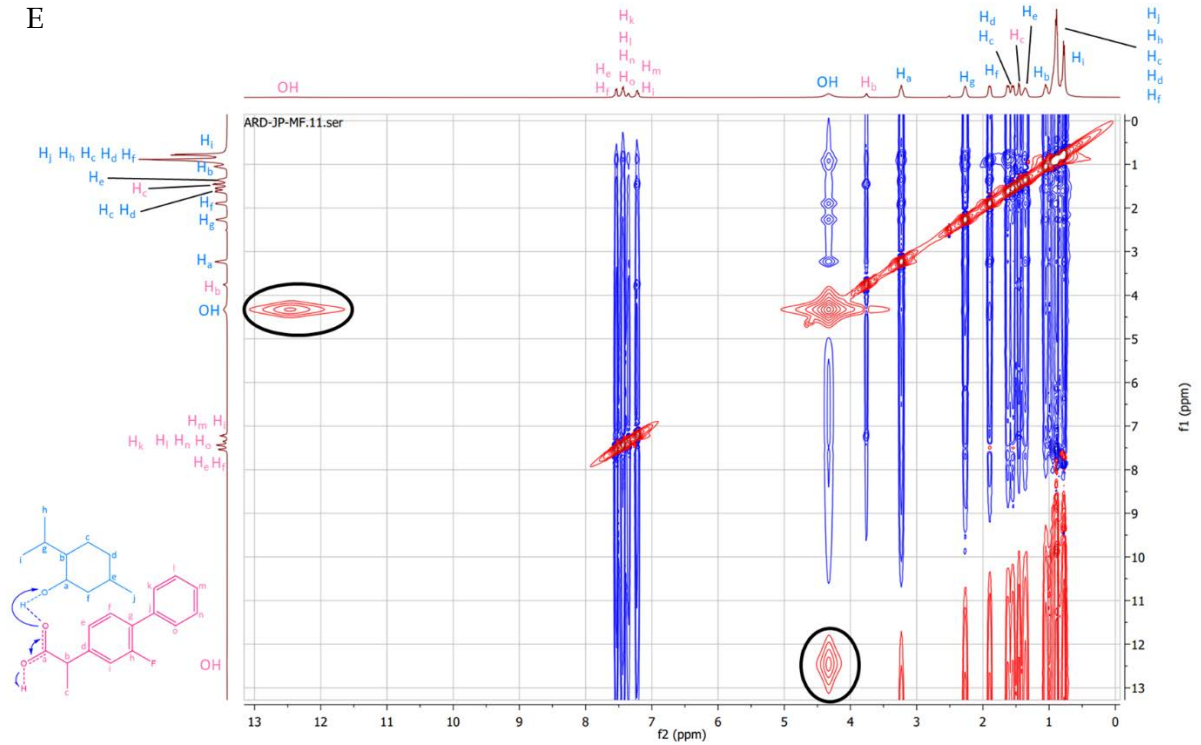
C



D

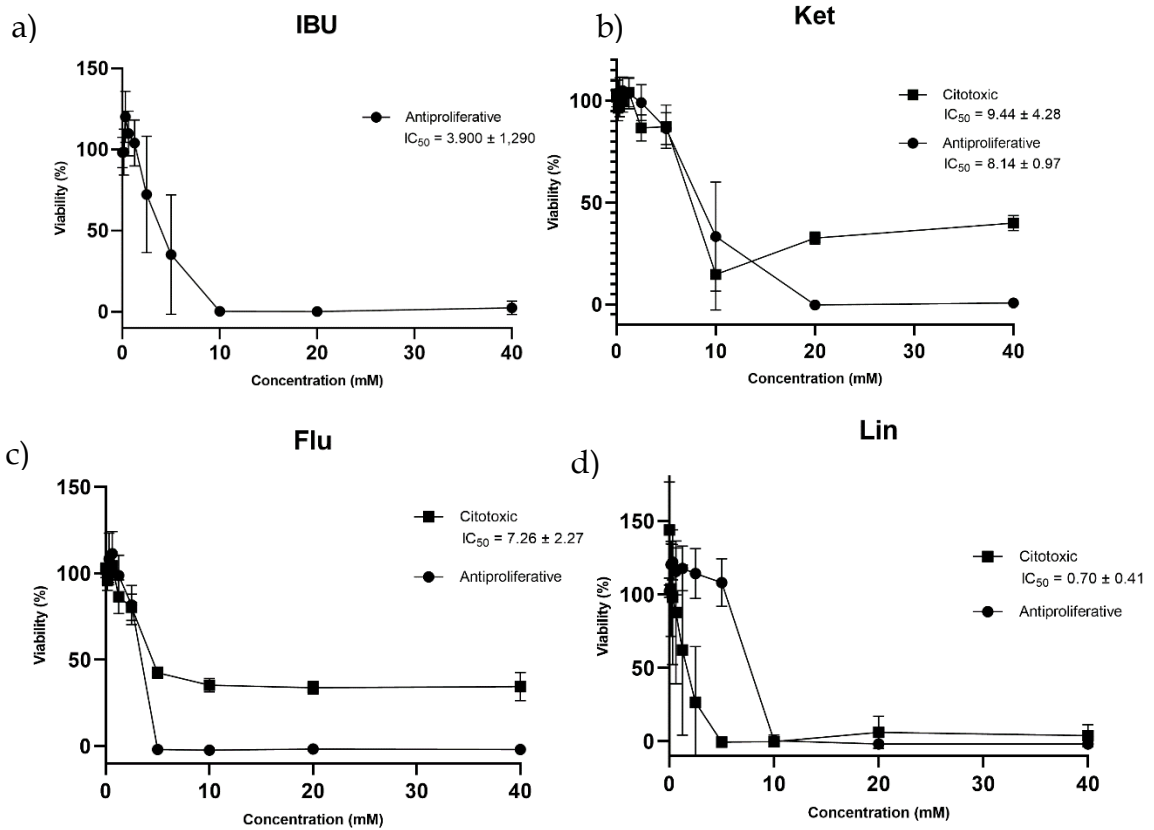


E



**Figure A.3.** NOESY NMR spectra, signal assignment and interactions assignment of THEDES (A) Saf:IBU (3:1), (B) Saf:IBU (4:1) (C) Lin:Flu (4:1), (D) Lin:Ket (4:1) and (E) Me:Flu (4:1). Samples prepared in DMSO- $d_6$ .

## A.2. THEDES Cytotoxicity and Antiproliferative Potentials



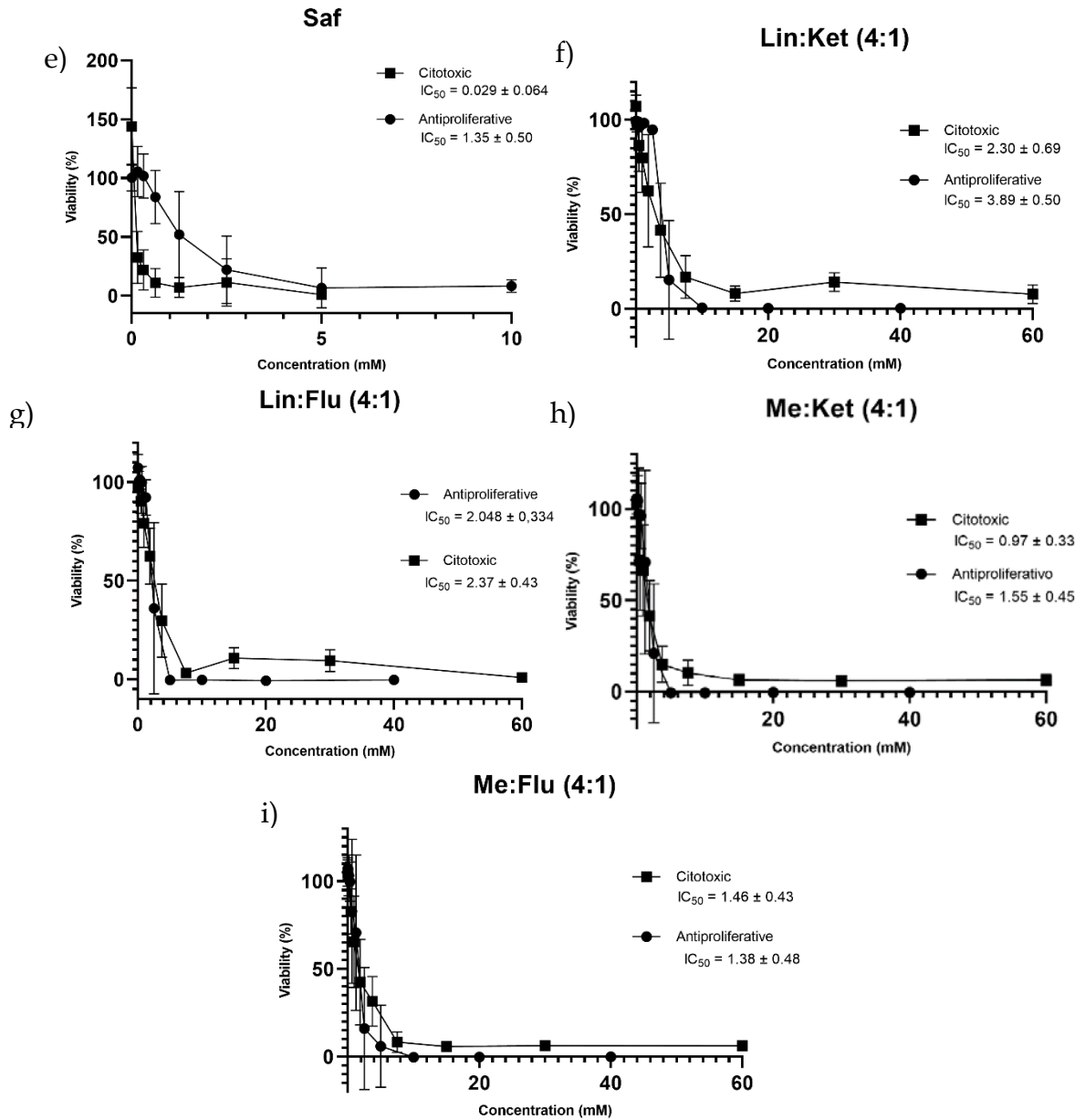


**Figure A.4.** Antiproliferative and cytotoxic graphic results obtain after HT29 and Caco-2 cells, respectively, had been exposed to different concentrations of a) IBU, b) Ket, c) Flu, d) Lin, e) Saf, f) Lin:Ket (4:1), g) Lin:Flu (4:1), h) Me:Ket (4:1) and i) Me:Flu (4:1).  $EC_{50}$  (effective concentration - concentration necessary to decrease 50 % of cell viability) results indicated in the graphics. Results were expressed relatively to the control as the mean  $\pm$  SD of three independent experiments performed in triplicate.

### A.3. LDH Release

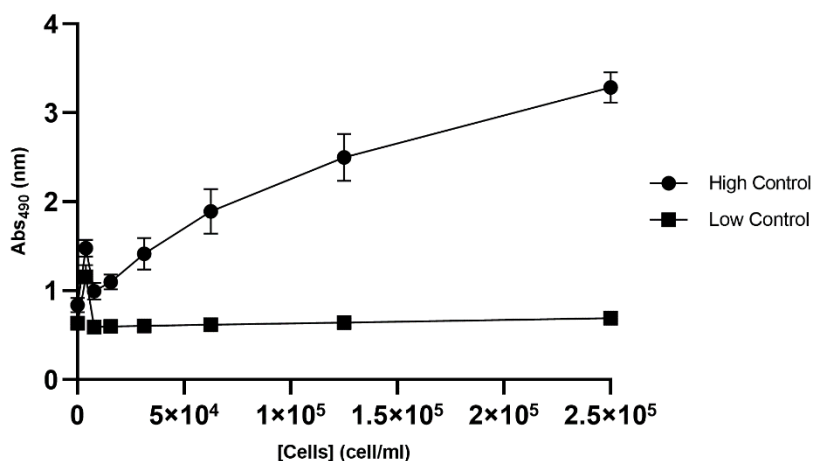


**Figure A.5.** Determination of optimal cell concentration to the LDH release assay. The optimal concentration is obtained when the Low Control has an absorbance value minor than 0,8 and when the greatest difference between the absorbance of the High Control and Low Control is observable. In this case, the optimal cell concentration is at  $2.5 \times 10^5$  cell/ml. Results were performed in triplicate.

### A.4. IL-8 Measurement

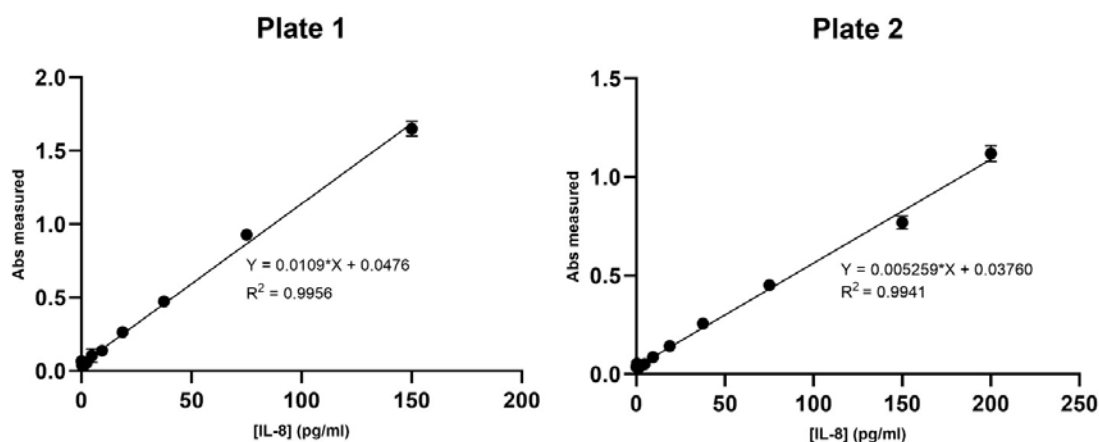


**Figure A.6.** IL-8 calibration curves obtained with the ELISA assay for both plates prepared. Abs measured obtained by the subtraction of Abs (450 nm) minus Abs (620 nm). Results were obtained from an experiment performed in triplicate.

### A.4.1. Bradford

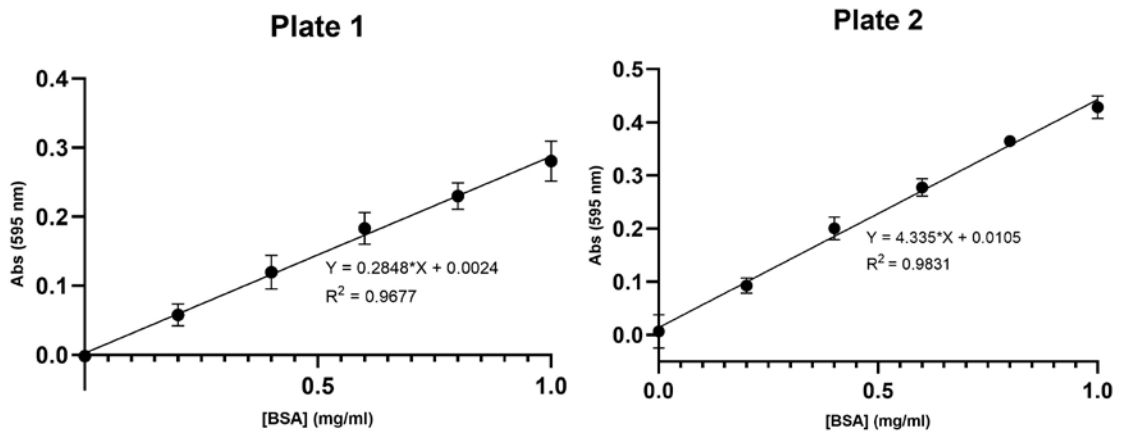


**Figure A.7.** BSA calibration curve obtained using the Bradford assay. Results were obtained from an experiment performed in triplicate.







2021

JOANA FÉLIX PEREIRA

THERAPEUTIC DEEP EUTECTIC SYSTEMS AS PROMISING  
NEW TOOLS IN THE ANTICANCER BATTLE